

A study of geomagnetic storm on the basis of magnetic observations in the Japanese chain observatories

by

Satoru Tsunomura, Takeshi Toya, Yoshiki Ishii and Satoshi Teshima

(Received December 14, 1998; Revised February 01, 1999)

Abstract

Characteristics of geomagnetic storms observed in Japanese chain observatories, Memambetsu, Kakioka and Kanoya are examined on the basis of routine reports, statistics of one-minute magnetic data and a numerical simulation. Stacked records of the one-minute magnetic data for geomagnetic storms starting with SSCs at Kakioka and Memambetsu, show a signature of direct contribution of the ring current in the Z-component for the period of one day or more, although somewhat reduced due to the shielding effect of the Earth's electromagnetic induction. A rough estimation of the ratio of the internal field to the external one using the H- and Z-components for that period range agrees well with that given by Rikitake and Sato (1957). It is imagined that the Z-component at Memambetsu, where the local conductivity anomaly effect is smaller than Kakioka, can be used as one of the realtime monitoring tools to estimate the ring current strength. It was shown that, however, the property of complicated secular variation of the Z-component around Japan should be sufficiently clarified before examining long term variations. Diurnal variation patterns in storm periods were shown in the stacked records dividing to local time blocks of Kakioka. They are possibly attributable to the effect of field-aligned currents and the resulting ionospheric current systems. The variation pattern of the geomagnetic storm of February, 11, 1958, which recorded an extremely large range for the D-component among the geomagnetic storms from the IGY to the present, is briefly examined as a case study. It is shown that the D-component variation associated with a negative bay in the H-component just after the SSC contributed to gain the range of the D-component. It is suggested that case studies of geomagnetic storms will remain to be important in future, including the studies for negative bays observed in middle and low latitudes in the noontime.

1. Introduction

Geomagnetic disturbances observed in middle and low latitudes show less spatial irregularities than those in high latitudes because these regions are distant from the origins of disturbance. Since the variation pattern looks simple, qualitative models or theories for geomagnetic disturbances in middle and low latitudes were constructed from the last century and almost established in the two decades after the International

Geophysical Year (IGY) which was operated from 1957 to 1958. As used to derive Dst index, the magnetic variations in low latitudes are now regarded as representing the whole magnetospheric process without severe locality. In 1980's, interests of scientists have been mainly directed to the phenomena in the interplanetary space, the inner and outer magnetosphere and the polar region.

Nevertheless, it is far from the truth that

geomagnetic disturbances in middle and low latitudes are fully understood quantitatively. Although many qualitative studies have been developed since the IGY using analogue data, precise discussions or statistical studies on the basis of digital data have not been completed. They show rather complicated time changes and/or spatial variations when they are examined precisely.

Recently, the number of studies for geomagnetic disturbances in middle and low latitudes is increasing as magnetic data have been accumulated in wide area. On the basis of high time resolution magnetic data, new findings and/or confirmations for the existing models of geomagnetic disturbances in middle and low latitudes have been obtained (e. g. Russell et al., 1992, 1994a, b; Yumoto et al., 1992, 1994, 1996; Yumoto and the 210° MM Magnetic Observation Group, 1995, 1996; Itonaga et al., 1992, 1995). On the other hand, some statistical results have been obtained using long-term data obtained at routine observatories (e. g., Takahashi et al., 1992; Tsunomura, 1995, 1998). Quantitative studies have been and will be further developed in the Solar Terrestrial Energy Program (STEP) and STEP-Results, Applications, and Modeling Phase (S-RAMP) periods, respectively, to clarify more precisely geomagnetic disturbances in middle and low latitudes, because the research is important as one of the subjects of the magnetosphere-ionosphere coupling problem.

In this paper, the average features of geomagnetic storms and their likely interpretations by the existing theories will be presented, on the basis of magnetic data and reports, accumulated for a long time in the routine observatories, and a numerical simulation. It is purposed to be one of the first steps of the quantitative analysis of geomagnetic storms in middle and low latitudes. The results will be useful for further studies in this field as a reference showing basic characteristics of geomagnetic storms observed in middle and low latitudes.

2. Average features of geomagnetic storm as observed in low latitudes

Since the IGY, routine reports for the parameters of geomagnetic storm, sudden impulse, bay and solar flare effect at the Kakioka Magnetic Observatory (KAK) and its two branch offices at Memambetsu (MMB) and Kanoya (KNY) have been continuously

issued in the series of 'Report of the Geomagnetic and Geoelectric Observations (Rapid Variations) (1957-1984)' and 'Report of Kakioka Magnetic Observatory (1985-1992)'. The reported parameters for the 20 high ranking geomagnetic storms in the range of the H-component from 1957 to 1997 are listed in Table 1 as a sample; it is noteworthy that the largest storm since the start of the magnetic observation at KAK was the event of July 04, 1941, the range in the H-component of which exceeded 700 nT. A machine-readable file for those at KAK from 1957 to 1985 were made by Okamoto and Fujita (1987) and updated to 1992 by Tsunomura (1995). There are two kinds of geomagnetic storm, that is, an SSC geomagnetic storm and an Sg one. The former starts with a storm sudden commencement (SSC), that is, a step-like increase of the H-component with a rise time of about a few minutes. The latter starts without a definite onset. Hereafter these will be called an SSC storm and an Sg storm, respectively.

Fig. 1 shows comparisons of time variations of the sunspot number and occurrence numbers of SSC and Sg storms detected at Kakioka. This figure is somewhat different from Fig. 10 of Nagai (1983) because the criterion to decide a geomagnetic storm is different from that of Nagai (1983) for the pre-IGY period. Here, the values for the period from 1924 to 1951 were taken from the lists of Yokouchi (1953) and those for the period from 1952 to 1956 from lists of the succeeding research (Yokouchi, private communication). It should be noted that the criteria to judge or classify a storm have not been completely the same before and after the IGY. There can be clearly seen that the time variation curve of the number of SSC is almost parallel with that of the sunspot number, whereas the occurrence number of the Sg storm shows a poor correlation with that of the sunspot number. These features are nearly the same as noted by Nagai (1983) though his result for the SSC storm shows much higher correlation with the sunspot number. There can be seen double peaks in the occurrence number of SSC in some solar cycles. This fact may be related with the double peaks of the ring current activity centering the sunspot maximum presented by Vernerstrøm and Friis-Christensen (1996). According to the empirical fact that the peak sunspot number has been larger for the odd number cycles than for the even number cycles, the peak sunspot number and the

Table 1 List of 20 high-ranking geomagnetic storms observed at Kakioka from 1957 to 1997.

Rank	Date y m d	Storm Time U.T.								Sudden commencement					K	Range		
		begin. h m	main phase d h	last phase d h	end. d h	Type	Q	H nT min	D nT min	Z nT min	H nT	D nT	Z nT					
1	1989 3 13	0127	13 01. 9	14 00. 4	15 22	SSC*	A	43	5	-7 47	0 3	18	5	9	644	351	205	
2	1982 7 13	1617	13 18. 0	14 00. 5	C	SSC*	A	114	4	-1 31	1 2	70	5	9	630	297	381	
3	1958 2 11	0126	11 03. 6	11 11. 3	13 06	SSC*	A	48 -72	1	40 -24	1 1	19 -31	1	8	617	469	237	
4	1959 7 15	0802	15 08. 7	15 19. 3	17 02	SSC	A	46	3	1	1	40	3	7	533	174	159	
5	1967 5 25	1235	25 20. 3	26 04. 4	29 20	SSC*	A	91	2	-8 47	0 3	55	3	8	509	138	192	
6	1991 3 24	0341				SSC	A	202	1	88	1	59	1	9	503	204	199	
7	1957 9 13	0045	13 01. 6	13 09. 8	14 16	SSC*	A	25	2	-5 38	1 2	12	2	8	486	224	163	
8	1958 7 8	0748	8 10. 9	8 21. 5	10 11	SSC*	A	116	2	-3 28	1 3	70	3	8	472	196	137	
9	1992 5 9	1958	10 03. 0	10 12. 1	12 07	SSC	A	101	2	12	1	55	2	7	426	209	109	
10	1960 11 12	1348	12 18. 2	13 10. 4	14 23	SSC	A	41	3	13	3	27	3	8	417	239	252	
11	1960 4 30	1213	30 12. 8	30 18. 8	01 20	SSC*	A	124	2	-2 62	0 2	47	2	8	380	150	174	
12	1991 11 8	0648	8 13. 3	9 08. 9	10 03	SSC	A	15	2	5	2	8	3	7	372	237	159	
13	1972 8 5	1400	5 19. 9	6 08. 7	07 18	SSC	B	54	3	16	3	35	3	9	359	332	230	
14	1990 4 9	0843	9 09. 6	9 12. 0	11 24	SSC	A	24	2	12	2	14	2	7	354	122	98	
15	1982 9 21	0339	21 22. 3	22 06. 6	23 21	SSC*	A	-2 39	1	-3 25	1	-1 16	1	7	341	175	129	
	1978 8 27	0246				SSC	A	27	4	10	3	14	4	7	341	146	127	
17	1991 7 8	1636	9 06. 2	9 11. 9	10 14	SSC	A	146	2	36	2	82	3	7	340	158	143	
18	1983 2 4	1615	4 17. 1	5 09. 5	06 20	SSC	A	92	1	23	2	50	2	8	335	168	125	
19	1961 7 13	1113	13 14. 6			SSC	A	53	4	21	3	31	4	7	334	99	132	
20	1959 7 17	1636	17 18. 2	18 07. 0	19 19	SSC	A	100	5	25	4	76	5	7	330	236	183	

occurrence number of SSCs will be possibly larger in the coming solar cycle 23 than the cycle 22.

Since there are many events reported so far, it is worth to examine the statistical features of the reported geomagnetic storms. One-minute magnetic data at KAK, MMB and KNY have been stored since 1976, 1985 and 1985, respectively, almost without data missing. There have been also one-minute magnetic data at an unmanned station, Chichijima (CBI) since 1989. Geographic and geomagnetic coordinates at these stations are listed in Table 2. Declination gap is the difference of the direction of the geomagnetic dipole meridian from that of the local geomagnetic north. Here, a superposed epoch analysis for SSC storms is made using the one-minute data at KAK and MMB similarly as Tsunomura (1995) and Tsunomura (1998). The data are converted to the geomagnetic dipole coordinate system at first and then a monthly diurnal variation pattern obtained by averaging the data

in the international five quiet days in each month is excluded. Figs. 2 and 3 show average variation patterns of geomagnetic storms at KAK from 1976 to 1992 and MMB from 1985 to 1992, respectively. The pattern is derived superposing SSC storms arranging to the onset of their SSCs; in the figure, the SSC is arranged at two hours after the start of each graph. The length of each graph is 48 hours in time and the vertical bars in the left indicate 20 nT magnetic variation. The number in the rightmost is that of the events stacked.

For both stations, the H-component shows a sharp increase immediately followed by a decrease with the time range of nearly two days and the D-component is almost flat. The pattern of the H-component reveals the average pattern of SSC and the succeeding development of the ring current, like the variation form usually observed. On the other hand, the pattern of the D-component is far from that of the actually observed; large disturbance fields are appeared superposing on

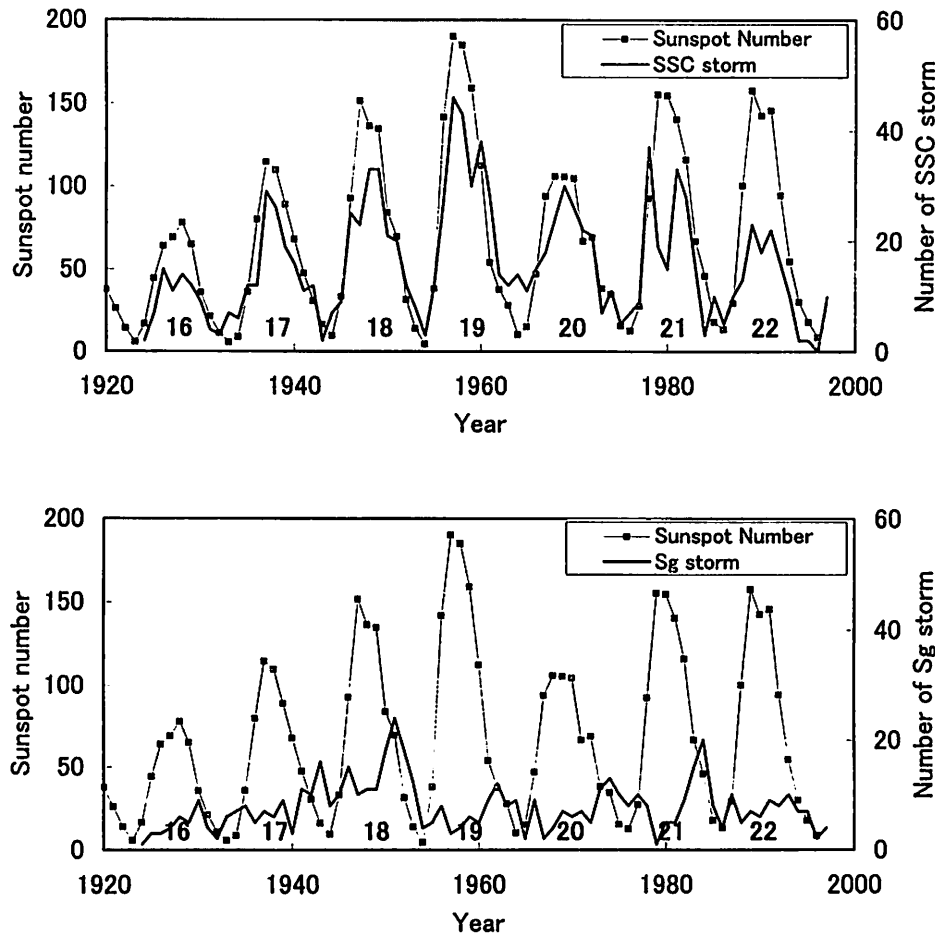


Fig. 1 Time variation of the occurrence numbers of SSC (upper panel) and Sg geomagnetic storms (lower panel) reported by the Kakioka Magnetic Observatory. The time variation of the sunspot number is shown for comparison; the solar cycle numbers are shown at the bottom. Note that the criteria to classify a storm have not been completely constant for all the period.

the Sq in the D-component during storm periods. The fact that the average pattern of the D-component is almost flat possibly reveals that the disturbance field in the storm field is a cyclic variation with local time or a completely random one for the D-component. Note that the SD field of the eastward component shows a sinusoidal variation (Sugiura and Chapman, 1960). This is different from the situation for the H-component for which the effect of the ring current acts

like a bias for all the local times.

The Z-component variations at both stations look quite different for the SSC and the succeeding period of nearly half a day. They show similar pattern for the period after about a half day after the SSC. For a time varying magnetic field the origin of which is located outside the Earth (external origin), the Z-component suffers the shielding effect of the conducting Earth. Meanwhile, the secondary Z-component magnetic field

Table 2 The Japanese geomagnetic observatories used in this paper.

Station Name	Abbreviation	Geographic		Geomagnetic		Declination Gap (degree)
		Latitude (Degree)	Longitude (Degree)	Latitude (Degree)	Longitude (Degree)	
Memambetsu	MMB	43.90	144.20	34.93	210.78	16.0
Kakioka	KAK	36.23	140.18	26.94	208.29	13.5
Kanoya	KNY	31.42	130.88	21.44	200.35	10.0
Chichijima	CBI	27.15	142.30	18.11	211.30	9.7

* The values are reprinted from World Data Center C2 for Geomagnetism DATA CATALOGUE (1996).

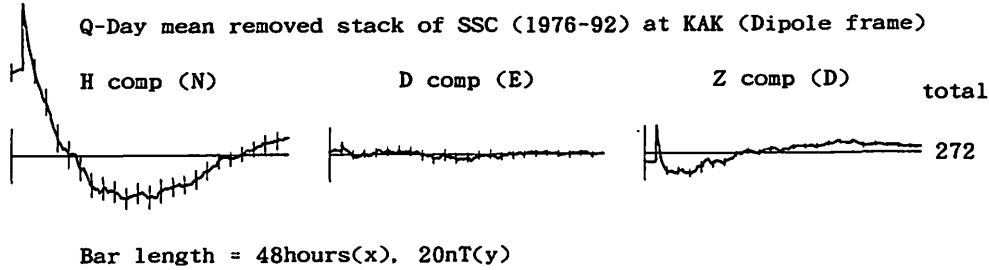


Fig. 2 The average magnetic variation of geomagnetic storms starting with SSC at KAK from 1976 to 1992. The length of each graph is 48 hours in time and the length of the bar at the left corresponds to 20 nT magnetic variation. The number in the right is that of the events to take the average. The bars on each graph denote standard errors.

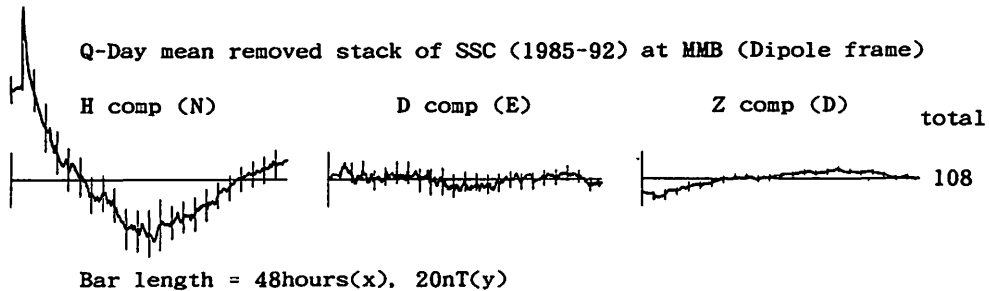


Fig. 3 The average magnetic variation of geomagnetic storms starting with SSC at MMB from 1985 to 1992. The style of the figure and the meanings of numbers are same as Fig. 2.

is produced by electromagnetically induced Earth-currents, which flow under the ground. This Z-component variation appears if the distribution of the Earth-current is inhomogeneous due to the anomaly of the electrical conductance under the observation site (e.g. Rikitake and Honkura, 1985, pp. 201 or 297). The rapid increase of the Z-component at KAK corresponding to the SSC is due to the CA effect which definitely appears at KAK (Yanagihara, 1965, 1972; Yanagihara and Nagano, 1976; Fujita, 1990; Fujiwara and Toh, 1996). The gradual variation for the later part in the Z-component, similarly seen for both the stations, is thought to denote the direct contribution of the ring current, which is not perfectly reduced by the Earth's electromagnetic induction. This situation is briefly illustrated in Fig. 4. For the case of the ring current, the ratio of the internal field to the external one can be roughly estimated by solving the following equations (Rikitake and Sato, 1957),

$$\begin{aligned}\Delta X &= -(e_1 + i_1) \cdot \sin \theta, \\ \Delta Z &= (e_1 - 2i_1) \cdot \cos \theta,\end{aligned}\quad (1)$$

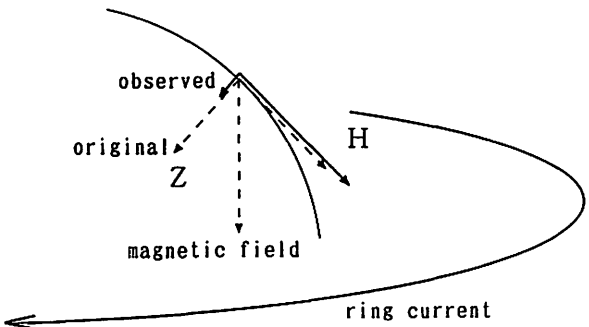


Fig. 4 Illustration of the modulation of the ring current magnetic field due to the Earth's induction.

where ΔX and ΔZ are the excursions of the H- and Z-components for the gradual variation, e_1 and i_1 the external and internal components of the first degree zonal harmonics for the corresponding magnetic potential and θ colatitude. The ratios of the internal to external potential strength thus obtained are 0.35 at both of KAK and MMB; this is nearly the same as the value, 0.37-0.39, derived from a case study by Rikitake and Sato (1957). Hence, the gradual variation of the Z-component most likely reveals the time variation of the ring current. That is apparent only for the later half of the curve at KAK (Fig. 2), whereas soon after the SSC

at MMB (Fig.3); this is because the CA effect is small at MMB. In the Z-component at MMB, variations due to the CA effect for SSCs and/or bay disturbances do not largely appear in usual.

If one can exclude the effect of the Sq , therefore, the Z-component at MMB can be used as one of the realtime monitoring tools to estimate the ring current strength. However, before using the Z component at MMB to discuss the long-term variation of the ring current strength, it is necessary to exclude the effect of the secular variation of the internal origin of the Earth. One of the methods to evaluate the secular variation of the internal field on the ground is to calculate the magnetic field using the DGRF and IGRF models. Time changes of the difference of the observed horizontal, vertical and total intensities and declination at KAK from those calculated using the DGRF and IGRF models to the tenth degree (Barton, 1997) are shown in Fig. 5. There can be seen large time changes in the figure except for the H-component. This may be due to the situation that the quality of the DGRF and IGRF coefficients, which basically depends on the number of the observation points to derive them, have not been constant for the long time period. Fujiwara et

al. (1998) reported that a finer resolution is necessary to discuss the long-term change of the F-component around Japan. The F-component is very much correlated with the Z-component as can be seen in the figure. It should be necessary to develop more accurate method to estimate the internal field contribution for the secular variation of the Z-component, before discussing the long-term variation of the external origin in the Z-component.

To see the variation forms of the SSC storm in another viewpoint, stacked records of SSC storms at KAK divided for eight local time blocks are shown in Fig. 6. Each graph is the average of the SSC storms whose onset is in the time range denoted in the leftmost. The onset is situated after two hours from the start of each graph in the figure. The length of each graph is 24 hours and the vertical bars in the left indicate 50 nT magnetic variation. The number in the rightmost is that of the events stacked. The H-component shows nearly the same variation forms with a slight difference due to a diurnal pattern being positive in the morning and negative in the evening. It can be seen a clearer diurnal pattern in the D-component; positive from the premidnight to the early

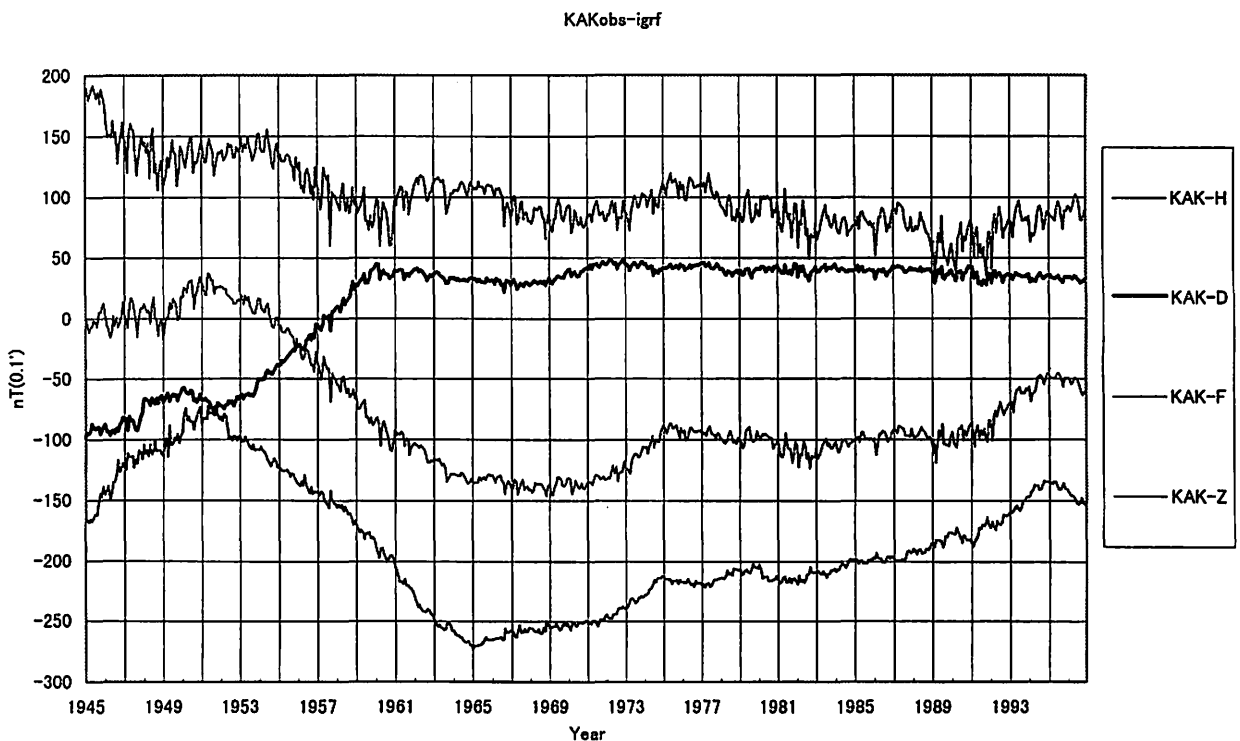


Fig. 5 Secular variation of the differences of the observed monthly means of horizontal intensity (KAK-H), declination (KAK-D), vertical intensity (KAK-Z) and total intensity (KAK-F) at KAK from the calculated values using DGRF and IGRF model fields. Note that the unit for KAK-D is different from those for others.

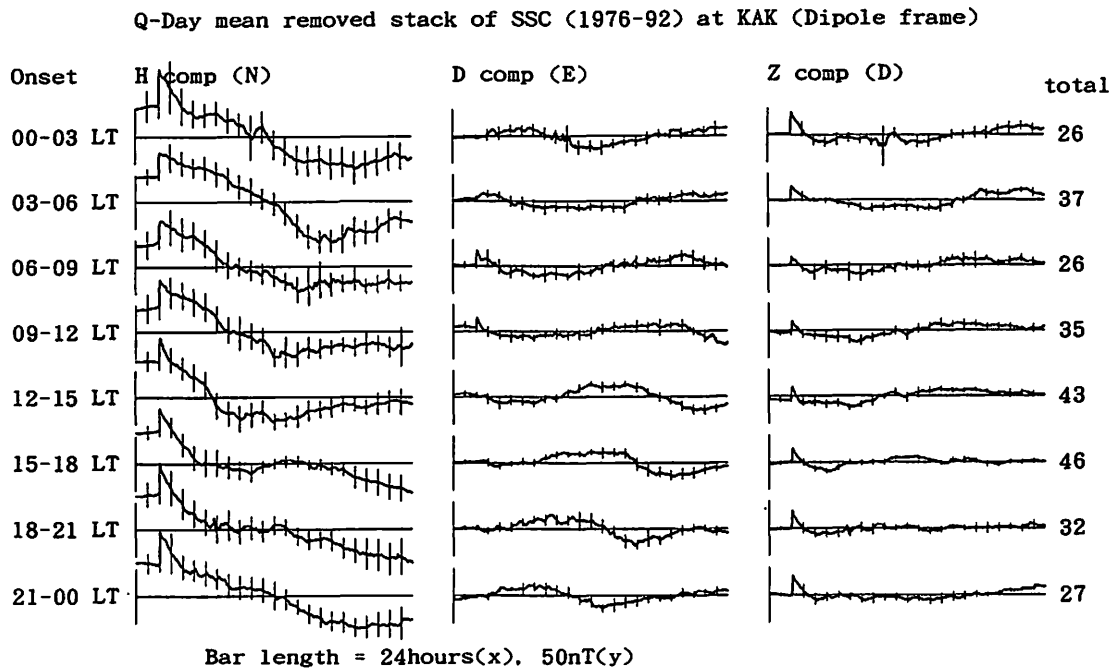


Fig. 6 Average magnetic variations of geomagnetic storms started with SSC at KAK from 1976 to 1992. The data are divided to eight local time blocks. The length of each graph is 24 hours in time and the length of the bar at the left corresponds to 50 nT magnetic variation. The number in the right is that of the events to take the average. The bars on each graph denote standard errors.

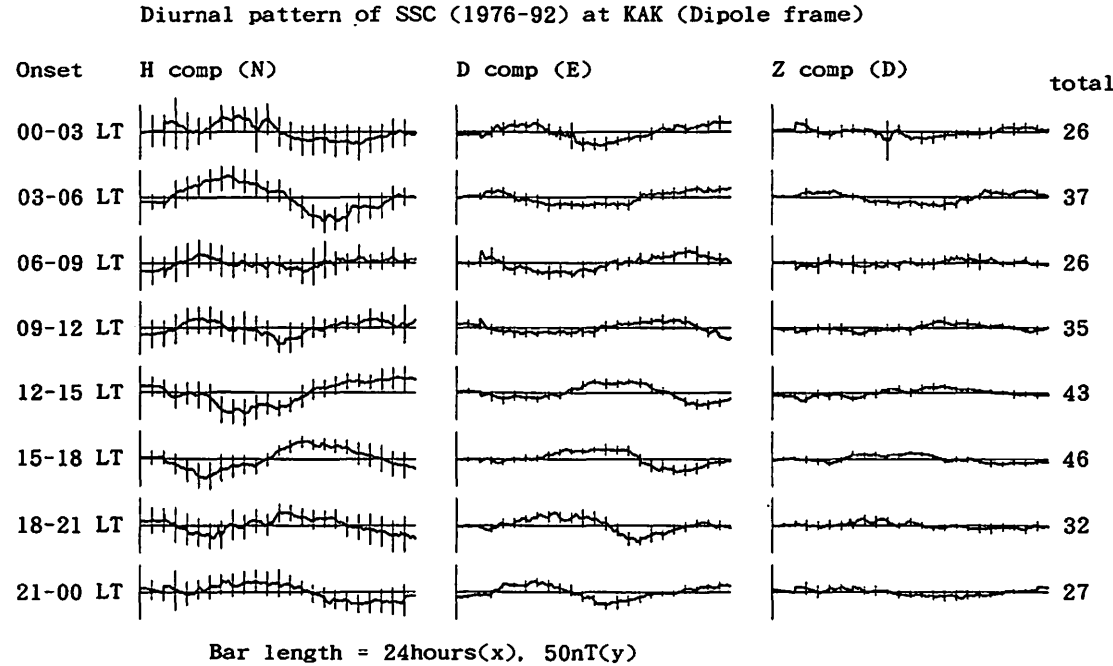


Fig. 7 Average diurnal variations during geomagnetic storms started with SSC at KAK from 1976 to 1992. The plot style is the same as that of Fig. 6.

morning and negative from the late morning to the evening. Fig. 7 shows the average diurnal variation patterns by subtracting the all-day means (shown in

Fig. 2) from the values in Fig. 6. Here, the diurnal variation patterns are clearly seen in all the components. The amplitude of the diurnal variation in

the H-component is larger than that of the D-component. These diurnal patterns are thought to be different from those of the solar diurnal variation because they are not apparent before the SSC; the patterns are similar to those of the SD fields of geomagnetic storm shown by Sugiura and Chapman (1960). It is expected that these diurnal variation patterns are most likely attributed to the field-aligned and the ionospheric currents' effects during geomagnetically disturbed periods.

There is an interaction between the ionosphere and the magnetosphere as a response to the impressed electric field from the solar wind. The magnetospheric electric field is reduced in the low latitude ionosphere by the shielding effect due to the electric charge produced in the Alfvén layer. The efficiency of the shielding effect depends on the time scale of the

phenomenon; the effect is apparent for the time-scale larger than about half an hour (Senior and Blanc, 1984). Kikuchi et al. (1996) discussed the penetration of the polar-originating DP2 electric field to low latitudes considering the shielding mechanism. In a storm period, when the magnetospheric convection is enhanced and the strength of the region 1 field-aligned current is enhanced, that of the region 2 field-aligned current will also be enhanced accordingly. The diurnal variation patterns of the H- and D-components possibly reveal the magnetic effects due to the combined effects of the enhanced field-aligned currents and the resulting ionospheric current systems. It is worth to examine whether the observed diurnal variation patterns are reproduced theoretically.

Fig. 8 is a copy of Fig. 7 of Tsunomura (to be published) showing local time profiles of the D- and

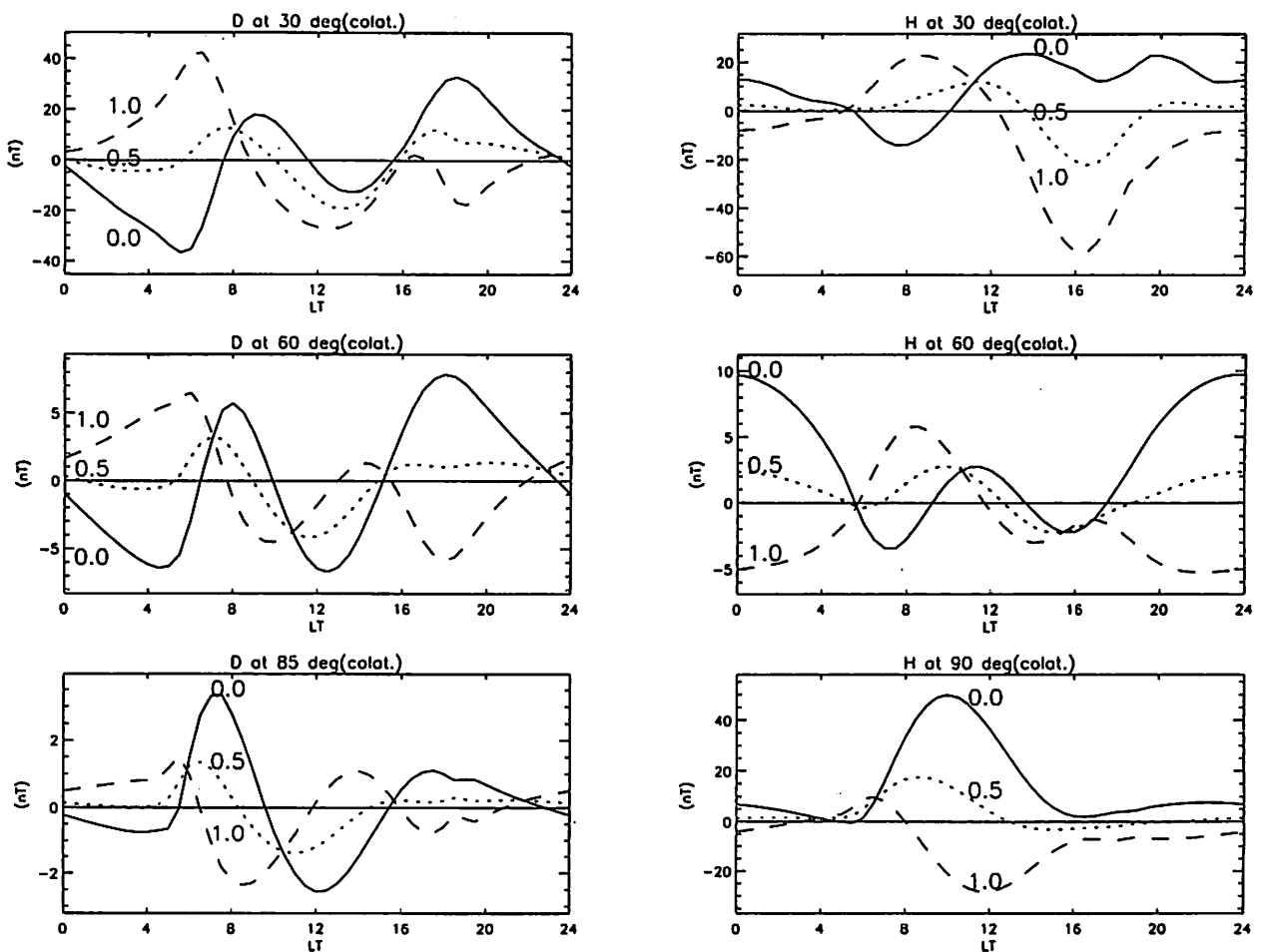


Fig. 8 Local time profiles of the D- (left panels) and H- (right panels) components of the magnetic fields at 60° , 30° latitudes and the equator calculated for three models of the source current composition. Solid, dotted and dashed lines are for the results with the ratio of the region 2 current intensity 0.0, 0.5 and 1.0 to that of the region 1 current, respectively as labeled on each curve.

H-components at 60°, 30° latitudes and the equator derived from a numerical simulation. The values shown in the figure are the ones obtained from the overhead ionospheric current and the field-aligned currents. The ionospheric current contribution at the equator is derived through the calculation by Biot-Savert's law for the electric current flowing in the narrow region of the equatorial electrojet. The figure shows the values putting the total strength of the region 2 field-aligned current as 0.0 (solid), 0.5 (dotted) and 1.0 (dashed) of that of the region 1 field-aligned current, respectively. The distribution of the field-aligned current density is given based on those in the quiet period shown by Iijima and Potemra (1976). Negative daytime fields are seen in the H-component at the equator (bottom right) for the curve of the ratio of 1.0; that means the strength of the shielding field is nearly twice as large as that of the original field. Thinking of the mechanism of the shielding, it is decided that the ratio of 1.0 is too large. It is noteworthy that the SD variations in the H-component do not show the equatorial enhancement as shown by Sugiura and Chapman (1960). The ratio of the strength of the region 2 field-aligned current to that of the region 1 was estimated nearly half in the steady state of Senior and Blanc's (1984) simulation. Considering these, the ratio of 0.5 is expected to describe the storm time signature best.

However, the curves for the ratio of 0.5 in the middle panels (for 30° latitude) do not match those of Fig. 7; the diurnal patterns are not clearly seen in Fig. 8. The difference in the amplitudes between the H- and D-components are not also apparent in Fig. 8. The simulation needs some modifications to explain the observed features. Crooker and Siscoe (1981) suggested a simple model which twists the double rings of the region 1 and 2 field-aligned current systems, to explain the low latitude asymmetric disturbance fields. In their model there appears an equivalent anti-sunward current in the noon-midnight meridian, which mainly contributes the asymmetry of the H-component during the developing stage of geomagnetic storms. By a rough estimation, the field-aligned currents suggested by Crooker and Siscoe (1981) give diurnal patterns in the low latitude magnetic fields. Iyemori (1990) showed that the similar current system is apparent during the main phase of geomagnetic storms. A numerical calculation

taking into account of the relative shift of the region 1 and 2 field-aligned currents and the partial ring current system should be made in future.

3. Variation forms of geomagnetic storms

In the previous section, the average magnetic variation patterns were shown and it is shown that they can be attributed to the contribution of the field-aligned currents and the resulting ionospheric current systems. However, it should be noted that the diurnal patterns shown in Figs. 6 and 7 are only the averages. The actual individual event must have some features different from the average pattern. One of the most pronounced events showing a characteristic variation pattern is the SSC storm of March 24, 1991. The morphology of the SSC of this event was precisely examined by Araki et al. (1997) and briefly by Tsunomura (1998) but is not fully understood. The study of each event, especially for large events such as those of March 24, 1940, July 04, 1941, February 11, 1958, August 05, 1972 and July 13, 1982, remains to be important to clarify the process of geomagnetic storms precisely.

Fig. 9 is a scatter plot of the ranges of the D-component against those of the H-component for the geomagnetic storms reported at KAK since the IGY. Although the ranges for the H- and D-components are controlled by different sources, these ranges show some relationship (the correlation coefficient is 0.43). It can be seen that there is an event with extremely

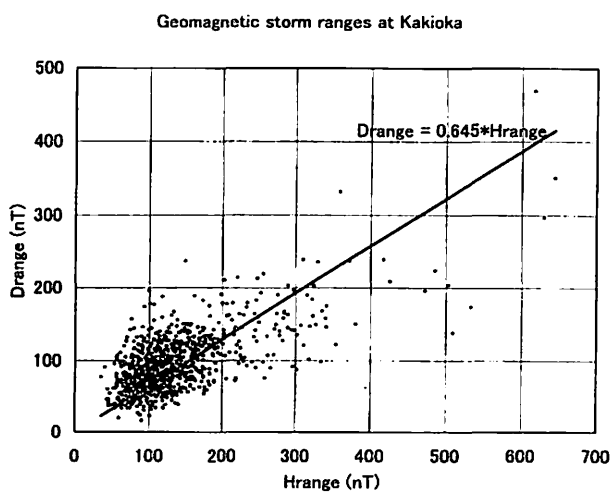


Fig. 9 Scatter plot of the ranges of the D-component vs. those of the H-component for the geomagnetic storms observed at KAK from 1957 to 1997.

large D-component range. This is the geomagnetic storm of February 11, 1958 whose range of the D-component is 469 nT, as listed in Table 1. This event was the famous one because an intense low latitude aurora was observed in Hokkaido district during its main phase ('REPORT OF THE AURORAS OBSERVED AT MEMAMBETSU THROUGH 1958 AND 1960', 1969; Tsunomura et al., 1990). The large-

scale equivalent currents originated in the polar region for this event were analyzed by Nagai (1964). Here, the variation form of this event observed at the Japanese stations is reexamined.

Fig. 10 shows the magnetic records at MMB, KAK and KNY for this event. Note that the upward direction is westward for the D-component in the figure. The hatched parts indicate the periods when the

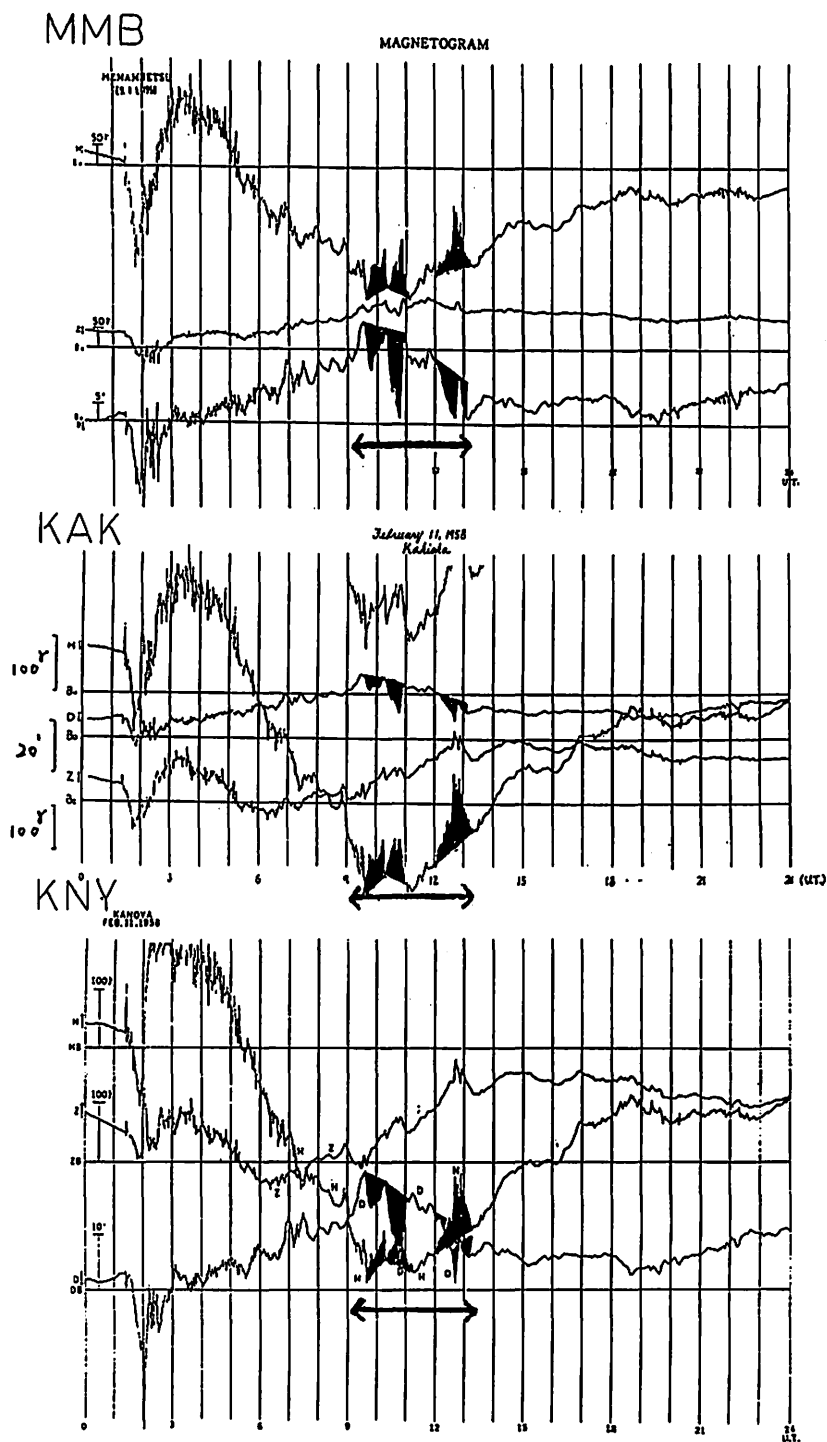


Fig. 10 Magnetic records at MMB, KAK and KNY for the geomagnetic storm of February 11, 1958. Note that the upward is westward for the D-component.

brightness of the low latitude aurora observed at MMB was enhanced (Tsunomura et al., 1990). It is noted that the variation form of the SSC in the H-component is quite different from the average form of SSCs; a rapid negative impulse followed immediately after the onset of the SSC. It can be inferred that this variation form manifests the signature of the D_{MI} -field in this area as suggested by Tsunomura (1998). It is also interesting that a negative variation with the duration of about one hour appeared just after the SSC in the H-component; the variation looks like a negative bay usually observed in high latitudes. A similar negative-bay-like variation was observed just after the SSC of March 24, 1991. These negative bay events may be one of the future subjects to be clarified. The long-term D-component variation is roughly parallel to the average variation pattern shown in Figs. 6 and 7, whereas a rapid variation corresponding to the negative bay in the H-component above mentioned is not included in the average pattern. The rapid variation contributes to make the range of the D-component very large. Therefore, the large D-component range for this event did not indicate only the enhanced magnetospheric convection. As this case shows, the full understanding of geomagnetic storms cannot be achieved without precise investigations of each event in the future analysis.

4. Concluding Remarks

In this paper, average variation patterns of SSC geomagnetic storms is presented by making a superposed epoch analysis of one-minute magnetic data at KAK and MMB. It was shown that the gradual time variation pattern in the Z-component reveals the direct contribution of the time change of the ring current. It is imagined that the Z-component at MMB can be used as one of the monitoring tools to estimate the ring current strength. After roughly checking the geomagnetic secular variations at Kakioka, it is very difficult to exclude the internal origin from the secular variation of the Z-component, which is necessary before examining long-term variations.

It is shown that the diurnal variation patterns are seen in the H- and D-components in the storm time. The patterns are basically the same as those of the SD fields of geomagnetic storm shown by Sugiura and Chapman (1960). The derived patterns are compared with the results of a numerical calculation but did not

match sufficiently. Calculations taking into account of the modified distribution of region 1 and 2 field-aligned currents suggested by Crooker and Siscoe (1981) and the partial ring current system should be operated in future.

Case studies remain to be important to discuss the process of geomagnetic storm. A brief case study for a geomagnetic storm with a large D-component range shows that the D-component range for the storm was enhanced due to the magnetic variation associated with a negative bay in the H-component in the daytime. The plots of magnetic records in Japanese stations for large geomagnetic storms from 1985 to 1997 were presented for the use of further studies and as a catalogue for the watching of geomagnetic storms, prepared for the coming solar maximum period of the solar cycle 23.

Appendix

The plots of the magnetic records at MMB, KAK, KNY and CBI for the geomagnetic storms from 1985 to 1997 with a range of the H-component at KAK larger than 150 nT are shown in Figs. A-1 to A-79. The start time, type and the ranges in the H-, D- and Z-components of the storms are listed in Table A-1. The type 'SSC*' means the SSC for the storm is preceded by a preliminary impulse. This set will be available as a catalogue of geomagnetic storm, prepared for the coming high-activity period of the solar cycle 23, where it is predicted that the maximum sunspot number will be in the range of 160 ± 30 (Joselyn et al., 1997).

Acknowledgments

The computer readable file for the list of SSC and Sg was based on that made by Okamoto and Fujita (1987). This study can be made using the long lasting magnetic data accumulated through the efforts of the colleagues of Kakioka Magnetic Observatory and its branch offices at Memambetsu and Kanoya.

References

- Araki, T., S. Fujitani, M. Emoto, K. Yumoto, K. Shiokawa, T. Ichinose, H. Luehr, D. Orr, D. K. Milling, H. Singer, G. Rostoker, S. Tsunomura, Y. Yamada, and C. F. Liu, Anomalous sudden commencement on March 24, 1991, *J. Geophys. Res.*, 102, 14075-14086, 1997.
- Barton, C. E., International geomagnetic reference

- field: The seventh generation, *J. Geomag. Geoelectr.*, 49, 123-148, 1997.
- Crooker, N. and G. L. Siscoe, Birkeland currents as the cause of the low-latitude asymmetric disturbance field, *J. Geophys. Res.*, 86, 11201-11210, 1981.
- Fujita, S., Monitoring of time changes of conductivity anomaly transfer functions at Japanese magnetic observatory network, *Mem. Kakioka Mag. Obs.*, 23, 53-87, 1990.
- Fujiwara, S. and H. Toh, Geomagnetic transfer functions in Japan obtained by first order geomagnetic survey, *J. Geomag. Geoelectr.*, 48, 1071-1101, 1996.
- Fujiwara, S., T. Tanabe, S. Nishi, S. Matsuzaka, V. Golovkov, and S. V. Filippov, Modeling of the geomagnetic total force changes in Japan and the far east, 'Proceedings of CA research meeting 1998' published by CA research group in Japan, 9-16, 1998. (in Japanese)
- Iijima, T. and T. A. Potemra, The amplitude distribution of field-aligned currents at northern high latitudes observed by Triad, *J. Geophys. Res.*, 81, 2165-2174, 1976.
- Itonaga, M., T.-I. Kitamura, O. Saka, H. Tachihara, M. Shinohara, and A. Yoshikawa, Discrete spectral structure of low-latitude and equatorial Pi2 pulsation, *J. Geomag. Geoelectr.*, 44, 253-259, 1992.
- Itonaga, M., K. Matsuzono, T.-I. Kitamura, I. Toshimitsu, N. B. Trivedi, R. Horita, T. Watanabe, and J. Riddick, Global structure of low-latitude and equatorial geomagnetic pulsations associated with sudden commencements, *J. Geomag. Geoelectr.*, 47, 441-457, 1995.
- Joselyn, J. A., J. B. Anderson, H. Coffey, K. Harvey, D. Hathaway, G. Heckman, E. Hildner, W. Mende, K. Schatten, R. Thompson, A. W. P. Thompson, and O. R. White, Panel achieves consensus prediction of solar cycle 23, *EOS Trans. AGU*, 78, 205, 211-212, 1997.
- Kikuchi, T., H. Lühr, T. Kitamura, O. Saka, and K. Schlegel, Direct penetration of the polar electric field to the equator during a DP2 event as detected by the auroral and equatorial magnetometer chains and the EISCAT radar, *J. Geophys. Res.*, 101, 17161-17173, 1996.
- Nagai, M., On the geomagnetic storm on February 11, 1958, *Mem. Kakioka Mag. Obs.*, 11, 39-53, 1964.
- Nagai, M., Characteristics of the geomagnetic storms based on the statistical analysis, *Mem. Kakioka Mag. Obs.*, 20, 17-38, 1983. (in Japanese)
- Okamoto, A., and S. Fujita, Statistics on the geomagnetic phenomena observed at Kakioka, *Mem. Kakioka Mag. Obs.*, 22, 21-42, 1987.
- REPORT OF THE AURORAS OBSERVED AT MEMAMBETSU THROUGH 1958 AND 1960, in REPORT OF THE GEOMAGNETIC AND GEOELECTRIC OBSERVATIONS 1967 (RAPID VARIATIONS), pp. 107-130, published by Kakioka Magnetic Observatory, 1969.
- Rikitake, T., and Y. Honkura, "Solid Earth Geomagnetism", *Developments in Earth and Planetary Sciences 05*, Terra Scientific Publishing Company, Tokyo, Japan, 1985.
- Rikitake, T. and S. Sato, The geomagnetic Dst field of the magnetic storm on June 18-19, 1936, *Bull. Earthq. Res. Inst., Univ. Tokyo*, 35, 7-21, 1957.
- Russell, C. T., M. Ginskey, S. Petrinec and G. Lee, The effect of solar wind dynamic pressure changes on low and mid-latitude magnetic records, *Geophys. Res. Lett.*, 19, 1227-1231, 1992.
- Russell, C. T., M. Ginskey, and S. M. Petrinec, Sudden impulses at low-latitude stations: Steady state response for northward interplanetary magnetic field, *J. Geophys. Res.*, 99, 253-261, 1994a.
- Russell, C. T., M. Ginskey, and S. M. Petrinec, Sudden impulses at low latitude stations: Steady state response for southward interplanetary magnetic field, *J. Geophys. Res.*, 99, 13403-13408, 1994b.
- Senior, C. and M. Blanc, On the control of magnetospheric convection by the spatial distribution of ionospheric conductivities, *J. Geophys. Res.*, 89, 261-284, 1984.
- Sugiura, M. and S. Chapman, The average morphology of geomagnetic storms with sudden commencements, *Abh. Akad. Wiss. Göttingen, Math.-phys., Kl., Sonderheft, Spec. Issue 4*, 1-53, 1960.
- Takahashi, K., S.-I. Ohtani, and K. Yumoto, AMPTE CCE observations of Pi2 pulsations in the inner magnetosphere, *Geophys. Res. Lett.*, 19, 1447-1450, 1992.
- Tsunomura, S., On the polarity of SSC and SI observed in low latitudes, *Mem. Kakioka Mag. Obs.*, 26, 15-36, 1995.
- Tsunomura, S., Characteristics of geomagnetic sudden

- commencement observed in middle and low latitudes, *Earth Planets Space*, 50, 755-772, 1998.
- Tsunomura, S., Numerical analysis of global ionospheric current system including the effect of equatorial enhancement, *Ann. Geophys.*, to be published.
- Tsunomura, S., T. Uwai, Y. Yamada, K. Hasegawa, F. Fukui, S. Toyodome, and M. Kuwashima, Characteristics of geomagnetic variations associated with low latitude auroras, *Mem. Kakioka Mag. Obs.*, 24, 25-38, 1990.
- Vennerstrøm, S. and E. Friis-Christensen, Long-term and solar cycle variation of the ring current, *J. Geophys. Res.*, 101, 24727-24735, 1996.
- Yanagihara, K., Estimate of the deep layer resistivity near Kakioka, *Mem. Kakioka Mag. Obs.*, 12, 115-122, 1965. (in Japanese)
- Yanagihara, K., Secular variation of the electrical conductivity anomaly in the central part of Japan, *Mem. Kakioka Mag. Obs.*, 15, 1-11, 1972.
- Yanagihara, K. and T. Nagano, Time change of transfer function in the Central Japan Anomaly, *J. Geomag. Geoelectr.*, 28, 157-163, 1976.
- Yokouchi, Y., Principal magnetic disturbances at Kakioka, 1924-1951, *Mem. Kakioka Mag. Obs.*, 6, 204-253, 1953. (in Japanese)
- Yumoto, K and the 210° MM Magnetic Observation Group, Initial results from the 210° magnetic meridian project-Review, *J. Geomag. Geoelectr.*, 47, 1197-1213, 1995.
- Yumoto, K and the 210° MM Magnetic Observation Group, The STEP 210° magnetic meridian network project, *J. Geomag. Geoelectr.*, 48, 1297-1309, 1996.
- Yumoto, K., Y. Tanaka, T. Oguchi, K. Shiokawa, Y. Yoshimura, A. Isono, B. J. Fraser, F. W. Menk, J. W. Lynn, M. Seto, and 210° MM Magnetic Observation Group, Globally coordinated magnetic observations along 210° magnetic meridian during STEP period: 1. Preliminary results of low latitude Pc3's, *J. Geomag. Geoelectr.*, 44, 261-276, 1992.
- Yumoto, K., H. Osaki, K. Fukao, K. Shiokawa, Y. Tanaka, S. I. Solovyev, G. Krymskij, E. F. Vershinin, V. F. Osinin, and 210° MM Magnetic Observation Group, Correlation of high- and low-latitude Pi2 magnetic pulsations observed at 210° magnetic meridian chain stations, *J. Geomag. Geoelectr.*, 46, 925-935, 1994.
- Yumoto, K., H. Matsuoka, H. Osaki, K. Shiokawa, Y. Tanaka, T. Kitamura, H. Tachihara, M. Shinohara, S. I. Solovyev, G. A. Makarov, E. F. Vershinin, A. V. Buzevich, S. L. Manurung, O. Sobari, M. Ruhimat, Sukmadradjat, R. J. Morris, B. J. Fraser, F. W. Menk, K. J. W. Lynn, D. G. Cole, J. A. Kennewell, J. V. Olson, and S.-I. Akasofu, North/south asymmetry of sc/si magnetic variations observed along the 210° magnetic meridian, *J. Geomag. Geoelectr.*, 48, 1333-1340, 1996.

Table A-1 List of geomagnetic storms

No.	Year	Month	Day	UT	Type	Range		
						H	D	Z
A-1	1985	1	27	17.7	Sg	174	79	52
A-2	1985	2	27	19.8	Sg	156	74	60
A-3	1985	4	20	0310	SSC*	227	145	82
A-4	1985	4	26	02.0	Sg	158	75	60
A-5	1985	4	30	0923	SSC*	176	58	70
A-6	1985	11	29	0806	SSC	157	150	86
A-7	1986	2	6	1312	SSC	310	239	156
A-8	1986	9	11	1835	SSC	229	162	98
A-9	1986	11	3	2354	SSC	173	107	70
A-10	1988	1	13	2330	SSC*	189	130	68
A-11	1988	2	21	0156	SSC	159	122	70
A-12	1988	4	3	1637	SSC	190	123	84
A-13	1988	5	6	0428	SSC	229	99	88
A-14	1988	9	10	20.2	Sg	151	92	73
A-15	1988	10	10	0231	SSC*	231	104	96
A-16	1988	11	30	0800	SSC	170	85	73
A-17	1989	1	20	1232	SSC*	234	93	83
A-18	1989	3	13	0127	SSC*	644	351	205
A-19	1989	3	16	0533	SSC*	183	82	92
A-20	1989	3	26	2250	SSC*	177	129	98
A-21	1989	4	25	10.3	Sg	171	131	75
A-22	1989	5	7	0512	SSC*	176	89	63
A-23	1989	5	23	1346	SSC*	198	109	89
A-24	1989	6	8	1953	SSC	173	183	109
A-25	1989	8	14	0613	SSC*	203	211	138
A-26	1989	9	18	1028	SSC	283	158	92
A-27	1989	9	26	05.7	Sg	190	116	63
A-28	1989	10	20	0917	SSC	307	148	135
A-29	1989	11	17	0926	SSC*	252	193	82
A-30	1990	3	12	1503	SSC	169	126	80
A-31	1990	3	30	0721	SSC	219	111	73
A-32	1990	4	9	0843	SSC	354	122	98
A-33	1990	4	12	0326	SSC*	206	178	77
A-34	1990	4	17	0719	SSC	170	84	55
A-35	1990	6	12	0820	SSC*	182	175	107
A-36	1990	7	28	0331	SSC*	282	127	87
A-37	1990	8	26	0543	SSC	164	89	82
A-38	1990	10	9	11.9	Sg	174	101	82
A-39	1991	3	24	0341	SSC	503	204	199
A-40	1991	4	4	1122	SSC	153	76	75
A-41	1991	5	16	2041	SSC	188	123	74
A-42	1991	6	4	08.5	Sg	297	197	177
A-43	1991	6	9	0040	SSC	194	128	108
A-44	1991	6	12	1012	SSC	284	167	156
A-45	1991	7	8	1636	SSC	340	158	143
A-46	1991	7	13	00.5	Sg	194	129	89
A-47	1991	8	11	0253	SSC*	164	113	50
A-48	1991	8	18	1834	SSC	223	164	108
A-49	1991	8	20	0759	SSC*	217	143	93
A-50	1991	10	1	1813	SSC*	188	107	102
A-51	1991	10	28	1054	SSC	327	149	161
A-52	1991	10	31	1650	SSC*	152	137	89
A-53	1991	11	8	0648	SSC	372	237	159
A-54	1992	2	2	1153	SSC	156	117	96
A-55	1992	2	8	1428	SSC	250	152	117
A-56	1992	2	20	0109	SSC*	278	140	106
A-57	1992	2	26	1658	SSC	173	92	83
A-58	1992	5	9	1958	SSC	426	209	109
A-59	1992	9	9	0139	SSC*	210	111	82
A-60	1992	9	17	02.1	Sg	182	118	91
A-61	1992	9	28	12.0	Sg	182	132	81
A-62	1992	10	8	1839	SSC	153	77	76
A-63	1992	11	9	05.8	Sg	172	84	74
A-64	1992	12	27	2010	SSC	159	103	55
A-65	1993	2	17	0301	SSC*	172	72	60
A-66	1993	3	8	2138	SSC	177	125	85
A-67	1993	4	4	1434	SSC	245	141	99
A-68	1993	9	12	11.7	Sg	223	126	105
A-69	1993	10	8	23.4	Sg	163	73	73
A-70	1993	11	3	1756	SSC	171	86	70
A-71	1994	2	21	0901	SSC*	214	179	83
A-72	1994	4	16	19.6	Sg	294	142	113
A-73	1994	10	2	17.2	Sg	154	76	78
A-74	1994	10	29	0025	SSC*	175	126	110
A-75	1994	11	26	05.9	Sg	219	76	92
A-76	1995	3	26	04.7	Sg	169	64	49
A-77	1997	1	10	01.1	Sg	163	61	65
A-78	1997	5	15	0159	SSC	170	128	73
A-79	1997	11	22	0949	SSC	152	91	77

Magnetogram for 1985 Jan. 27-29

at Memambetsu(MMB), Kakioka(KAK), Kanoya(KNY)

Upward: increase(H), westward(D), downward(Z)

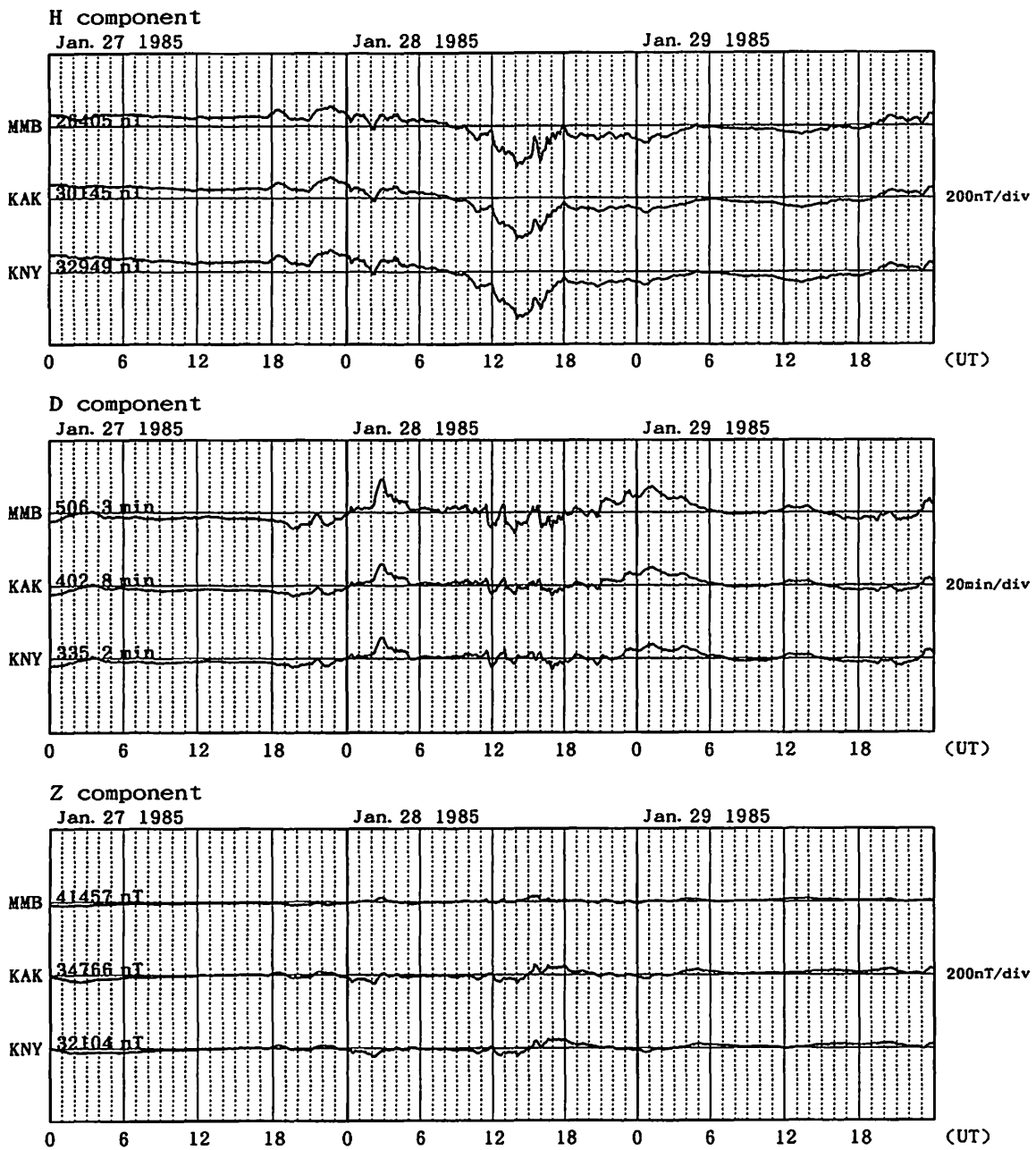


Fig. A-1 Magnetic records at MMB, KAK and KNY for the geomagnetic storm of January 27, 1985.

Magnetogram for 1985 Feb. 27-Mar. 01

at Memambetsu(MMB), Kakioka(KAK), Kanoya(KNY)

Upward: increase(H), westward(D), downward(Z)

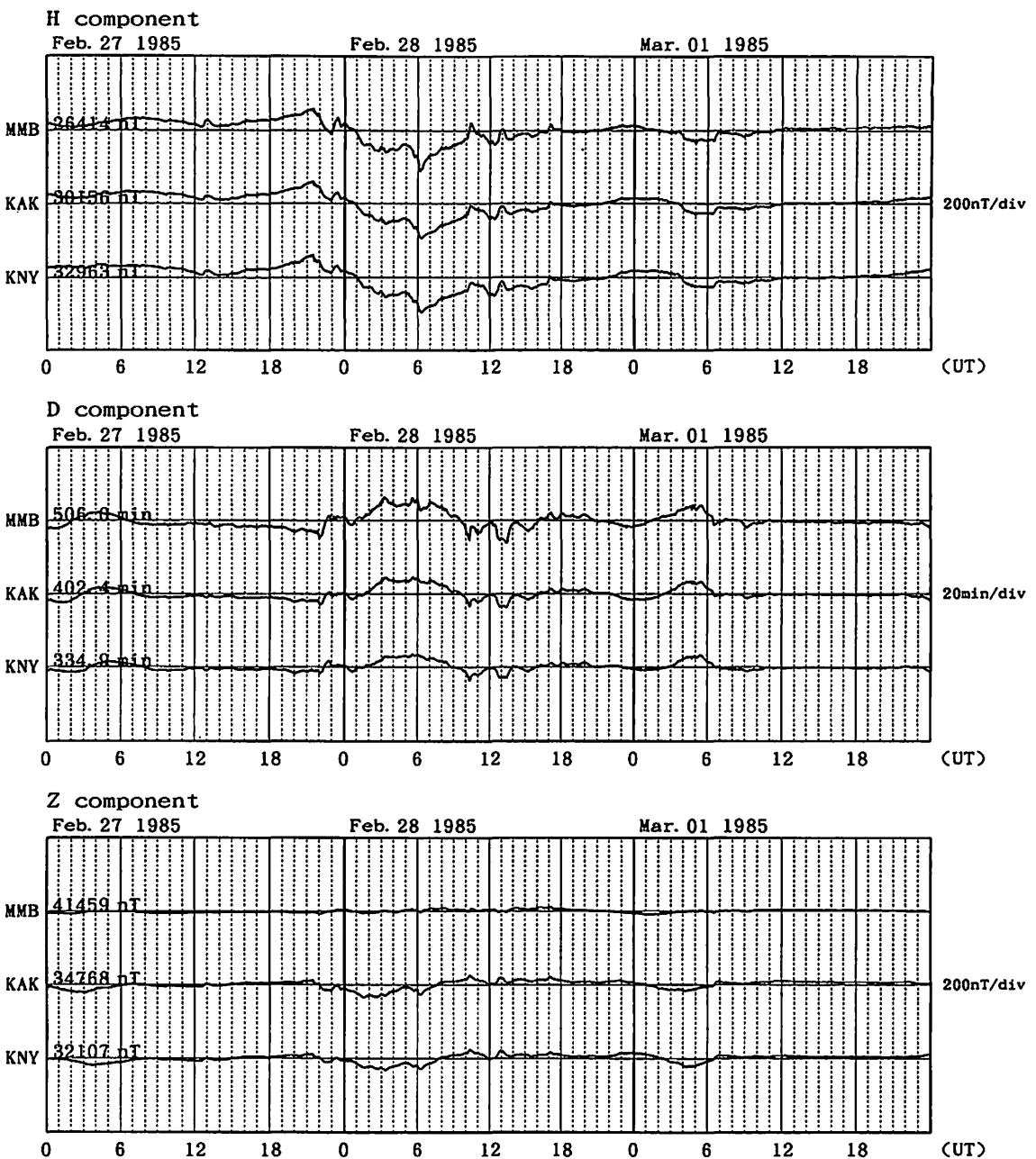


Fig. A-2 Magnetic records at MMB, KAK and KNY for the geomagnetic storm of February 27, 1985.

Magnetogram for 1985 Apr. 20-22

at Nemambetsu(MMB), Kakioka(KAK), Kanoya(KNY)

Upward: increase(H), westward(D), downward(Z)

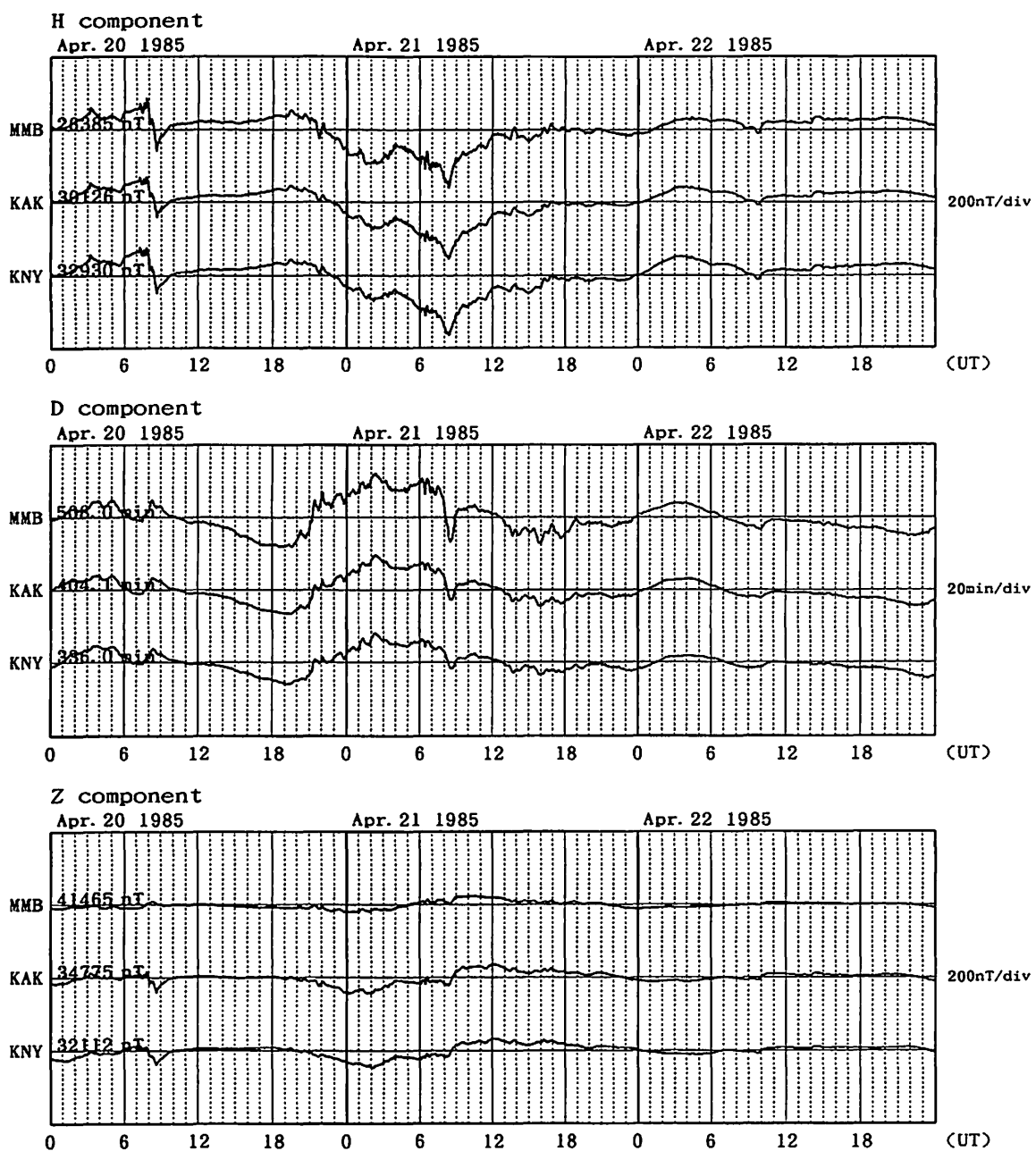


Fig. A-3 Magnetic records at MMB, KAK and KNY for the geomagnetic storm of April 20, 1985.

Magnetogram for 1985 Apr. 26-28

at Memambetsu(MMB), Kakioka(KAK), Kanoya(KNY)

Upward: increase(H), westward(D), downward(Z)

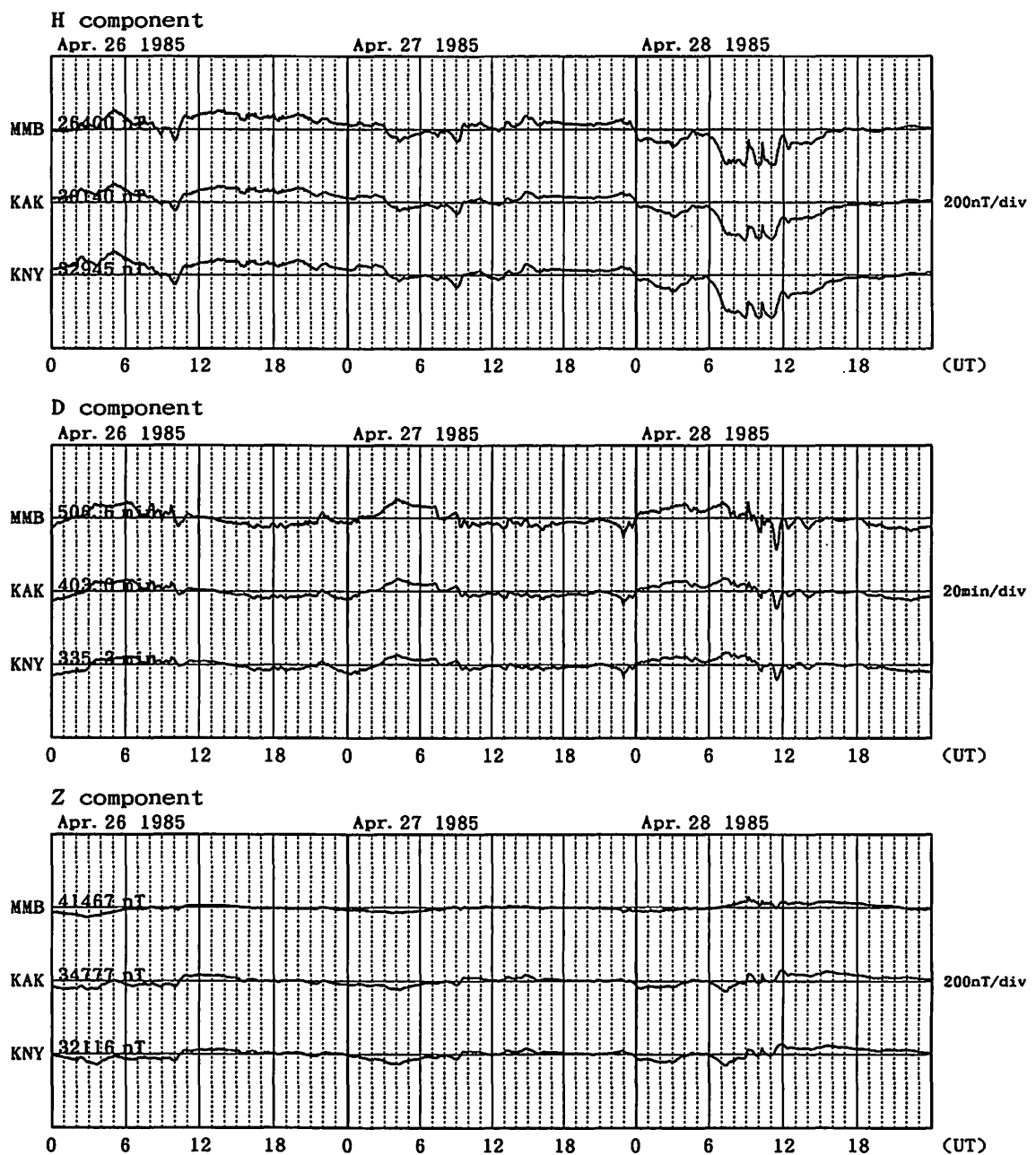


Fig. A-4 Magnetic records at MMB, KAK and KNY for the geomagnetic storm of April 26, 1985.

Magnetogram for 1985 Apr. 30-May 02

at Memambetsu(MMB), Kakioka(KAK), Kanoya(KNY)

Upward: increase(H), westward(D), downward(Z)

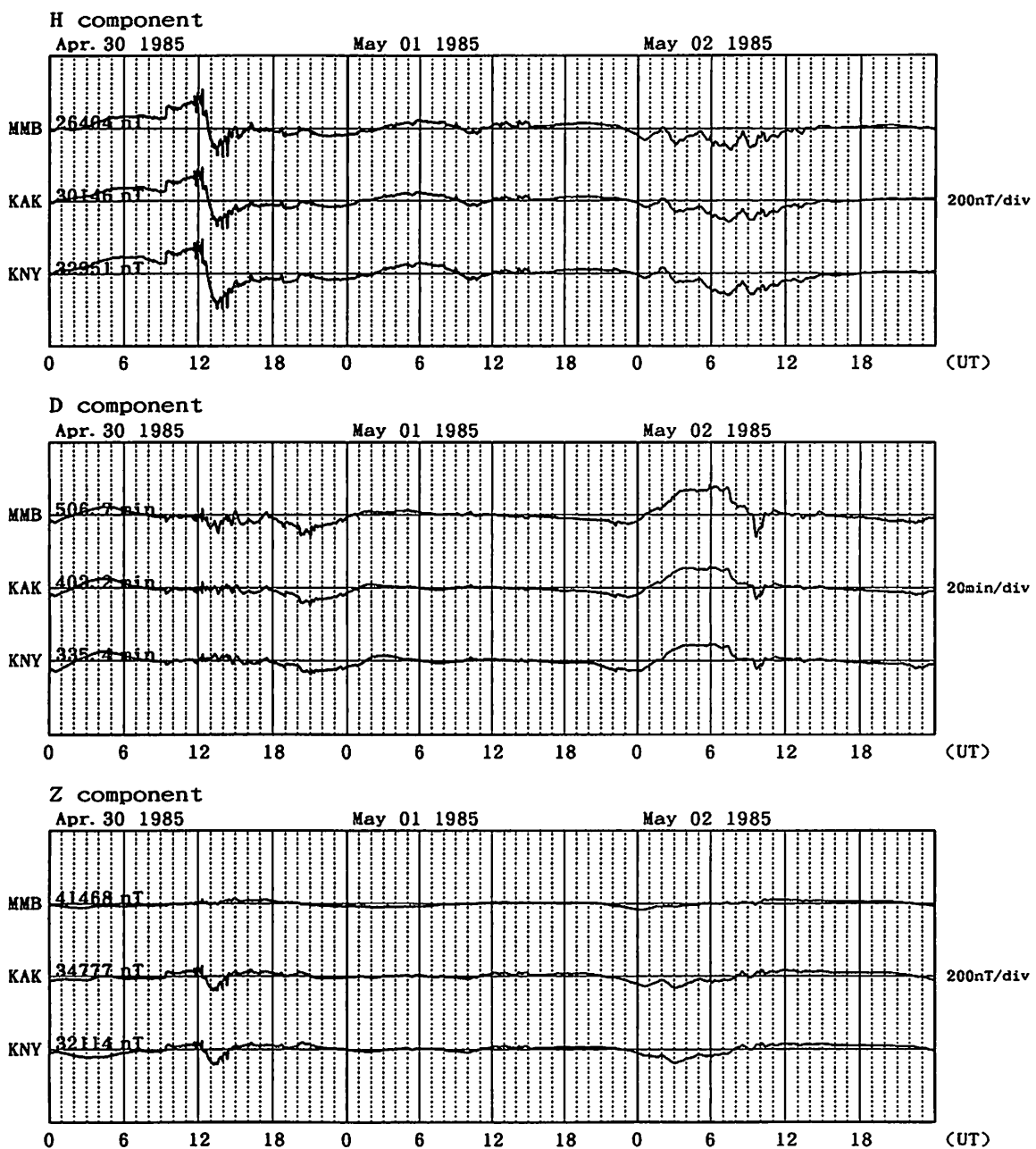


Fig. A-5 Magnetic records at MMB, KAK and KNY for the geomagnetic storm of April 30, 1985.

Magnetogram for 1985 Nov. 29-Dec. 01

at Memambetsu(MMB), Kakioka(KAK), Kanoya(KNY)

Upward: increase(H), westward(D), downward(Z)

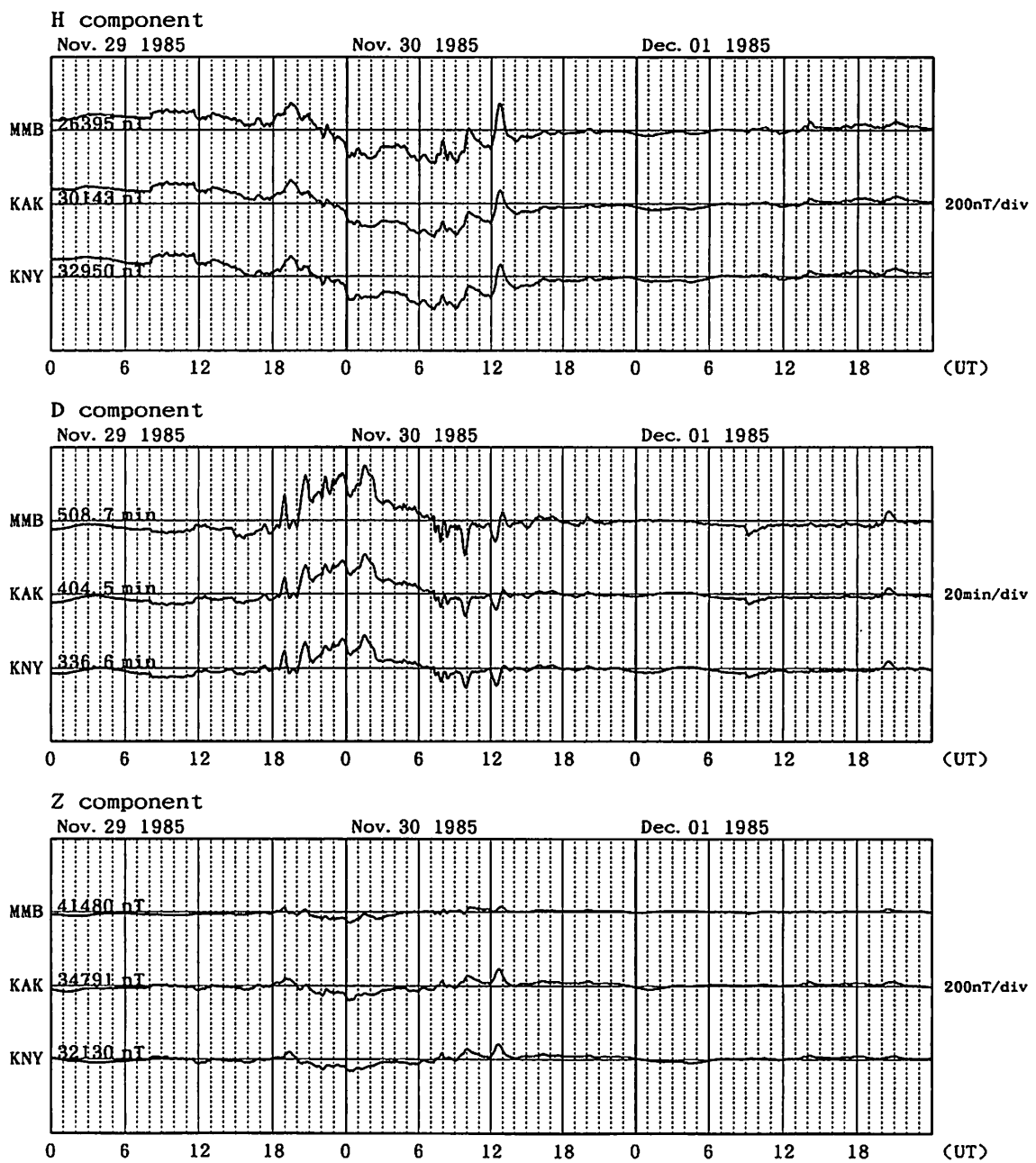


Fig. A-6 Magnetic records at MMB, KAK and KNY for the geomagnetic storm of November 29, 1985.

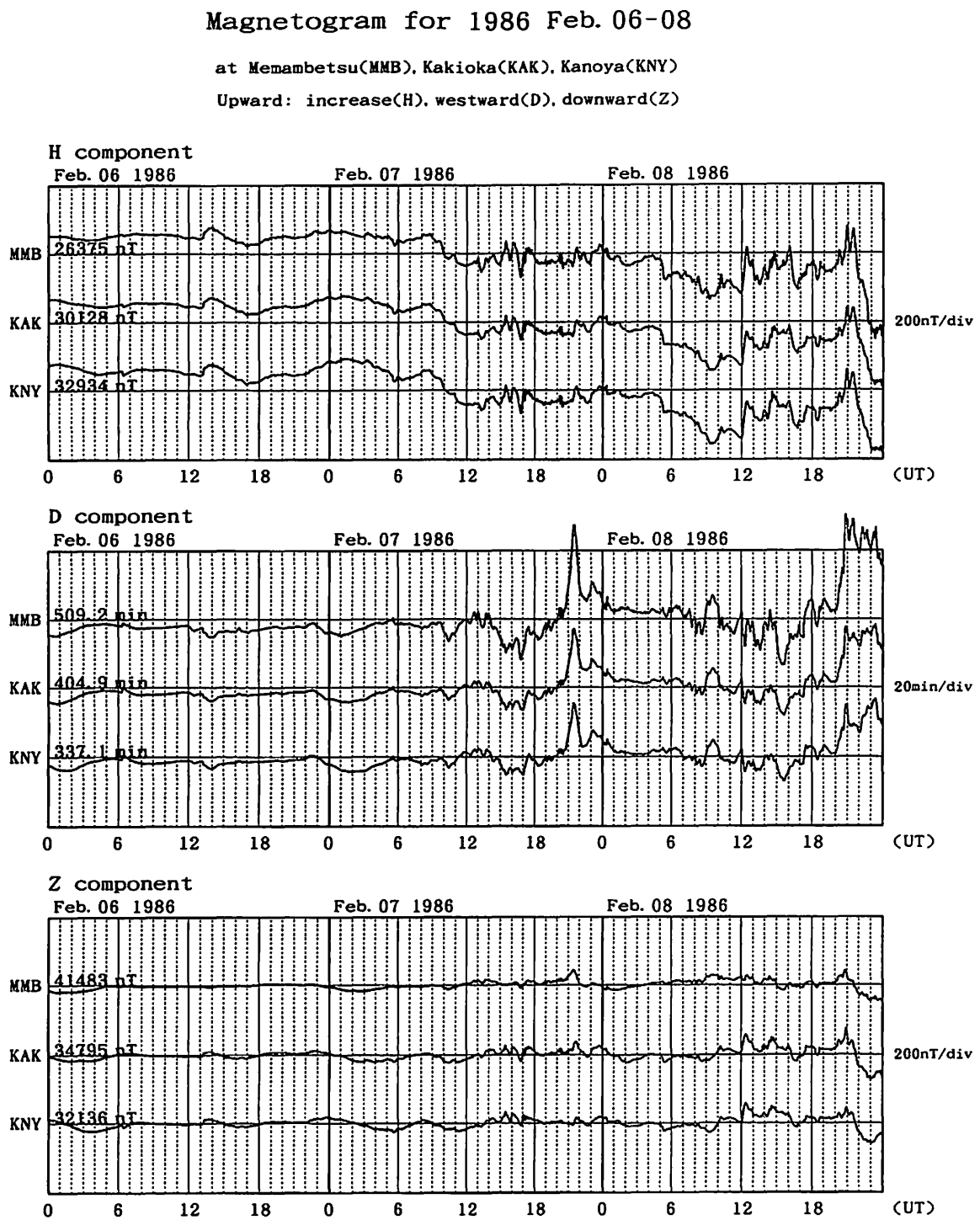


Fig. A-7(a) Magnetic records at MMB, KAK and KNY for the geomagnetic storm of February 6, 1986.

Magnetogram for 1986 Feb. 09-11

at Memambetsu(MMB), Kakioka(KAK), Kanoya(KNY)

Upward: increase(H), westward(D), downward(Z)

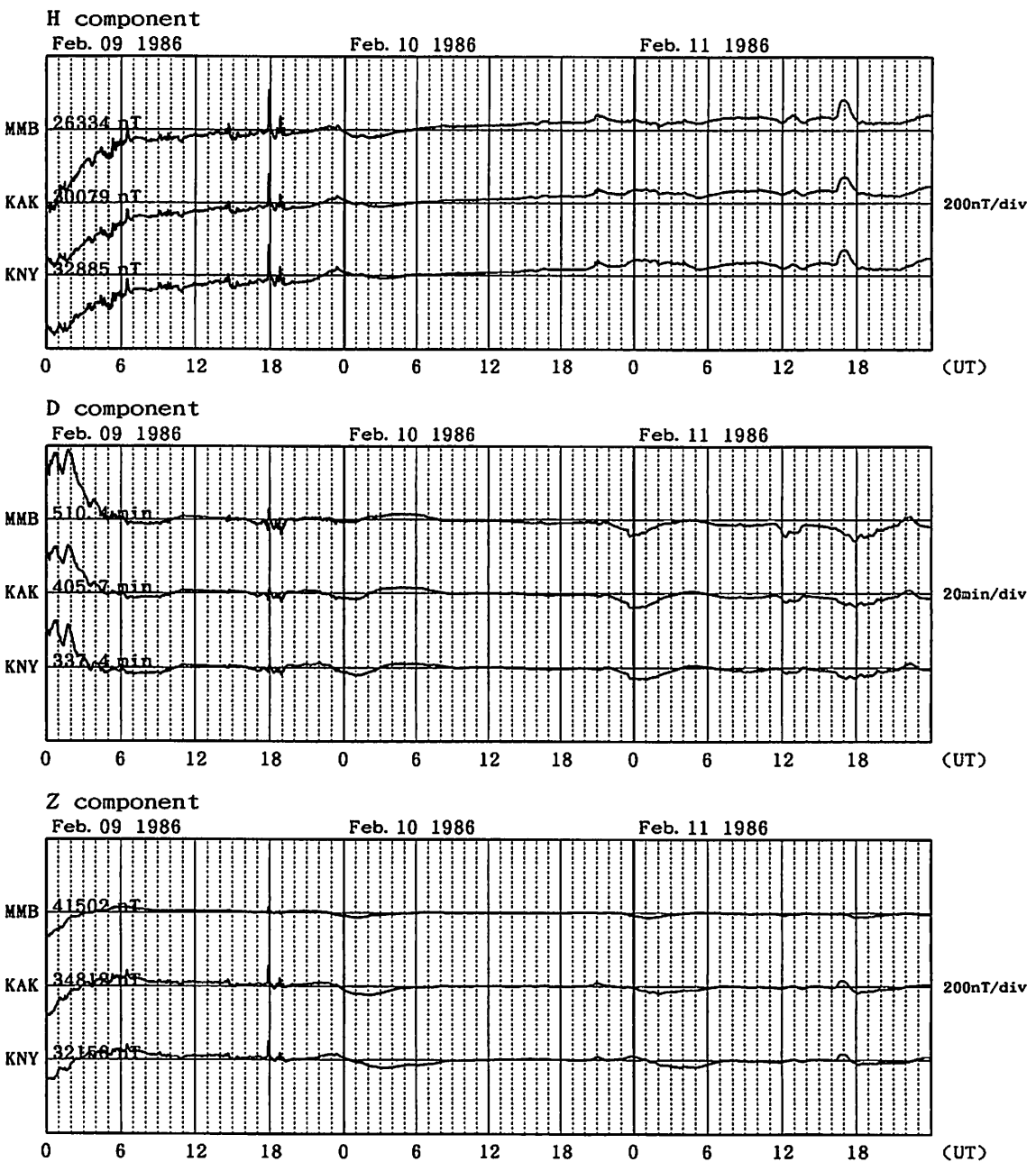


Fig. A-7(b) Magnetic records at MMB, KAK and KNY for the geomagnetic storm of February 6, 1986 (succeeding Fig. A-7(a)).

Magnetogram for 1986 Sep. 11-13

at Memambetsu(MMB), Kakioka(KAK), Kanoya(KNY)

Upward: increase(H), westward(D), downward(Z)

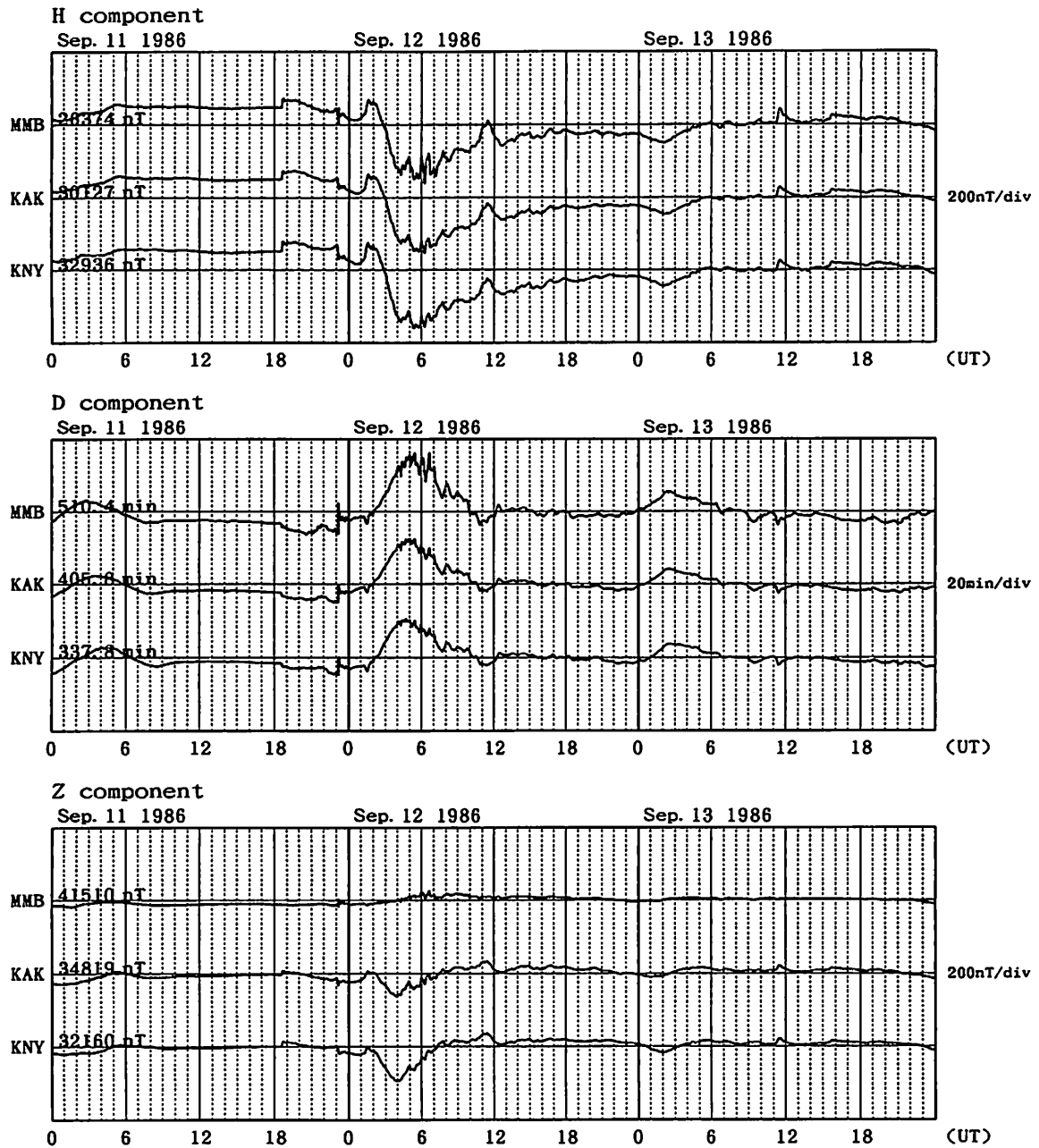


Fig. A-8 Magnetic records at MMB, KAK and KNY for the geomagnetic storm of September 11, 1986.

Magnetogram for 1986 Nov. 03-05

at Memambetsu(MMB), Kakioka(KAK), Kanoya(KNY)

Upward: increase(H), westward(D), downward(Z)

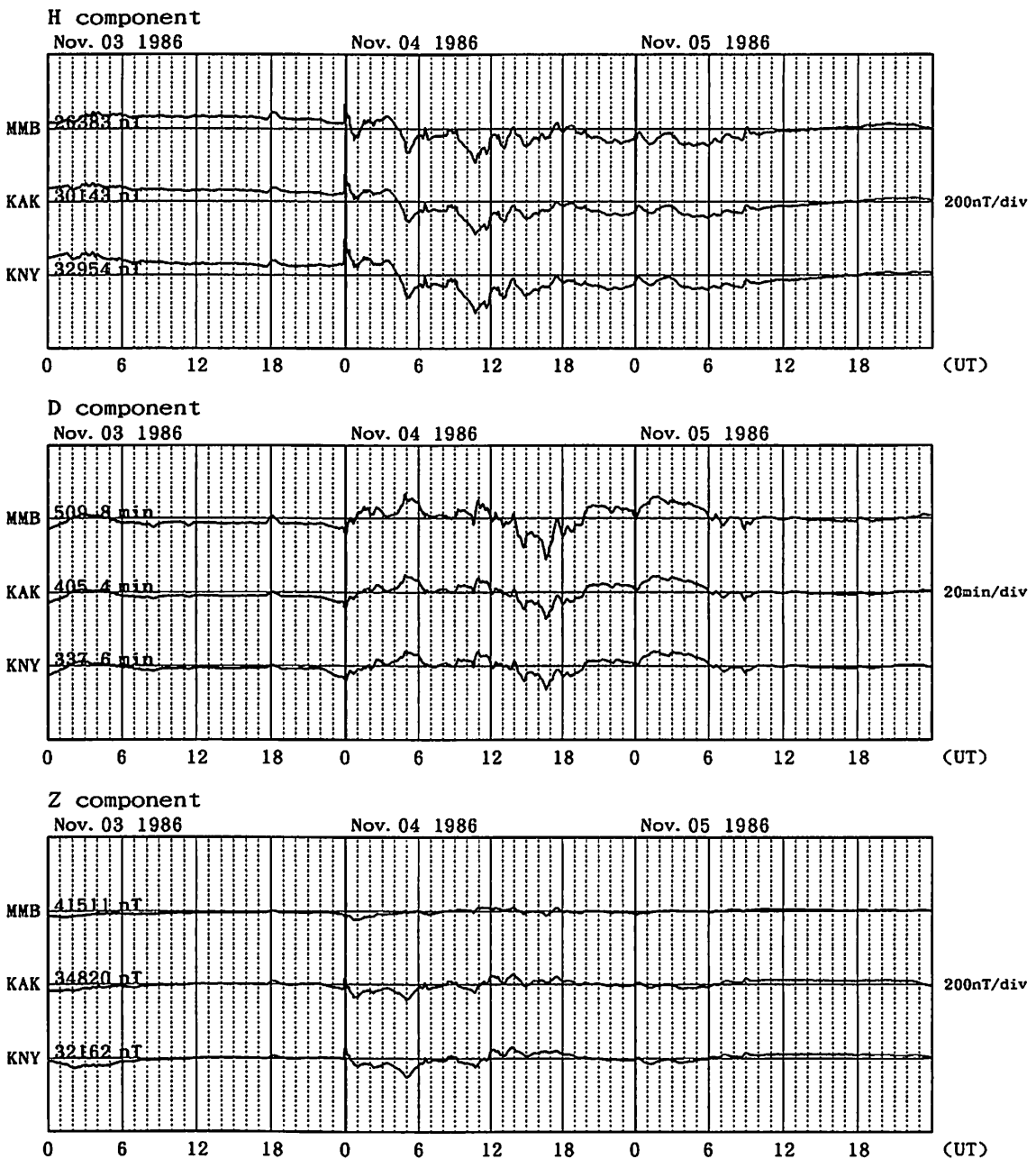


Fig. A-9 Magnetic records at MMB, KAK and KNY for the geomagnetic storm of November 3, 1986.

Magnetogram for 1988 Jan. 13-15

at Memambetsu(MMB), Kakioka(KAK), Kanoya(KNY)

Upward: increase(H), westward(D), downward(Z)

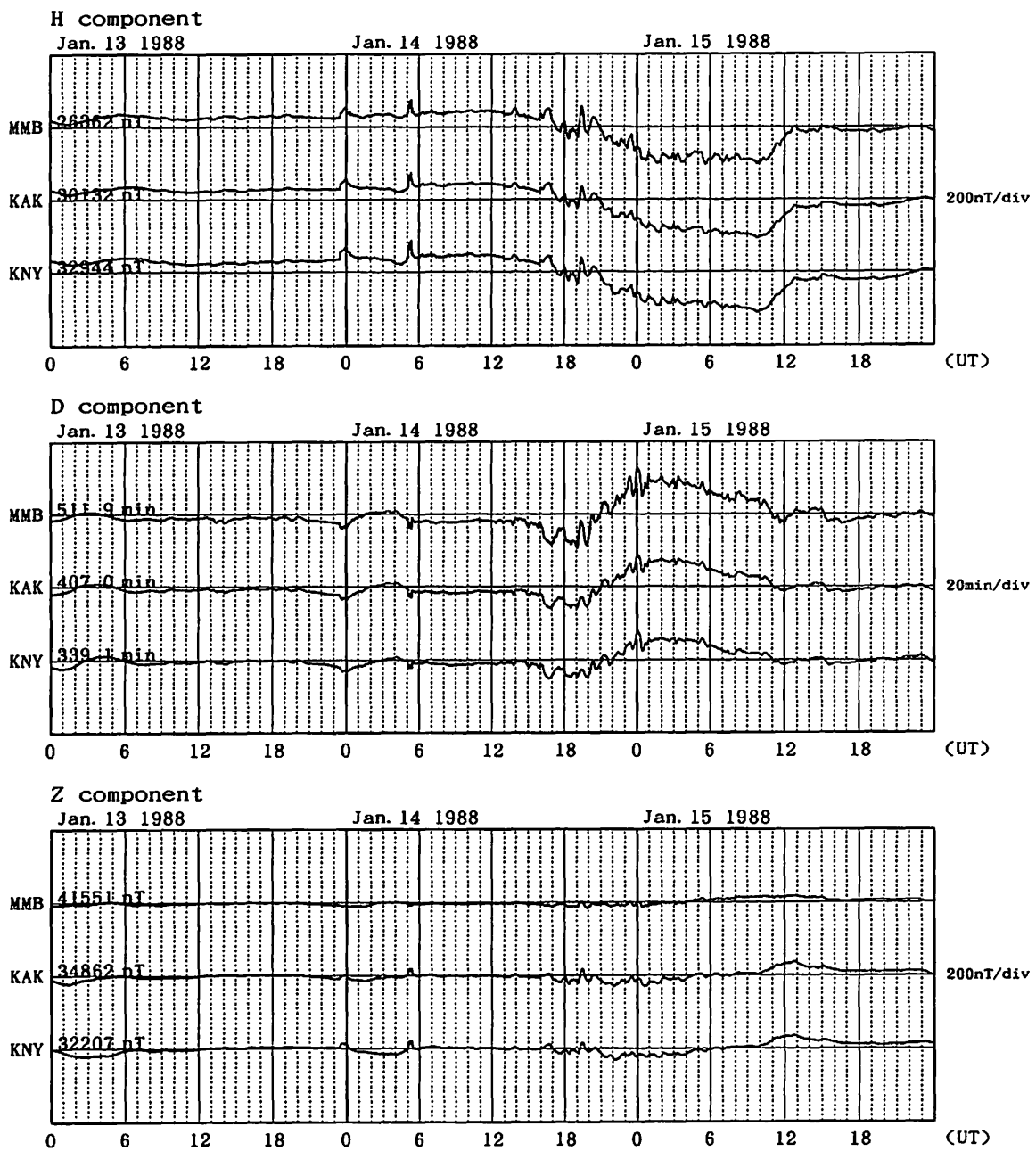


Fig. A-10 Magnetic records at MMB, KAK and KNY for the geomagnetic storm of January 13, 1988.

Magnetogram for 1988 Feb. 21-23

at Memambetsu(MMB), Kakioka(KAK), Kanoya(KNY)

Upward: increase(H), westward(D), downward(Z)

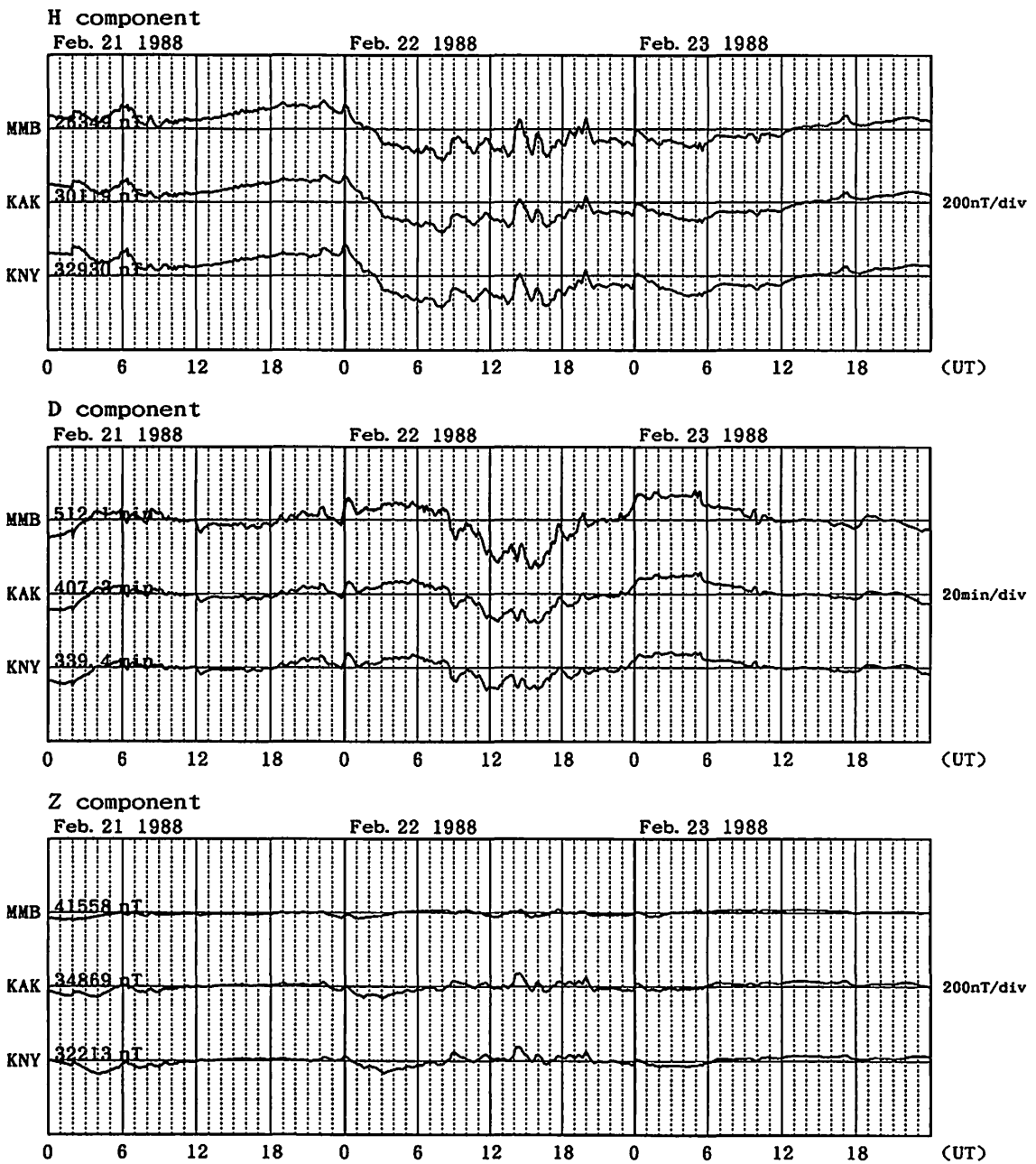


Fig. A-11 Magnetic records at MMB, KAK and KNY for the geomagnetic storm of February 21, 1988.

Magnetogram for 1988 Apr. 03-05

at Memambetsu(MMB), Kakioka(KAK), Kanoya(KNY)

Upward: increase(H), westward(D), downward(Z)

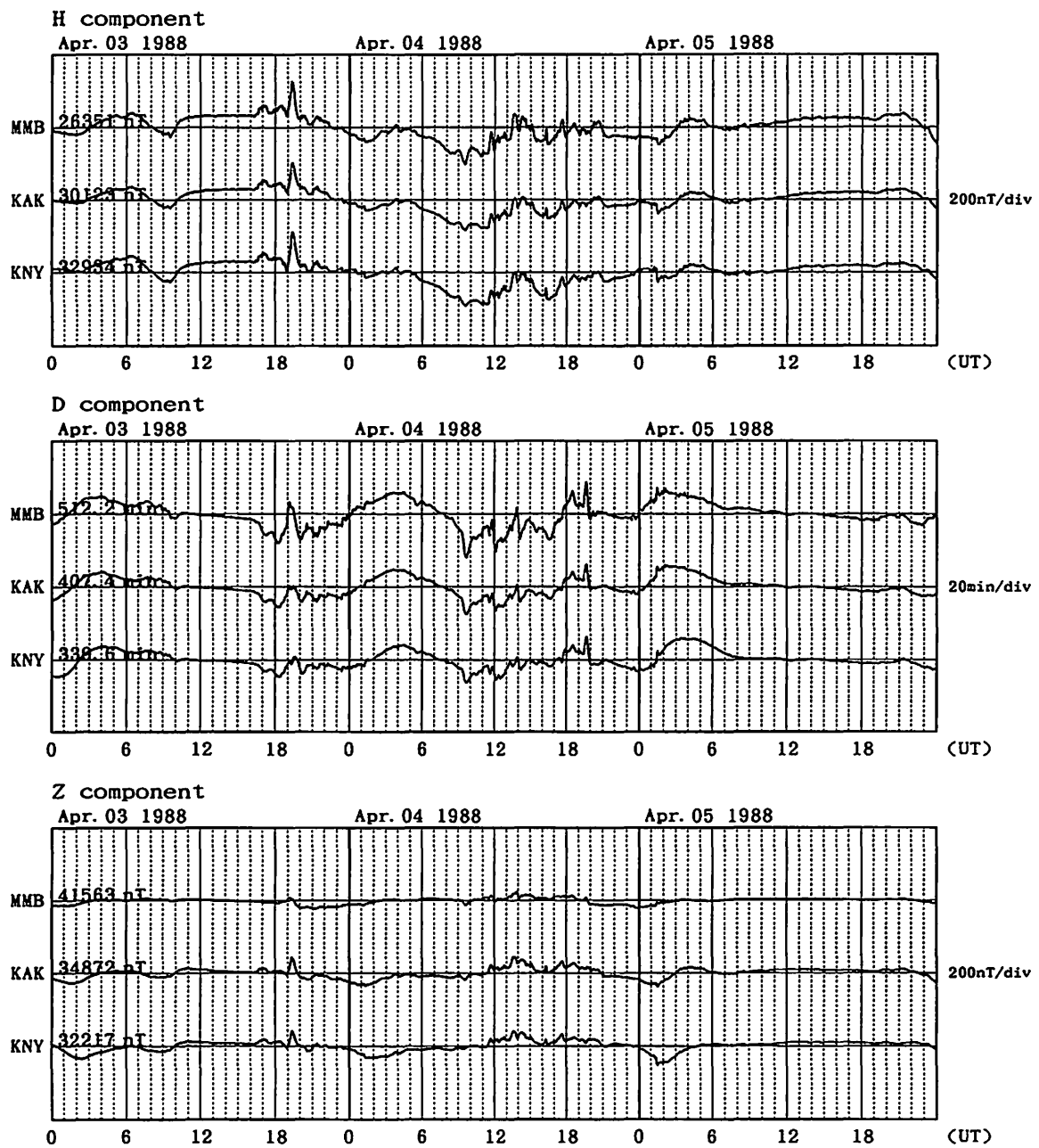


Fig. A-12 Magnetic records at MMB, KAK and KNY for the geomagnetic storm of April 3, 1988.

Magnetogram for 1988 May 06-08

at Memambetsu(MMB), Kakioka(KAK), Kanoya(KNY)

Upward: increase(H), westward(D), downward(Z)

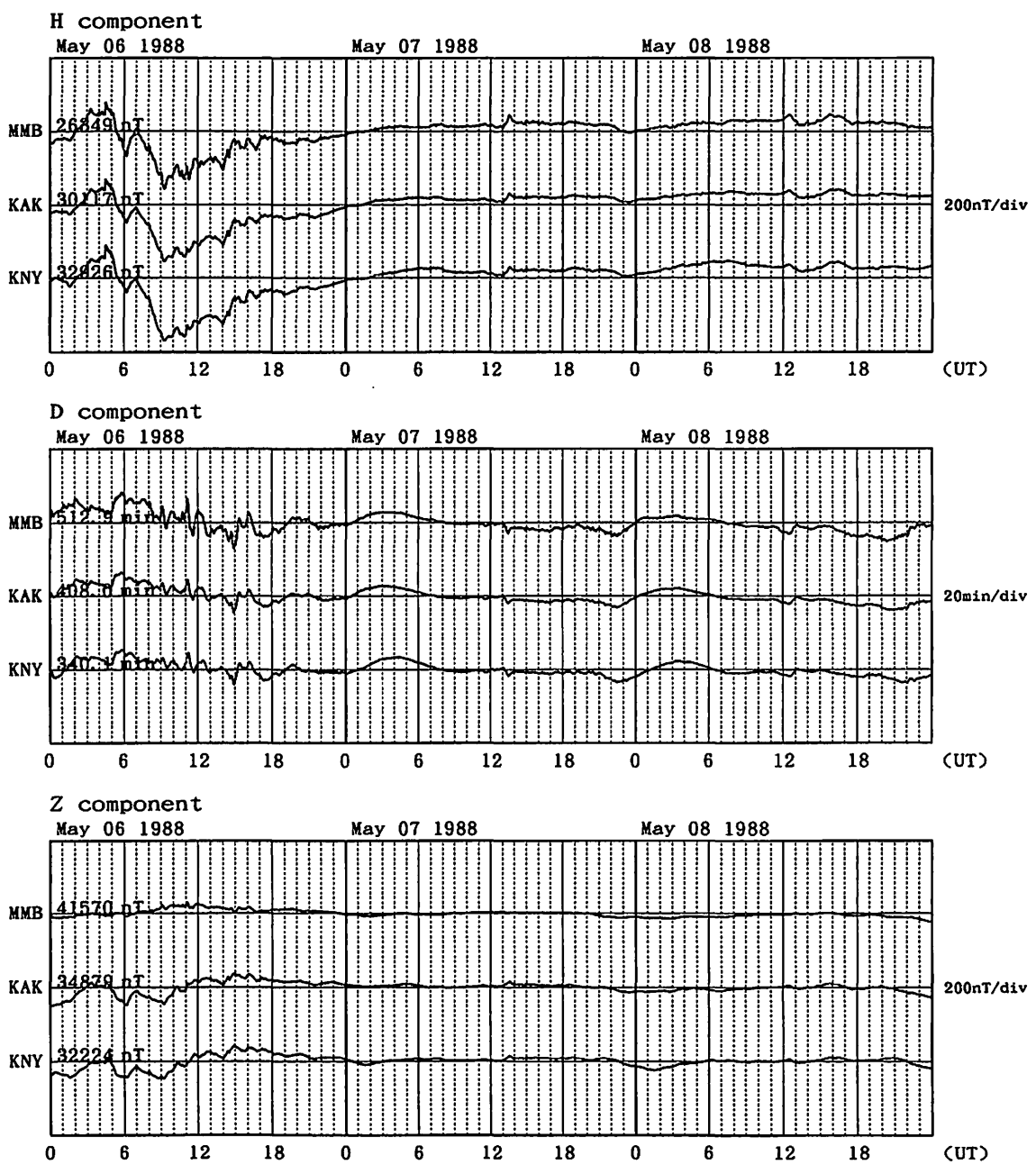


Fig. A-13 Magnetic records at MMB, KAK and KNY for the geomagnetic storm of May 6, 1988.

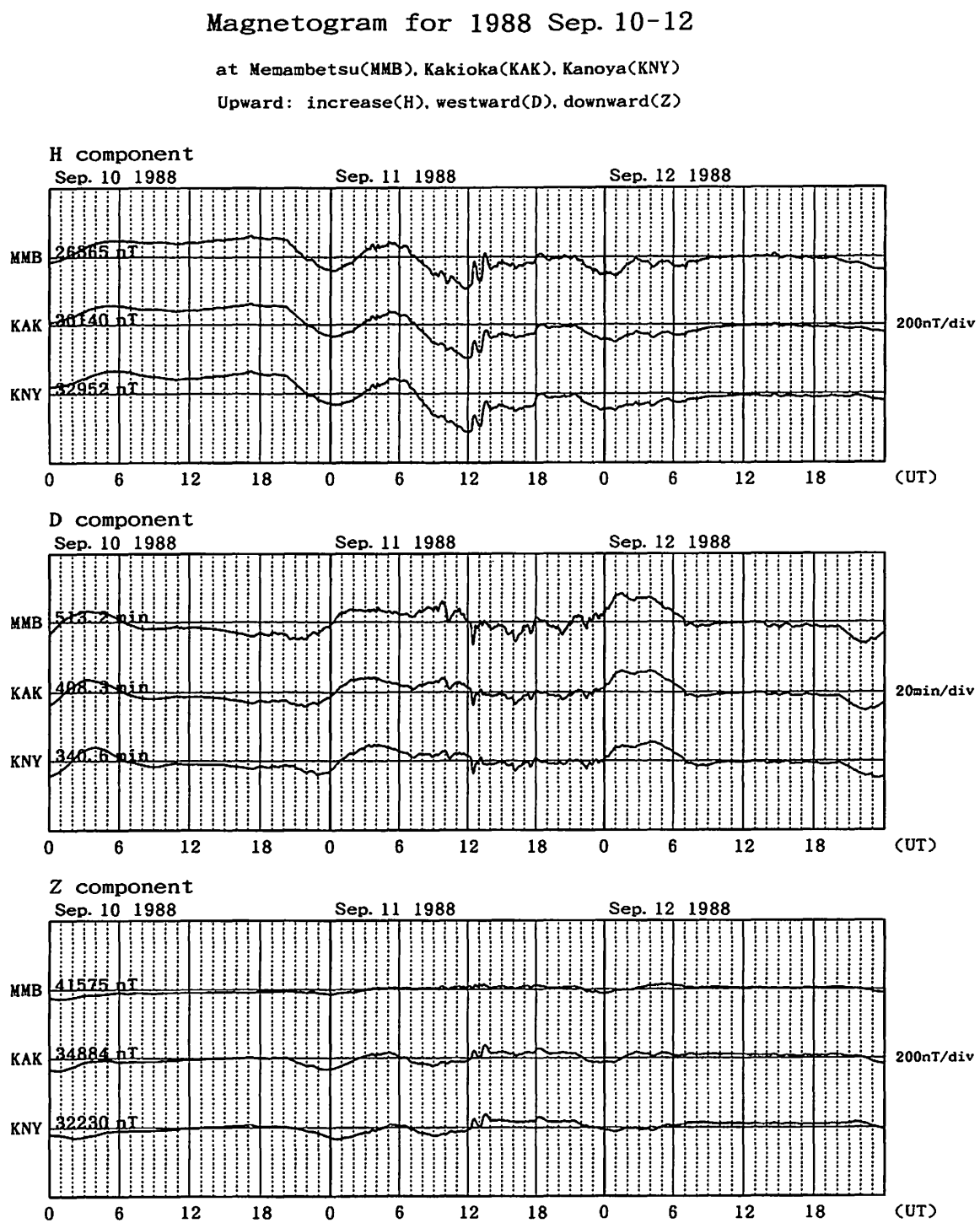


Fig. A-14 Magnetic records at MMB, KAK and KNY for the geomagnetic storm of September 10, 1988.

Magnetogram for 1988 Oct. 10-12

at Memambetsu(MMB), Kakioka(KAK), Kanoya(KNY)

Upward: increase(H), westward(D), downward(Z)

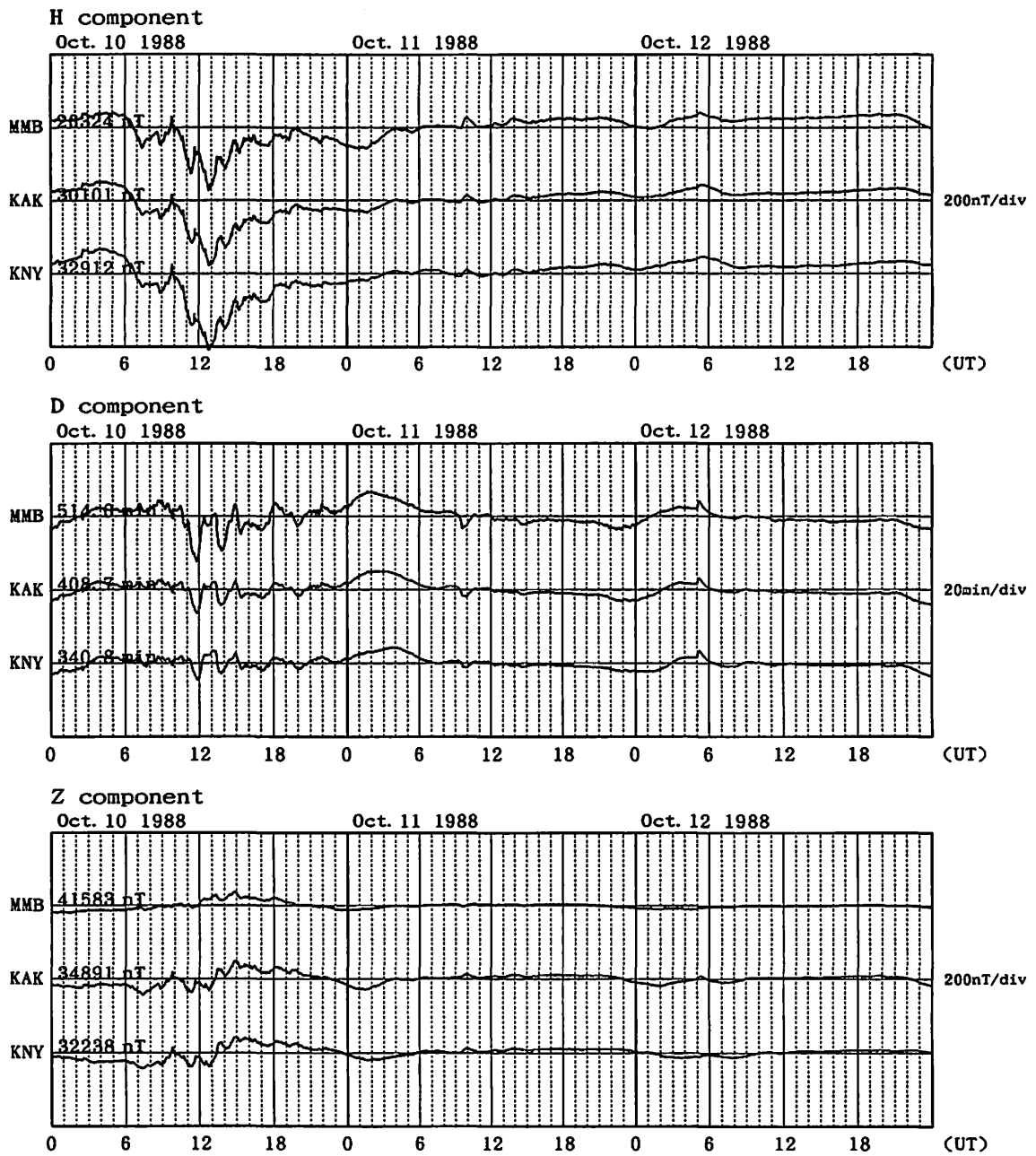


Fig. A-15 Magnetic records at MMB, KAK and KNY for the geomagnetic storm of October 10, 1988.

Magnetogram for 1988 Nov. 30-Dec. 02

at Memambetsu(MMB), Kakioka(KAK), Kanoya(KNY)

Upward: increase(H), westward(D), downward(Z)

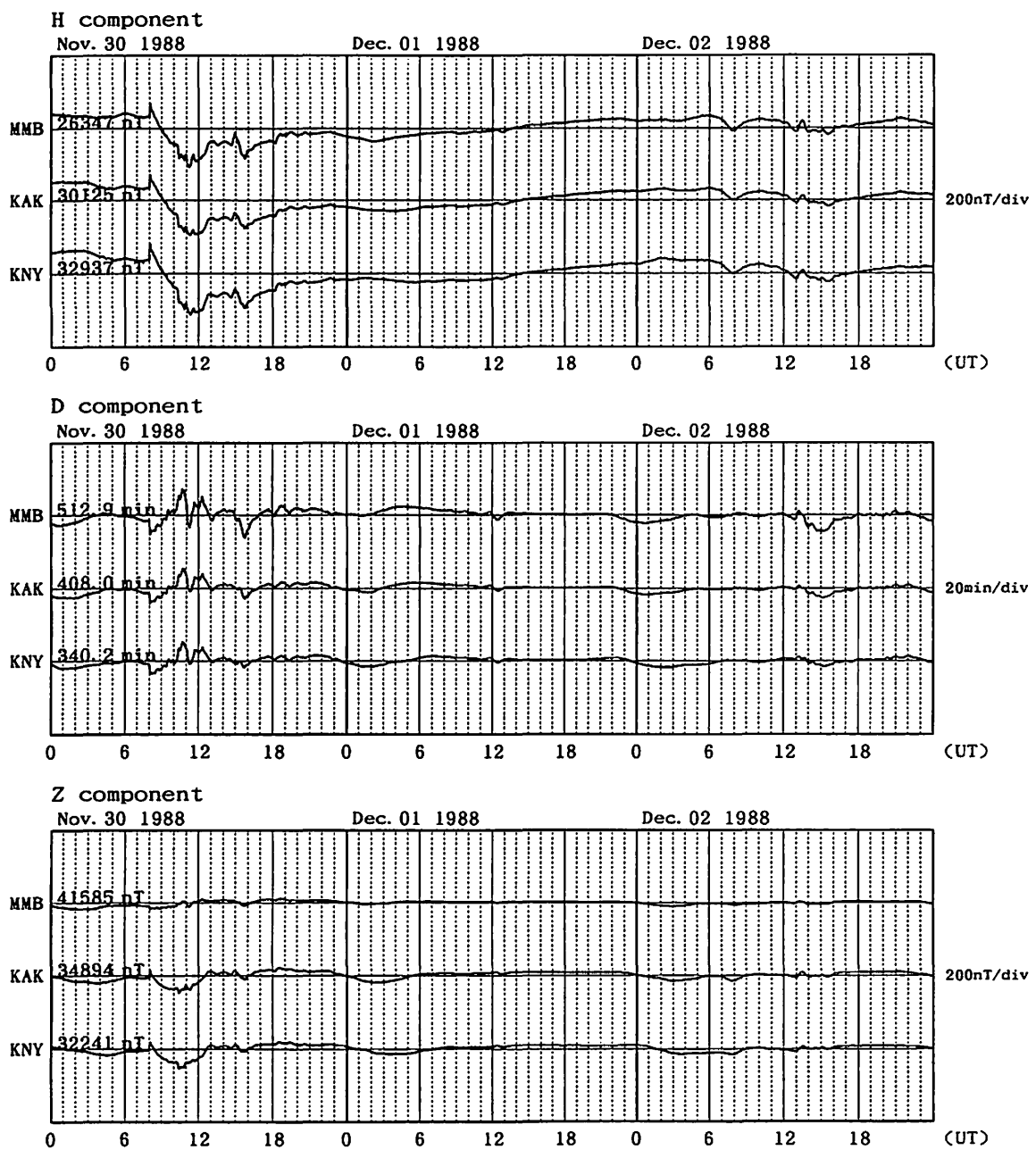


Fig. A-16 Magnetic records at MMB, KAK and KNY for the geomagnetic storm of November 30, 1988.

Magnetogram for 1989 Jan. 20-22

at Memambetsu(MMB), Kakioka(KAK), Kanoya(KNY)

Upward: increase(H), westward(D), downward(Z)

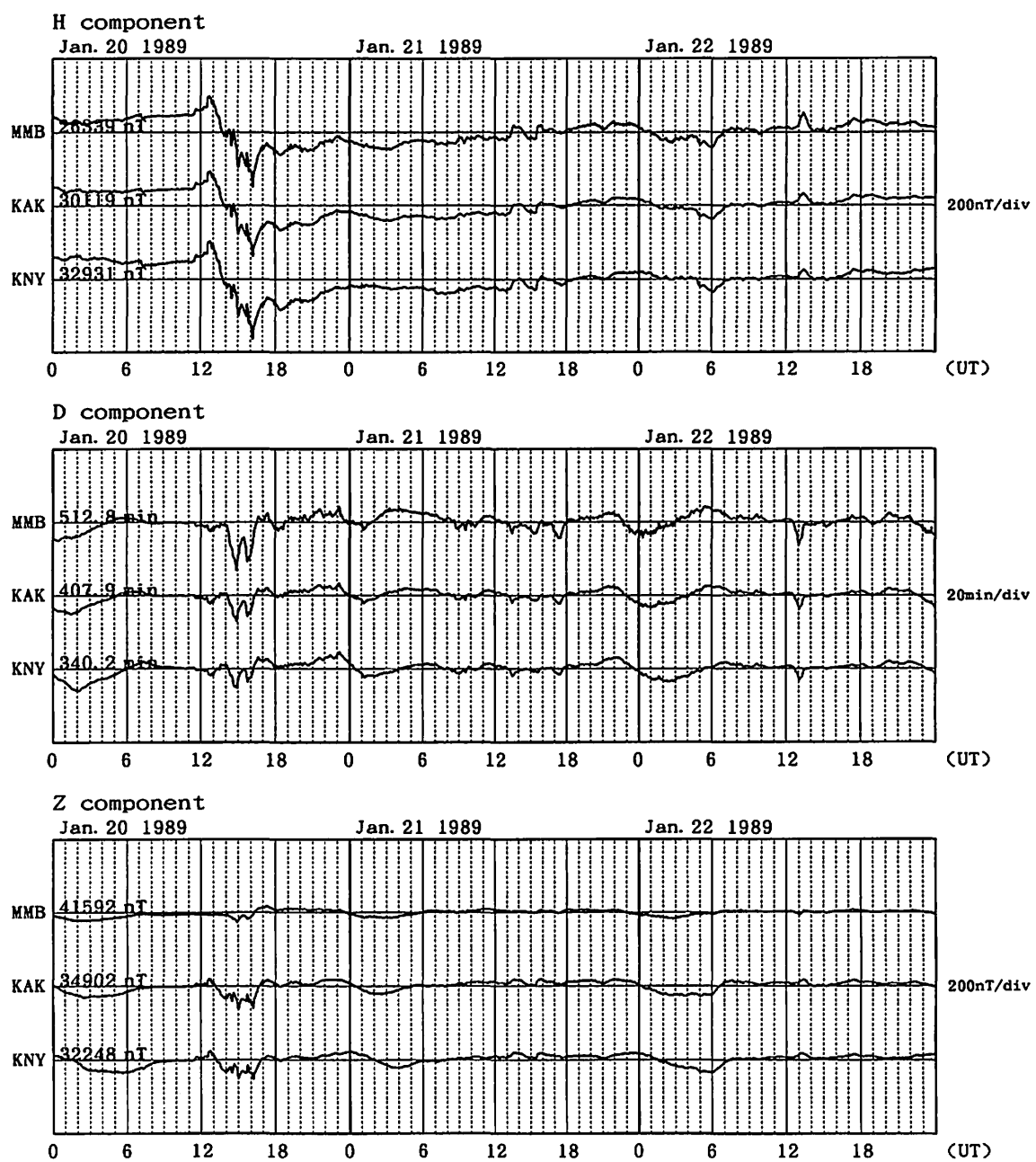


Fig. A-17 Magnetic records at MMB, KAK and KNY for the geomagnetic storm of January 20, 1989.

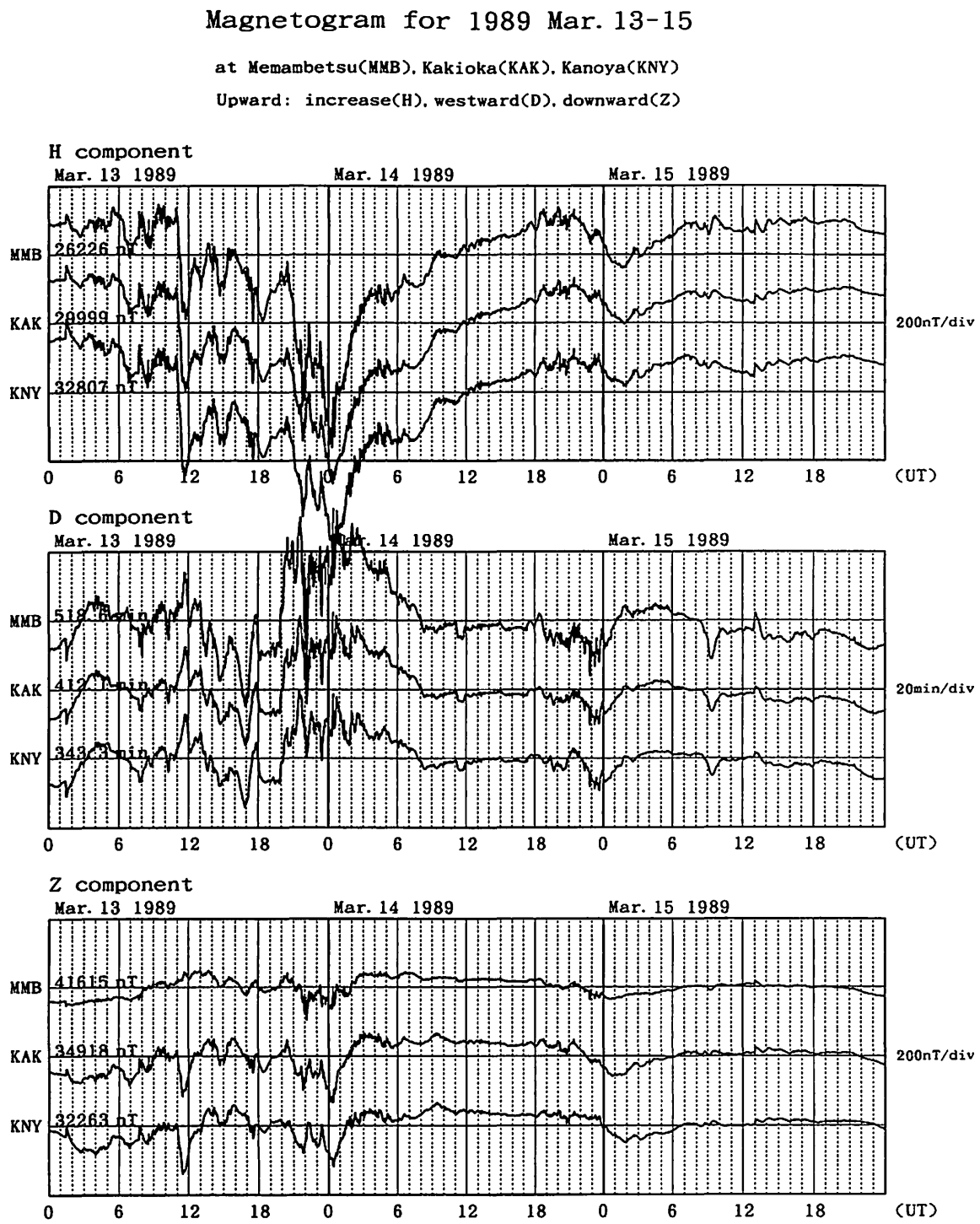


Fig. A-18 Magnetic records at MMB, KAK and KNY for the geomagnetic storm of March 13, 1989.

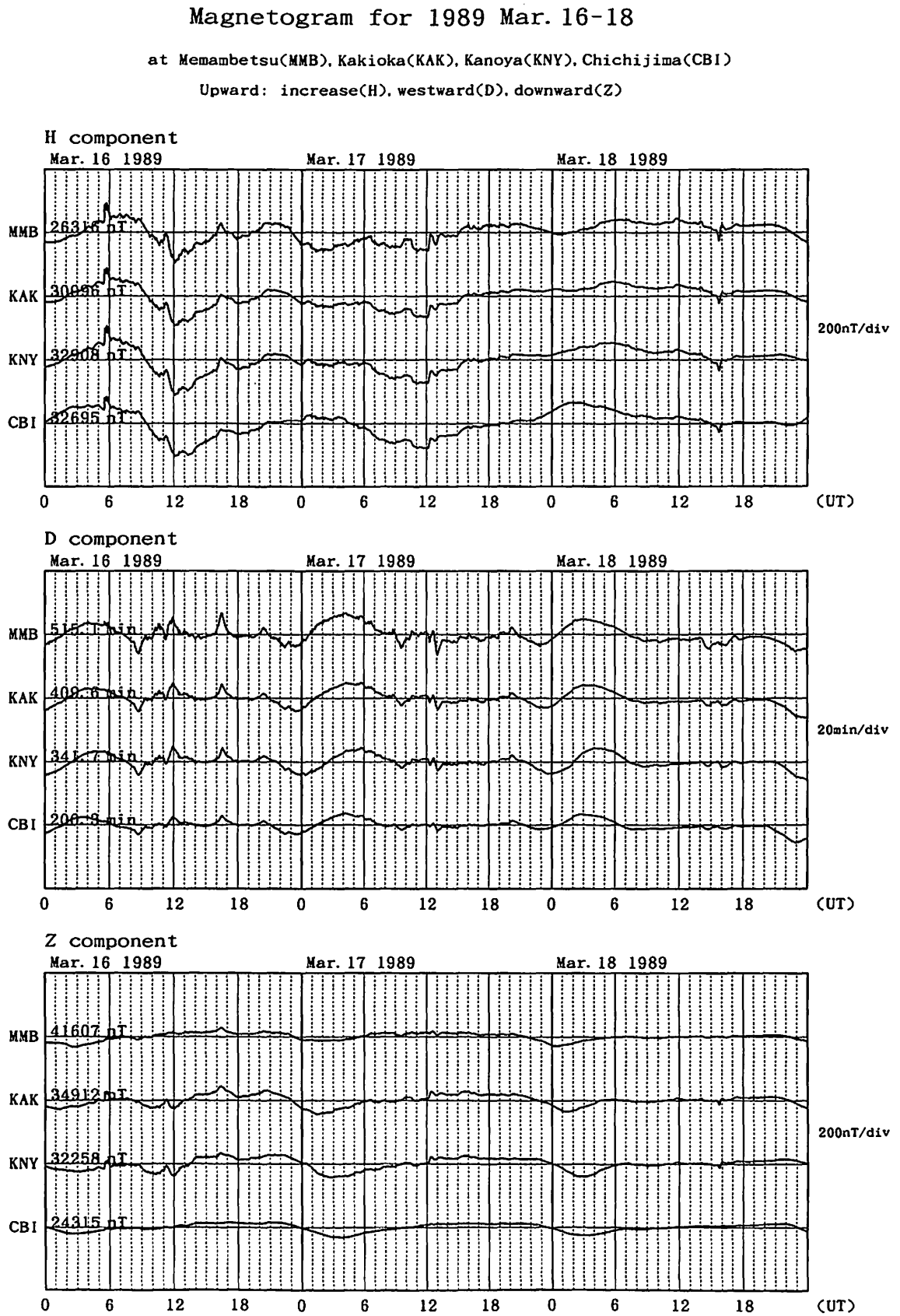


Fig. A-19 Magnetic records at MMB, KAK, KNY and CBI for the geomagnetic storm of March 16, 1989.

Magnetogram for 1989 Mar. 26-28

at Memambetsu(MMB), Kakicka(KAK), Kanoya(KNY), Chichijima(CBI)

Upward: increase(H), westward(D), downward(Z)

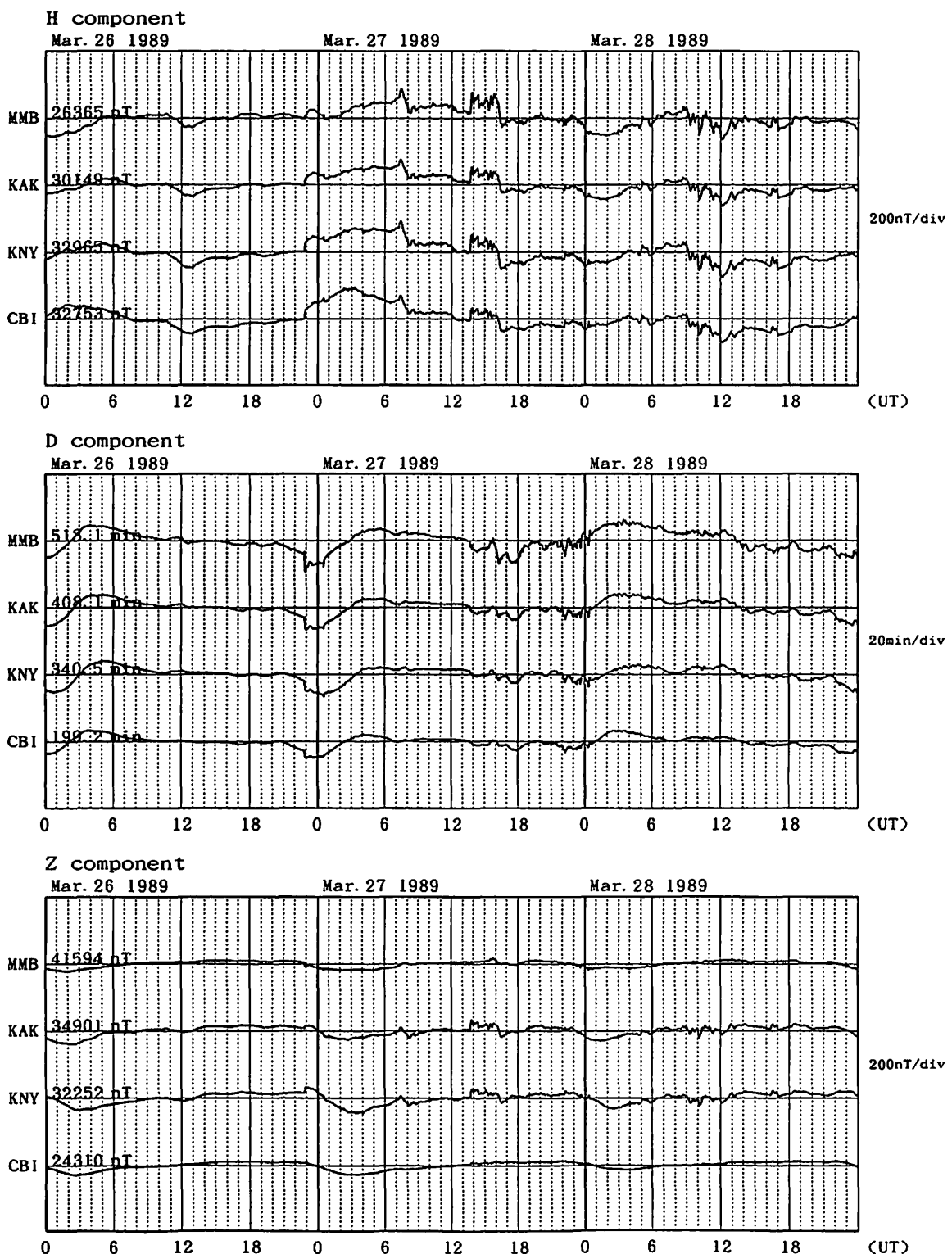


Fig. A-20(a) Magnetic records at MMB, KAK, KNY and CBI for the geomagnetic storm of March 26, 1989.

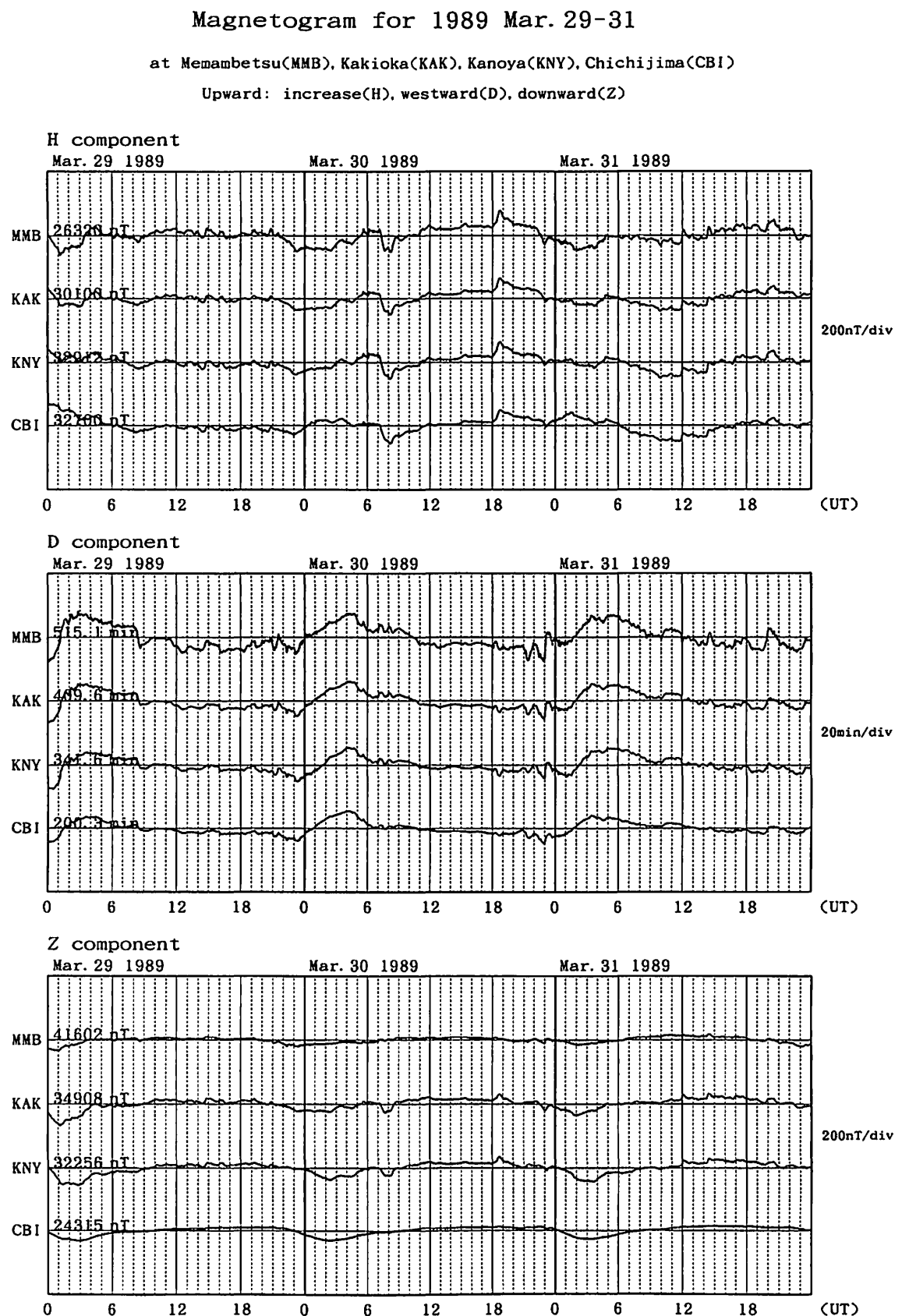


Fig. A-20(b) Magnetic records at MMB, KAK, KNY and CBI for the geomagnetic storm of March 26, 1989 (succeding Fig. A-20(a)).

Magnetogram for 1989 Apr. 25-27

at Memambetsu(MMB), Kakioka(KAK), Kanoya(KNY)

Upward: increase(H), westward(D), downward(Z)

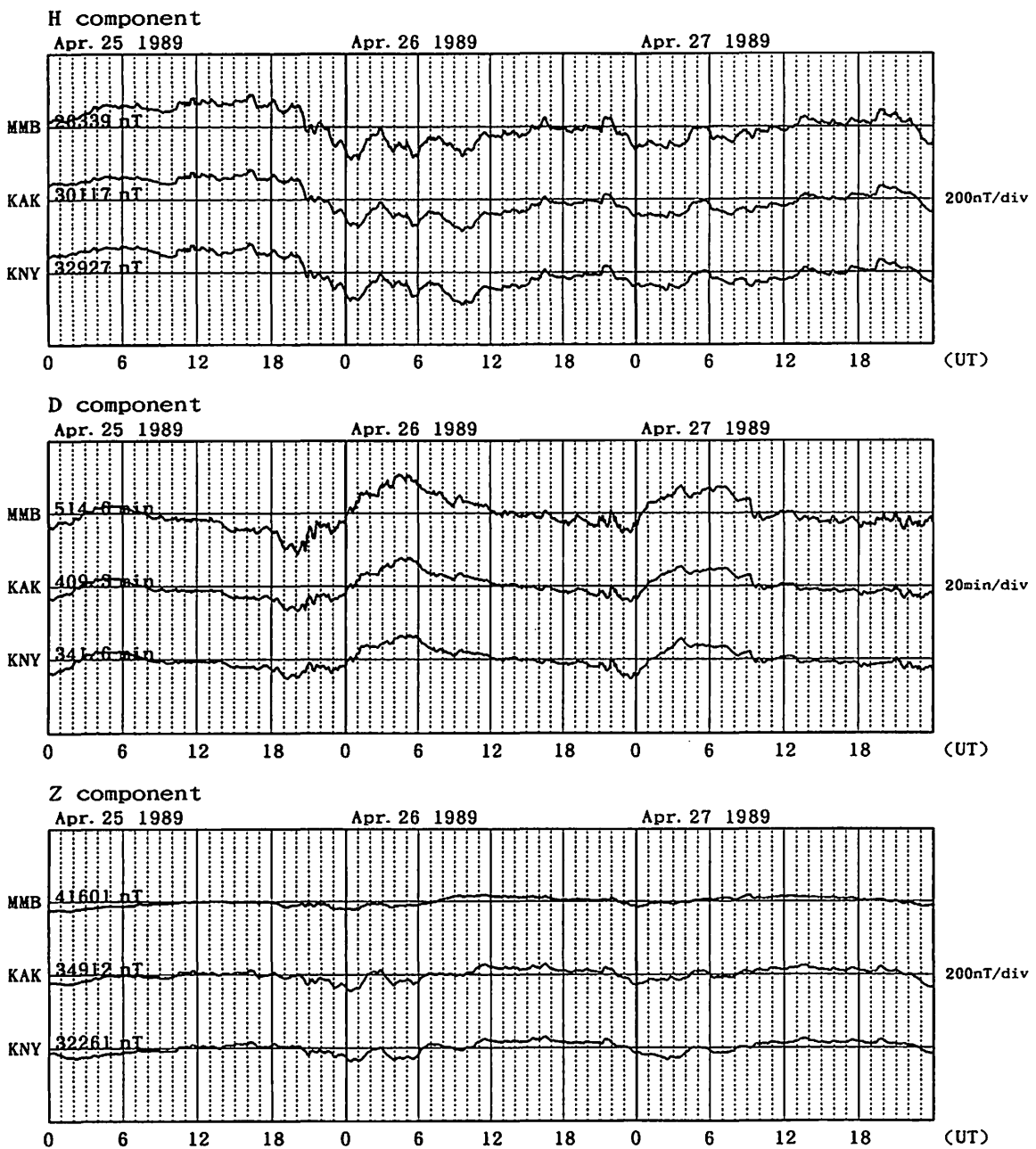


Fig. A-21(a) Magnetic records at MMB, KAK and KNY for the geomagnetic storm of April 25, 1989.

Magnetogram for 1989 Apr. 28-30

at Memambetsu(MMB), Kakioka(KAK), Kanoya(KNY)

Upward: increase(H), westward(D), downward(Z)

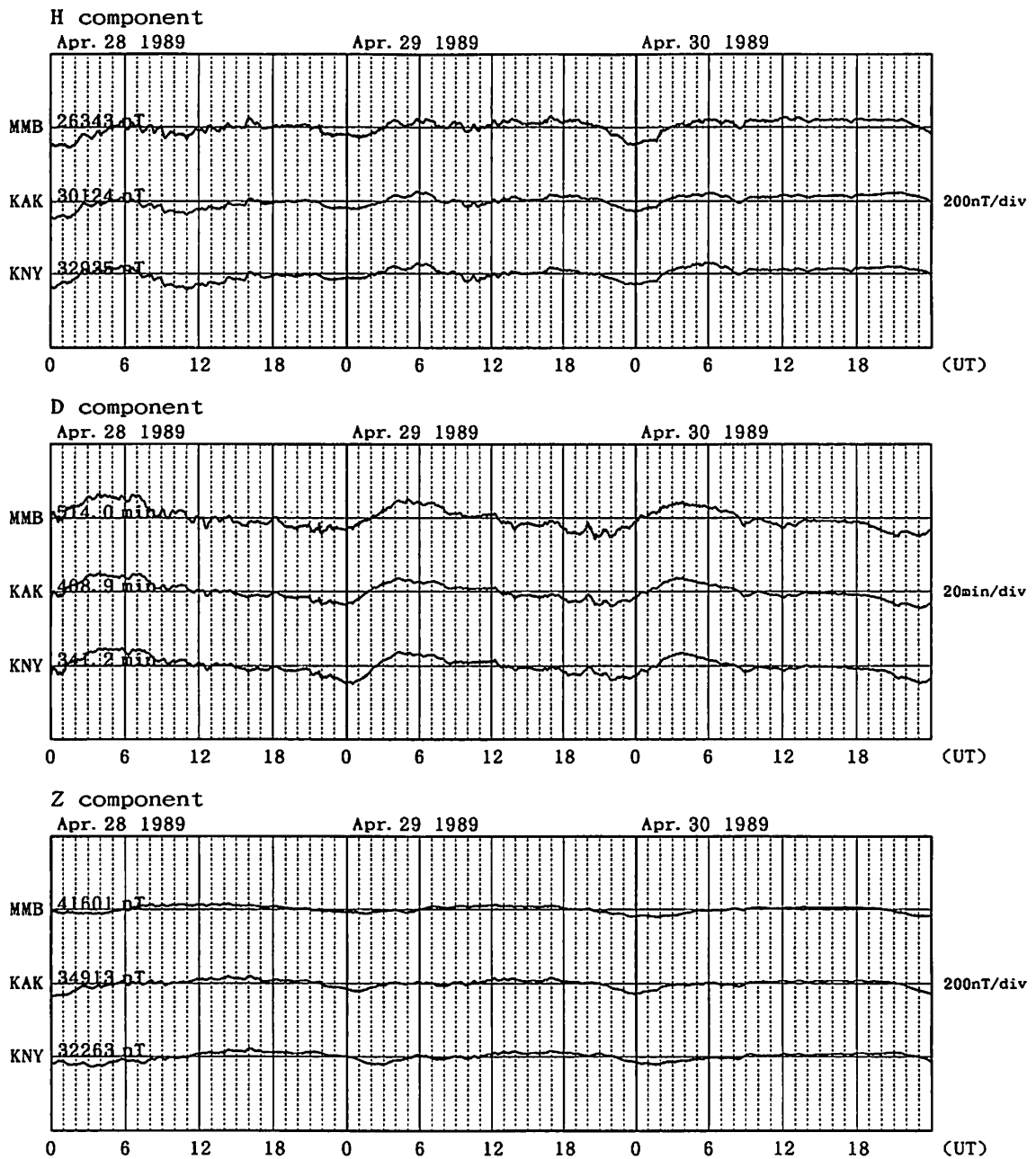


Fig. A-21(b) Magnetic records at MMB, KAK and KNY for the geomagnetic storm of April 25, 1989 (succeding Fig. A-21(a)).

Magnetogram for 1989 May 07-09

at Memambetsu(MMB), Kakioka(KAK), Kanoya(KNY)

Upward: increase(H), westward(D), downward(Z)

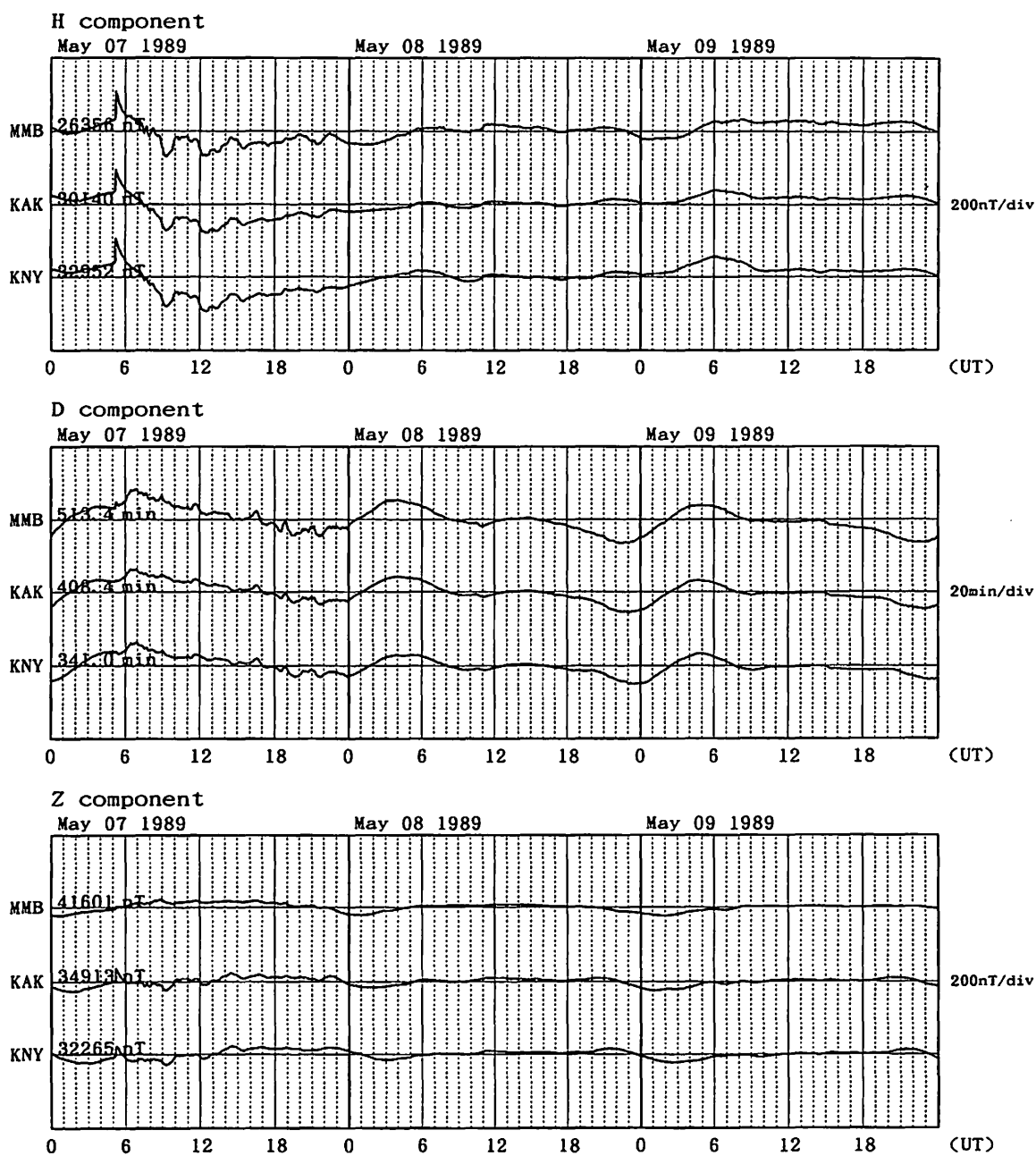


Fig. A-22 Magnetic records at MMB, KAK and KNY for the geomagnetic storm of May 7, 1989.

Magnetogram for 1989 May 23-25

at Memambetsu(MMB), Kakioka(KAK), Kanoya(KNY), Chichijima(CBI)

Upward: increase(H), westward(D), downward(Z)

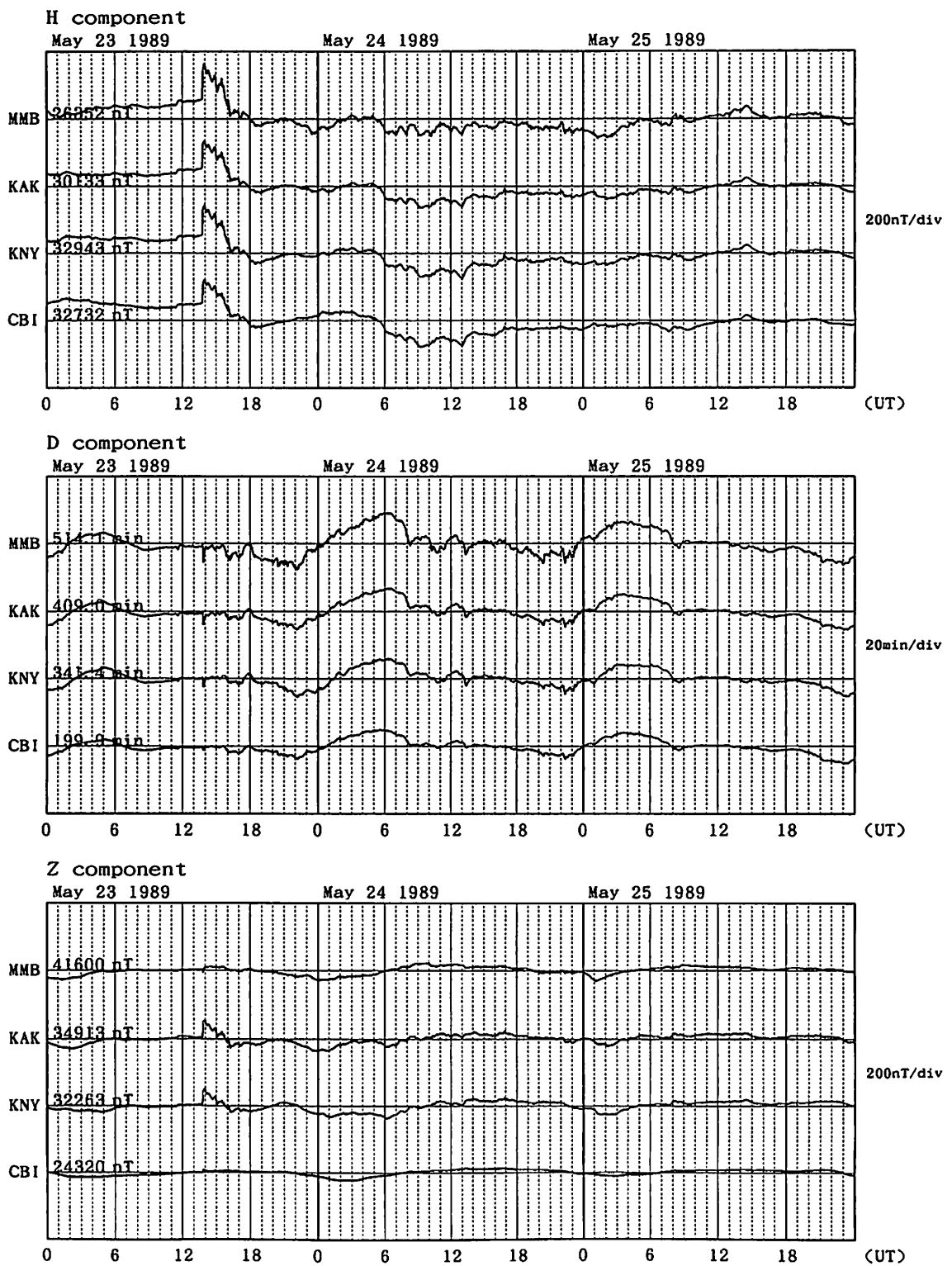


Fig. A-23 Magnetic records at MMB, KAK, KNY and CBI for the geomagnetic storm of May 23, 1989.

Magnetogram for 1989 Jun. 08-10

at Memambetsu(MMB), Kakioka(KAK), Kanoya(KNY), Chichijima(CBI)

Upward: increase(H), westward(D), downward(Z)

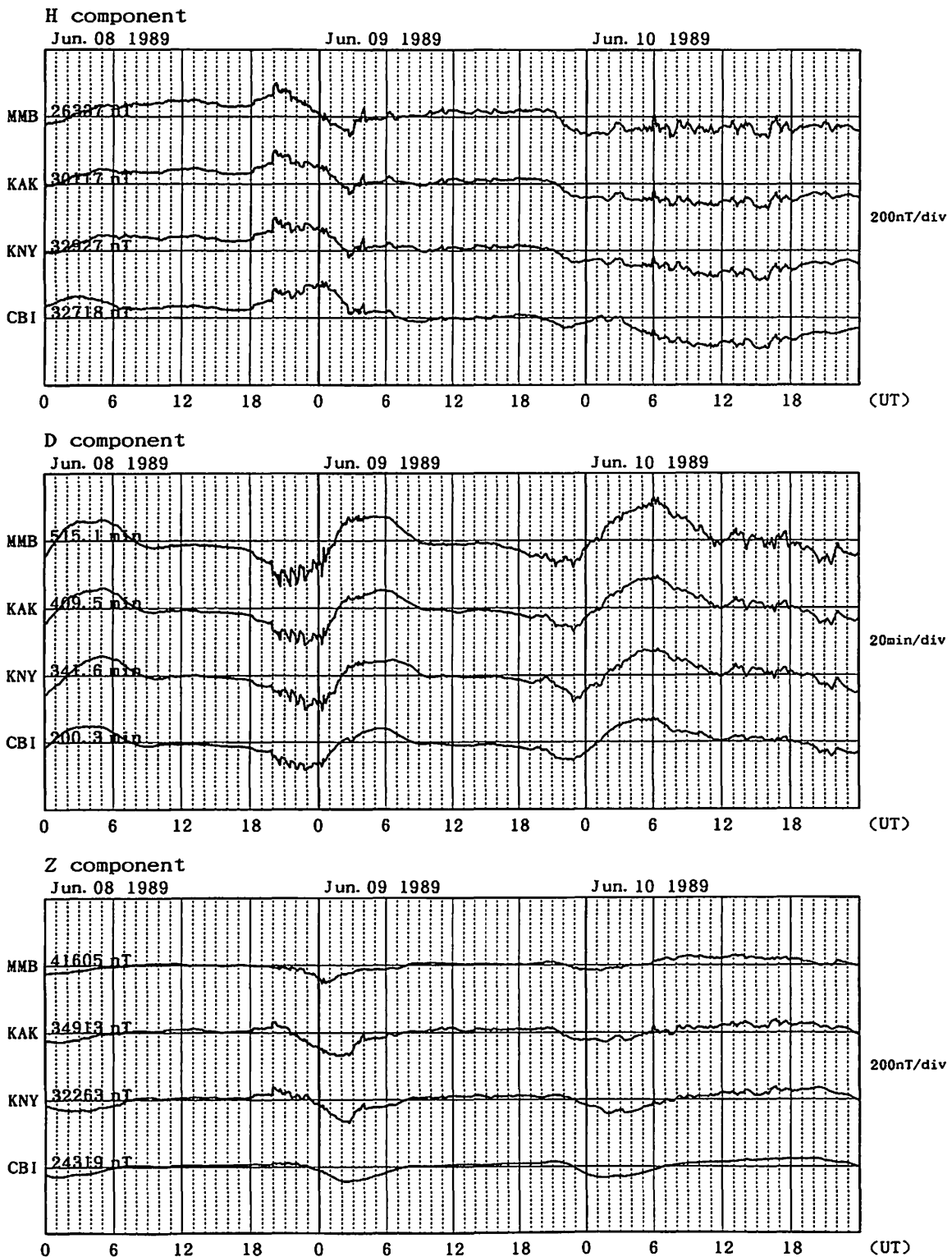


Fig. A-24(a) Magnetic records at MMB, KAK, KNY and CBI for the geomagnetic storm of June 8, 1989.

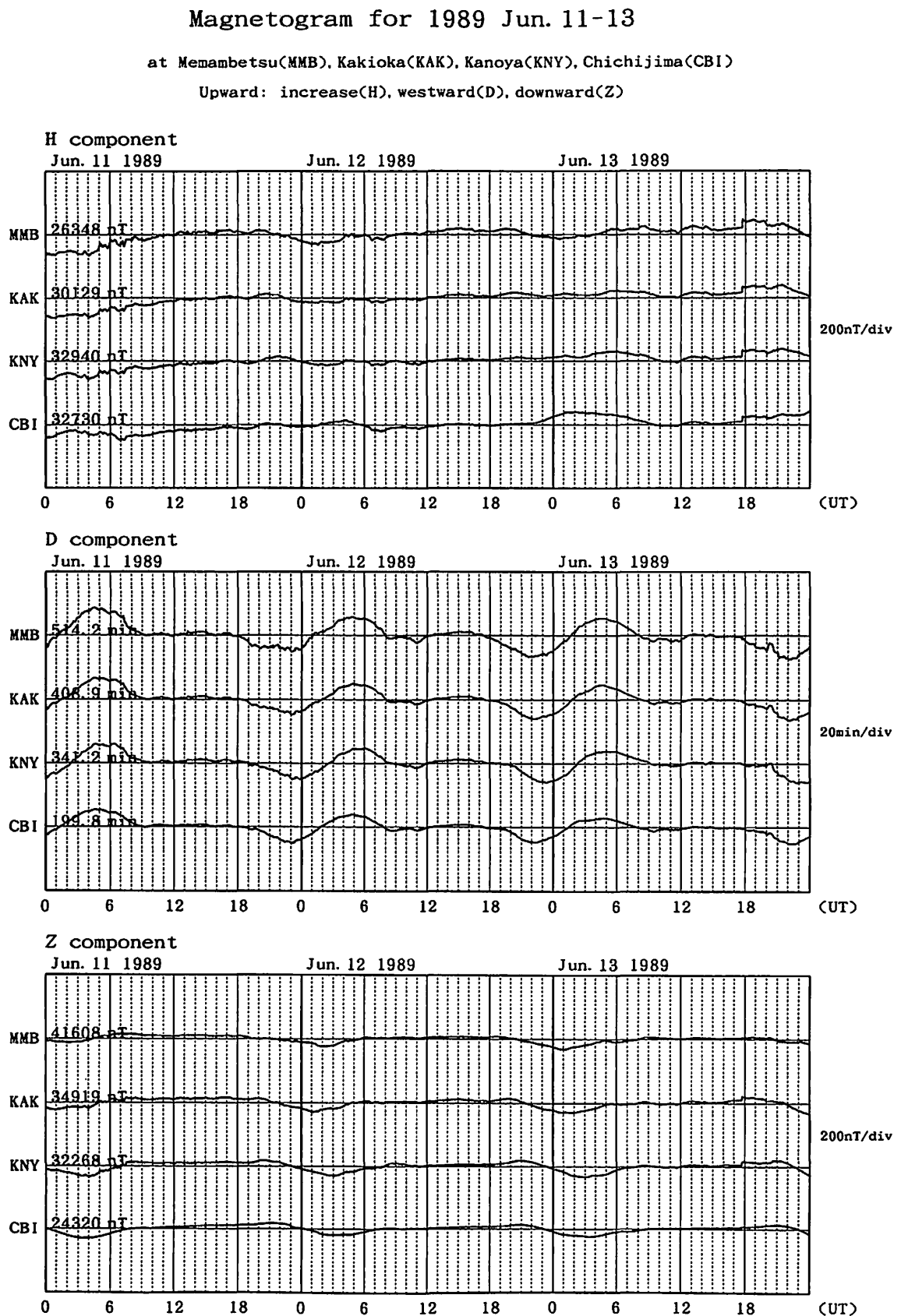


Fig. A-24(b) Magnetic records at MMB, KAK, KNY and CBI for the geomagnetic storm of June 8, 1989 (succeeding Fig. A-24(a)).

Magnetogram for 1989 Aug. 14-16

at Memambetsu(MMB), Kakioka(KAK), Kanoya(KNY), Chichijima(CBI)

Upward: increase(H), westward(D), downward(Z)

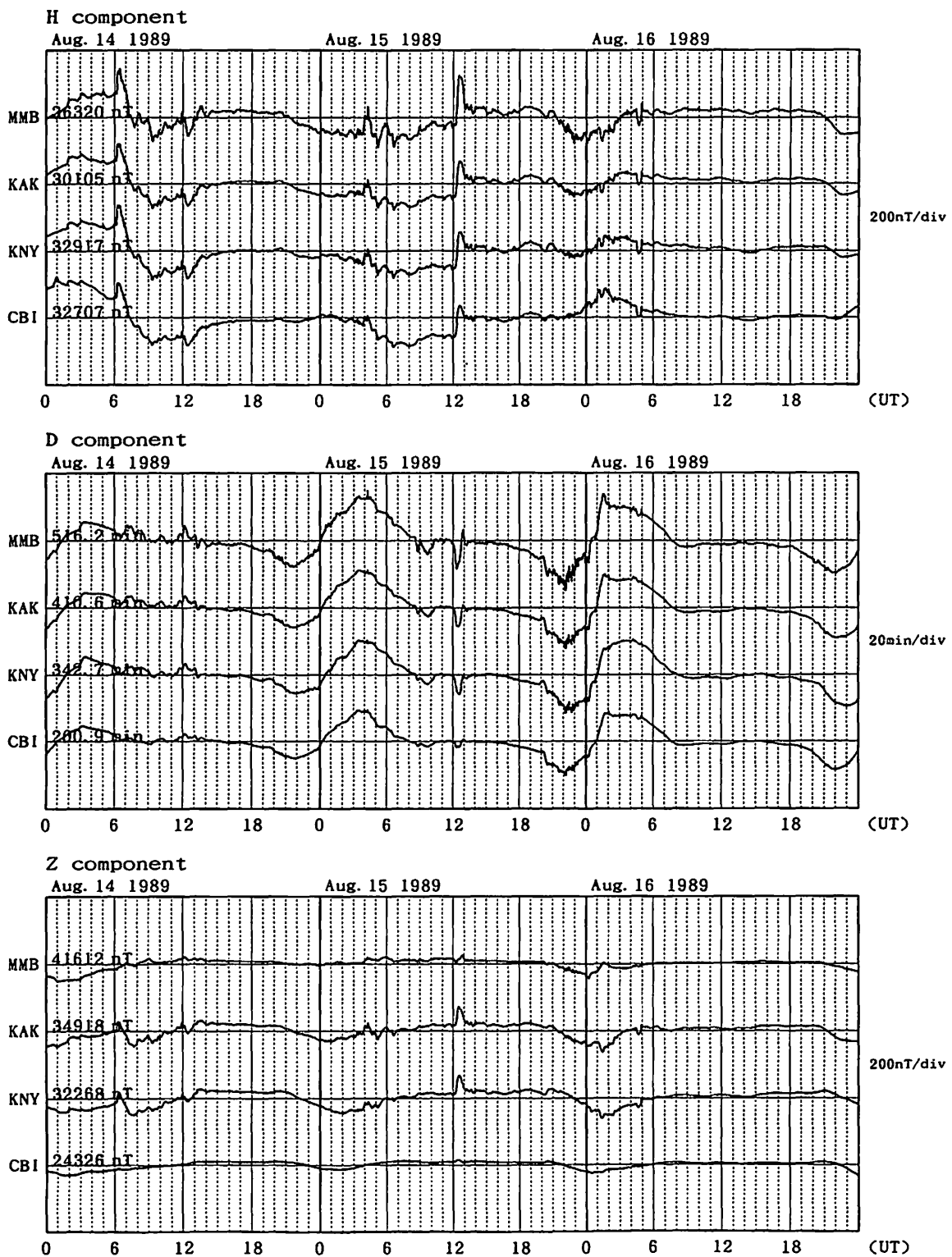


Fig. A-25 Magnetic records at MMB, KAK, KNY and CBI for the geomagnetic storm of August 14, 1989.

Magnetogram for 1989 Sep. 18-20

at Memambetsu(MMB), Kakioka(KAK), Kanoya(KNY)

Upward: increase(H), westward(D), downward(Z)

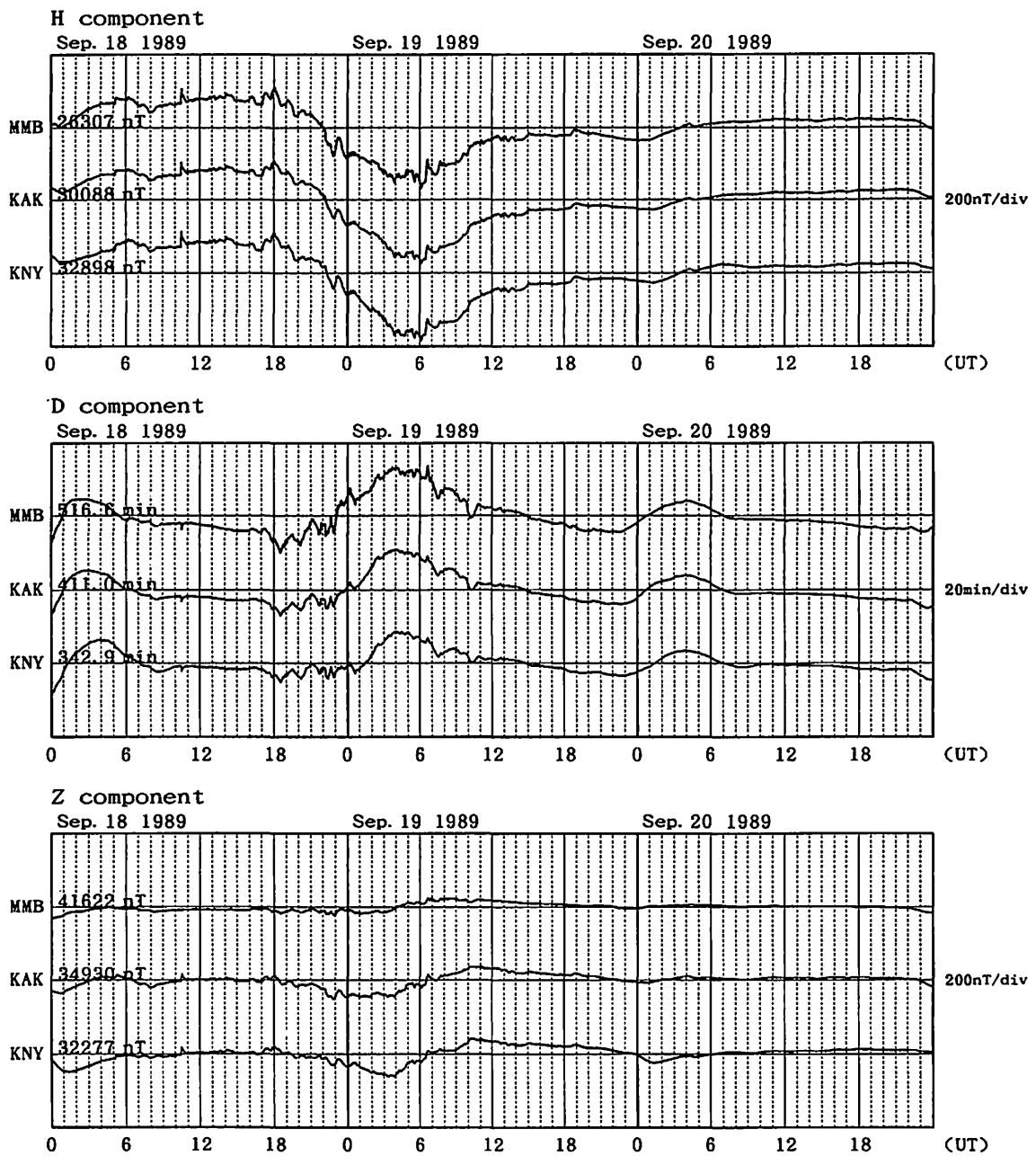


Fig. A-26 Magnetic records at MMB, KAK and KNY for the geomagnetic storm of September 18, 1989.

Magnetogram for 1989 Sep. 26-28

at Memambetsu(MMB), Kakioka(KAK), Kanoya(KNY)

Upward: increase(H), westward(D), downward(Z)

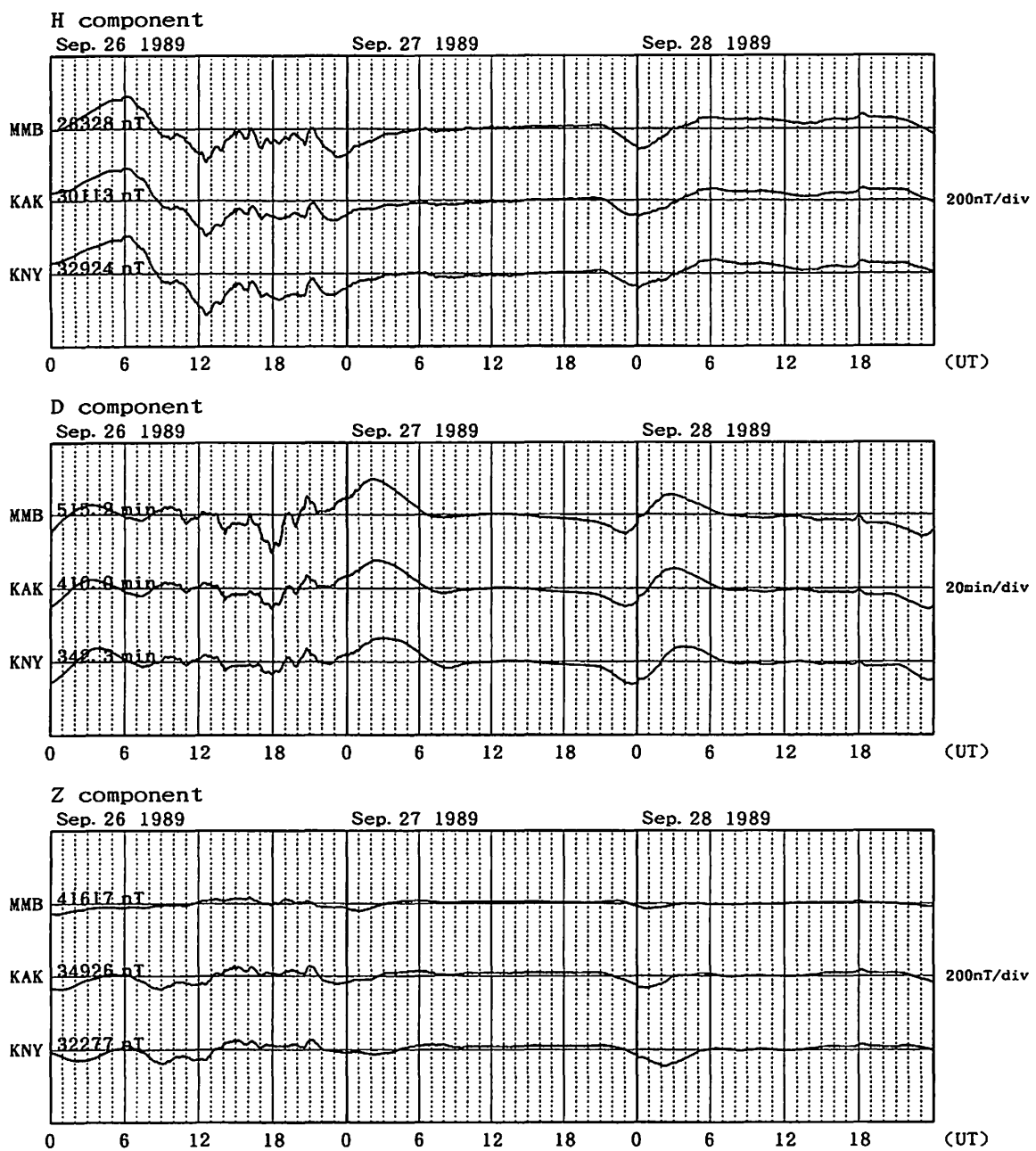


Fig. A-27 Magnetic records at MMB, KAK and KNY for the geomagnetic storm of September 26, 1989.

Magnetogram for 1989 Oct. 20-22

at Memambetsu(MMB), Kakioka(KAK), Kanoya(KNY)

Upward: increase(H), westward(D), downward(Z)

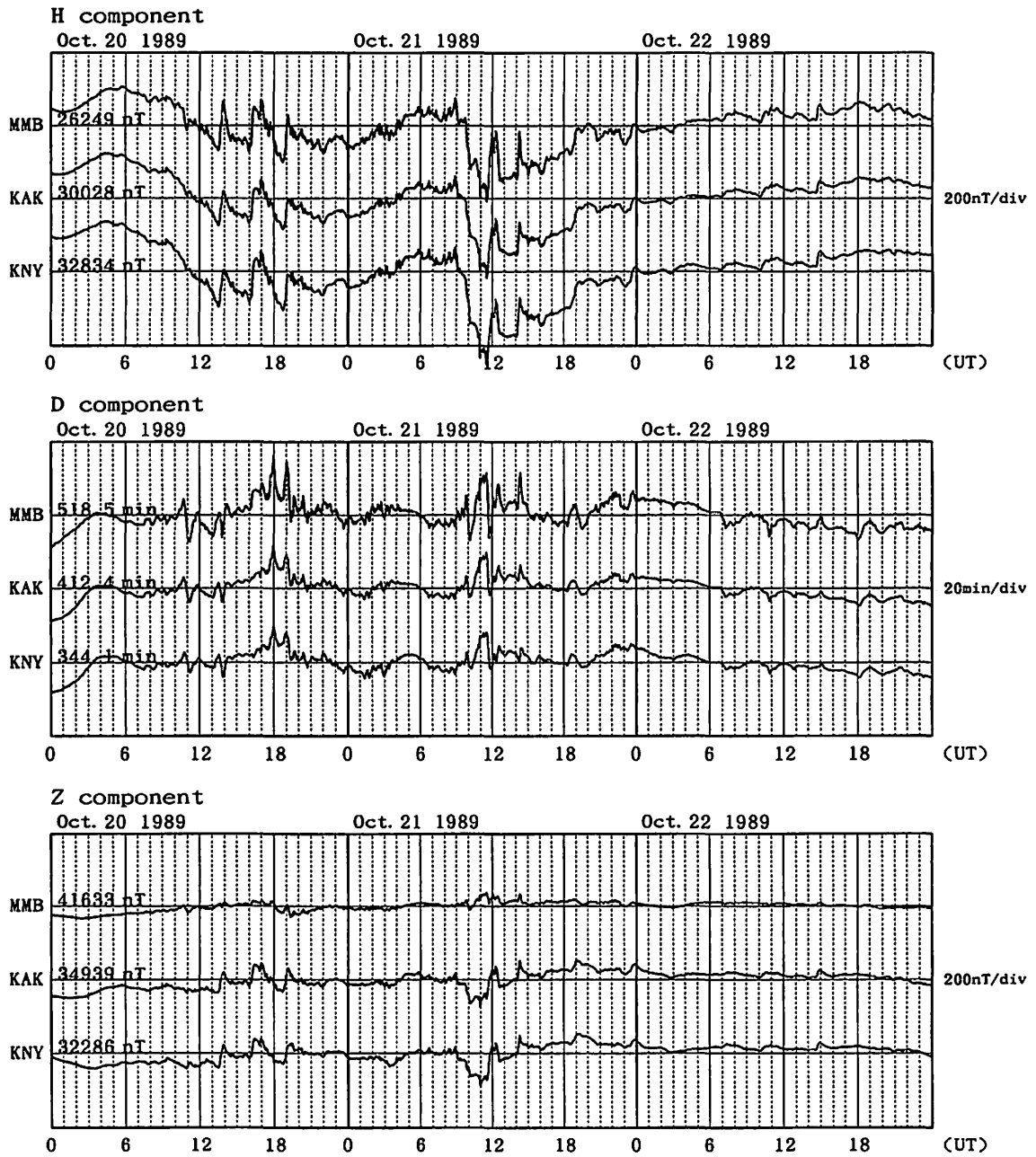


Fig. A-28(a) Magnetic records at MMB, KAK and KNY for the geomagnetic storm of October 20, 1989.

Magnetogram for 1989 Oct. 23-25

at Memambetsu(MMB), Kakioka(KAK), Kanoya(KNY)

Upward: increase(H), westward(D), downward(Z)

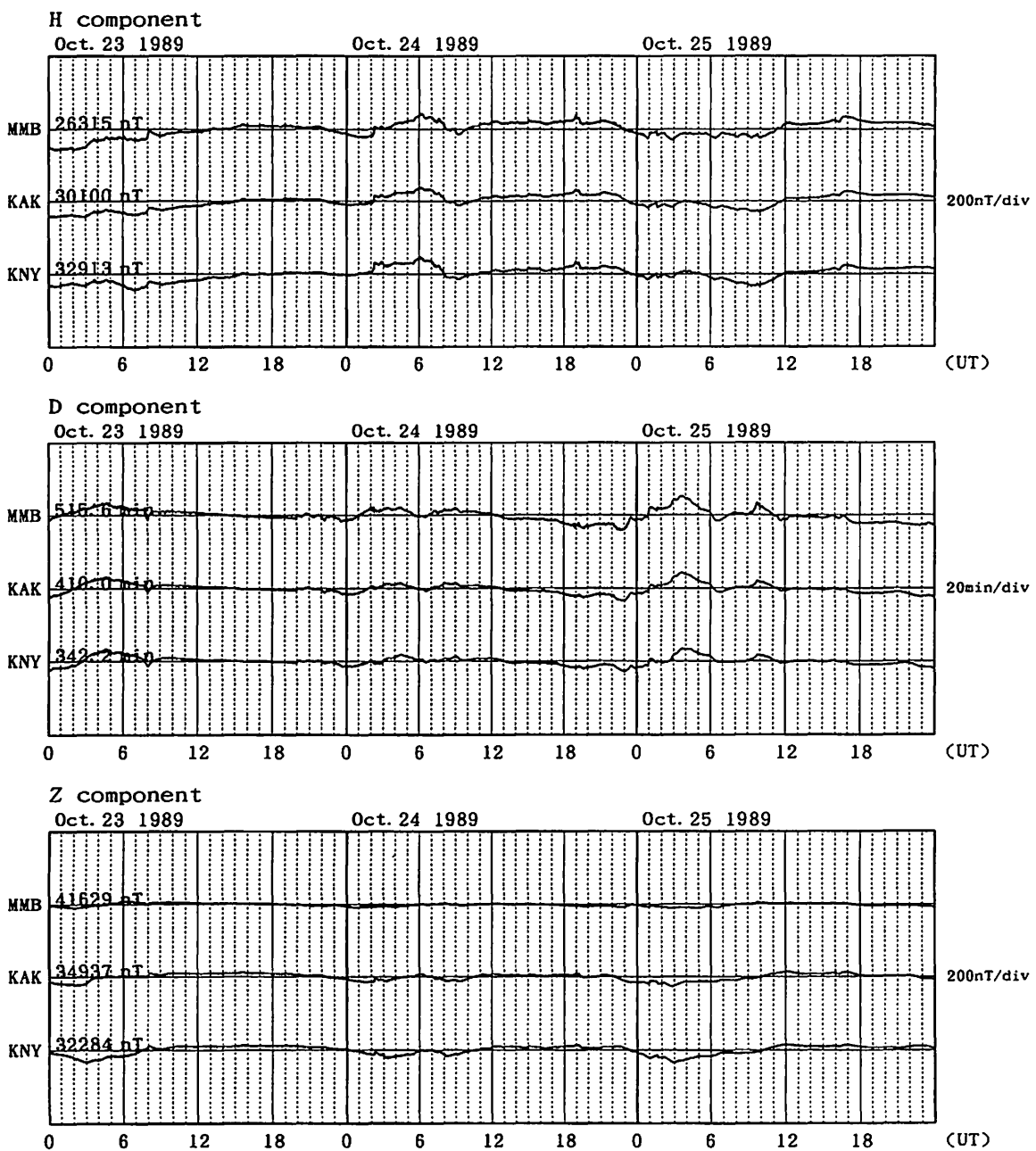


Fig. A-28(b) Magnetic records at MMB, KAK and KNY for the geomagnetic storm of October 20, 1989 (succeeding Fig. A-28(a)).

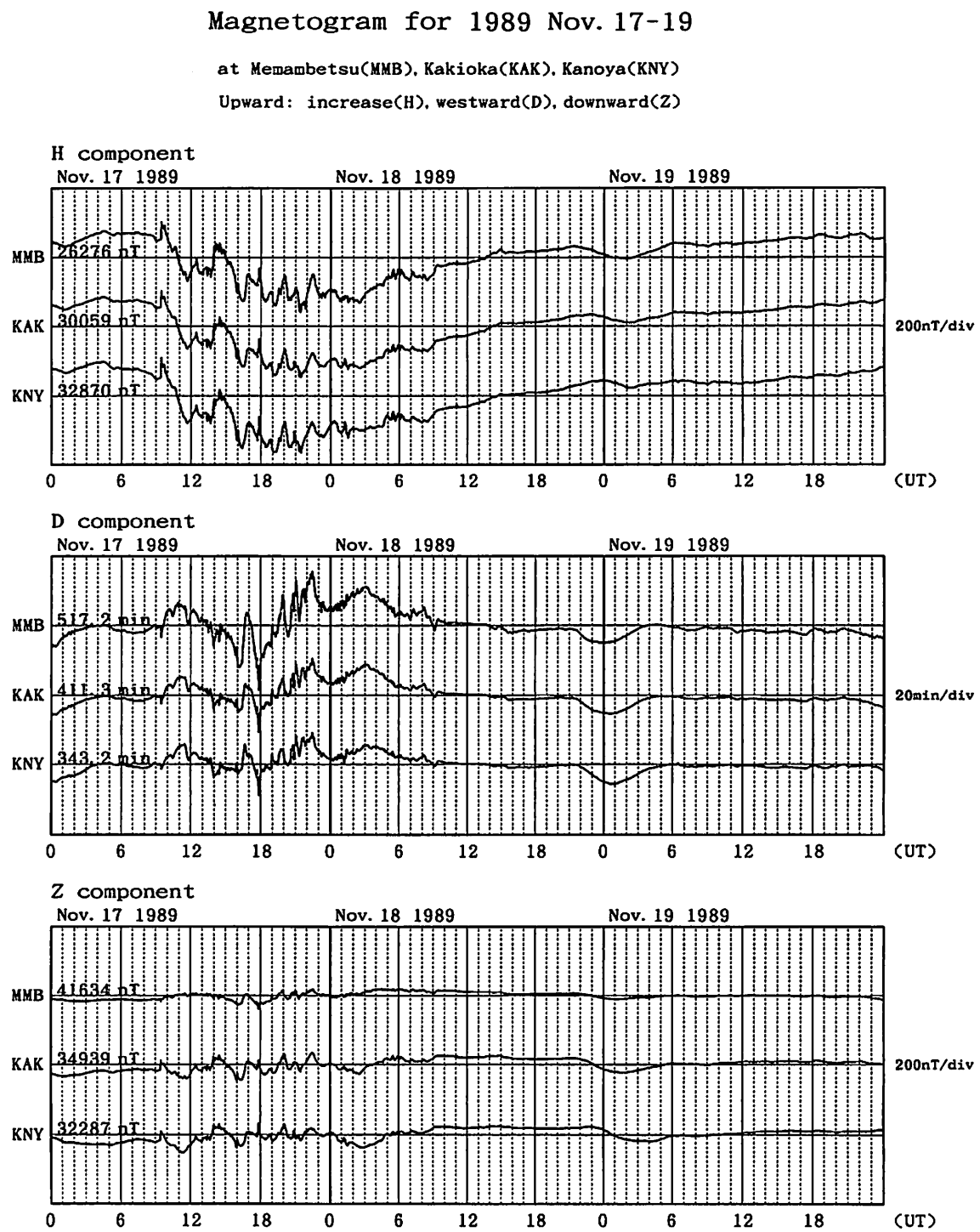


Fig. A-29 Magnetic records at MMB, KAK and KNY for the geomagnetic storm of November 17, 1989.

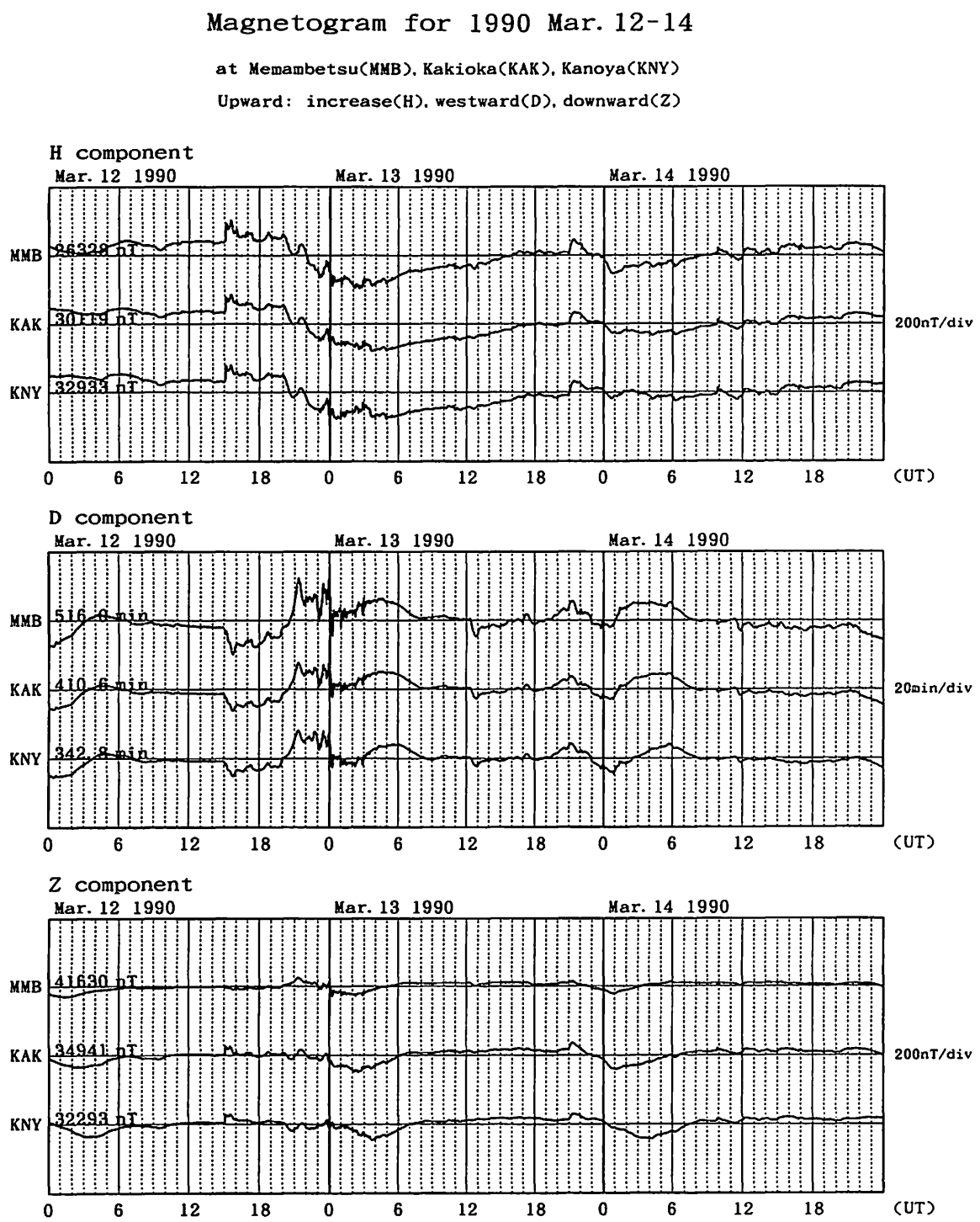


Fig. A-30 Magnetic records at MMB, KAK and KNY for the geomagnetic storm of March 12, 1990.

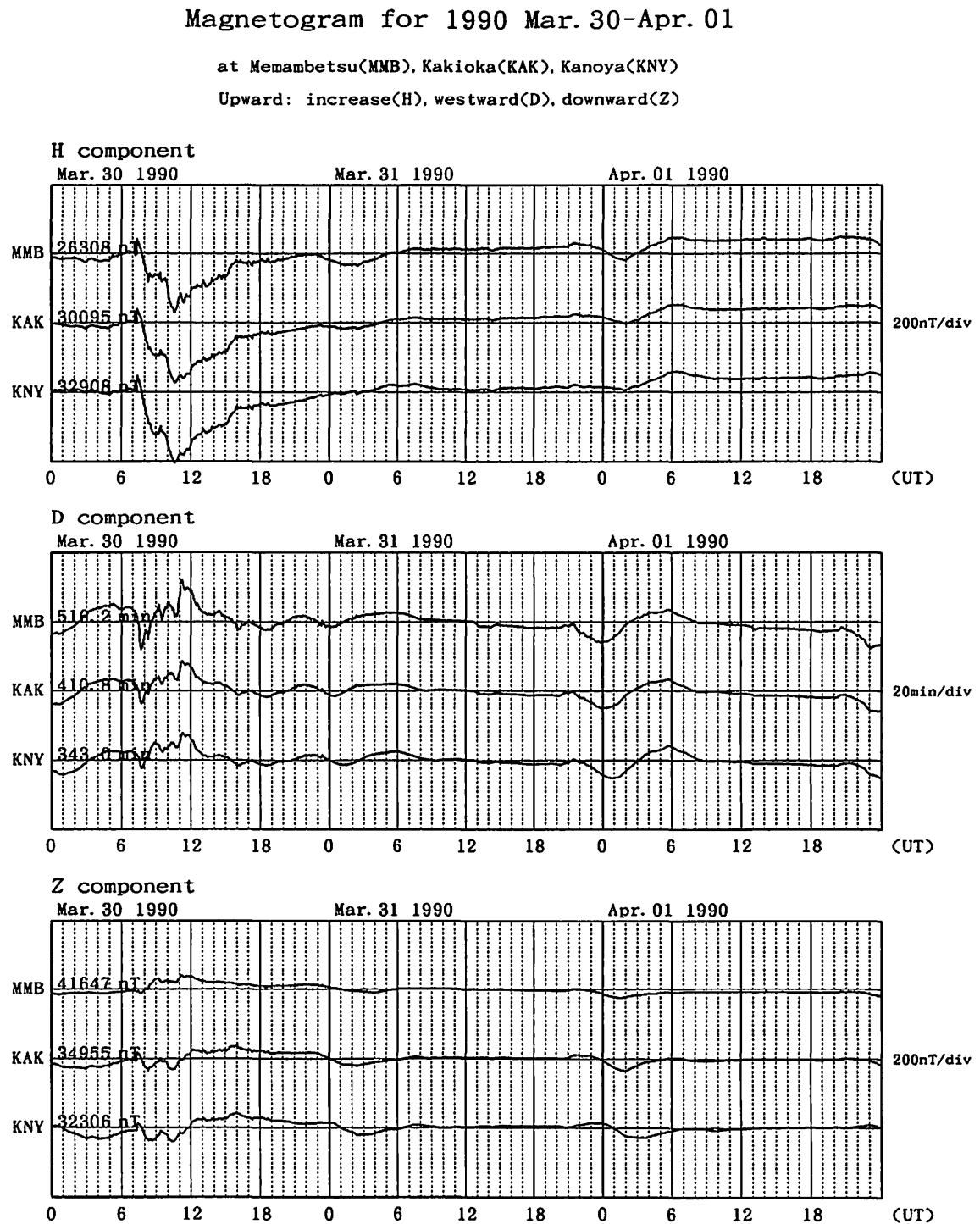


Fig. A-31 Magnetic records at MMB, KAK and KNY for the geomagnetic storm of March 30, 1990.

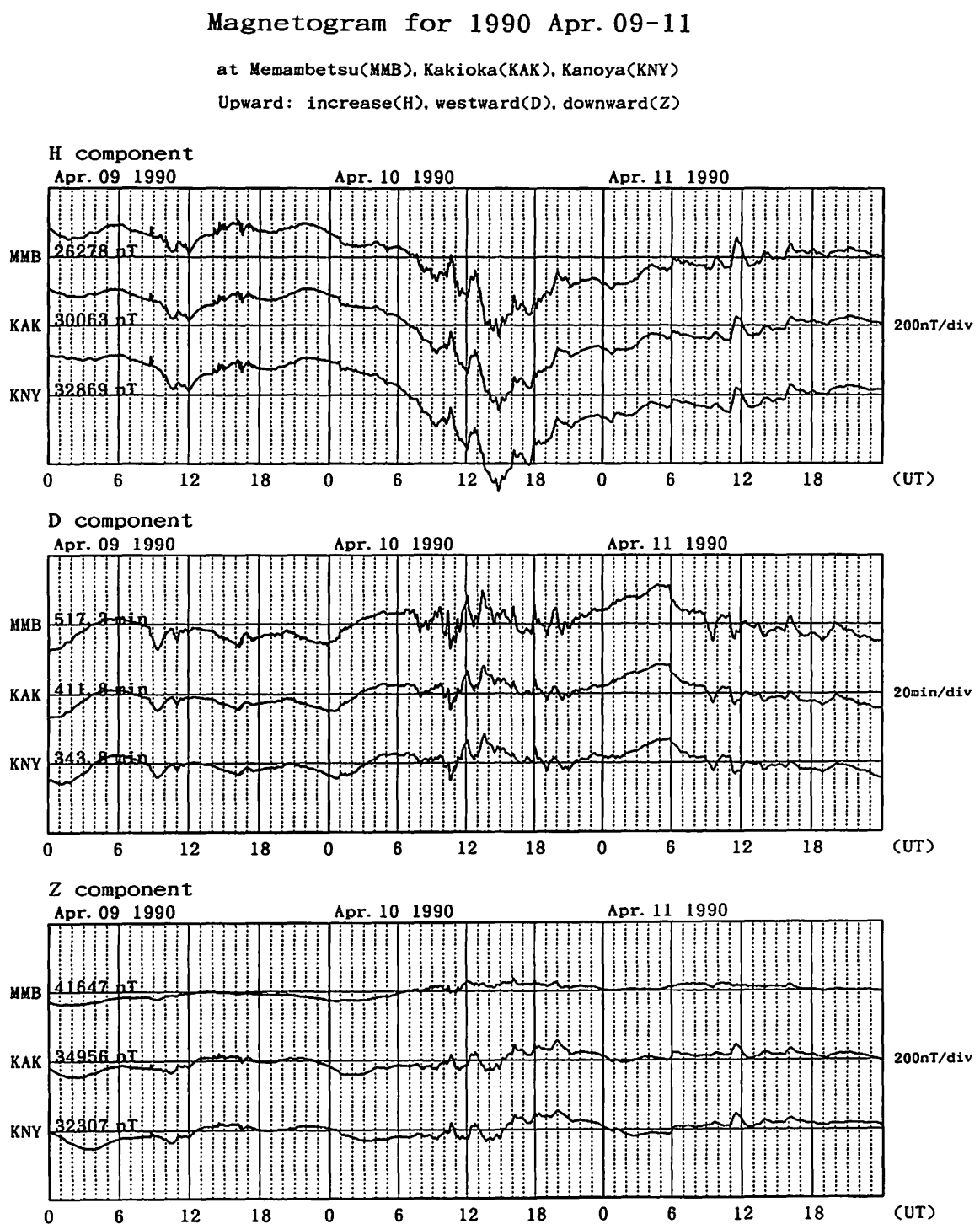


Fig. A-32 Magnetic records at MMB, KAK and KNY for the geomagnetic storm of April 9, 1990.

Magnetogram for 1990 Apr. 12-14

at Memambetsu(MMB), Kakioka(KAK), Kanoya(KNY)

Upward: increase(H), westward(D), downward(Z)

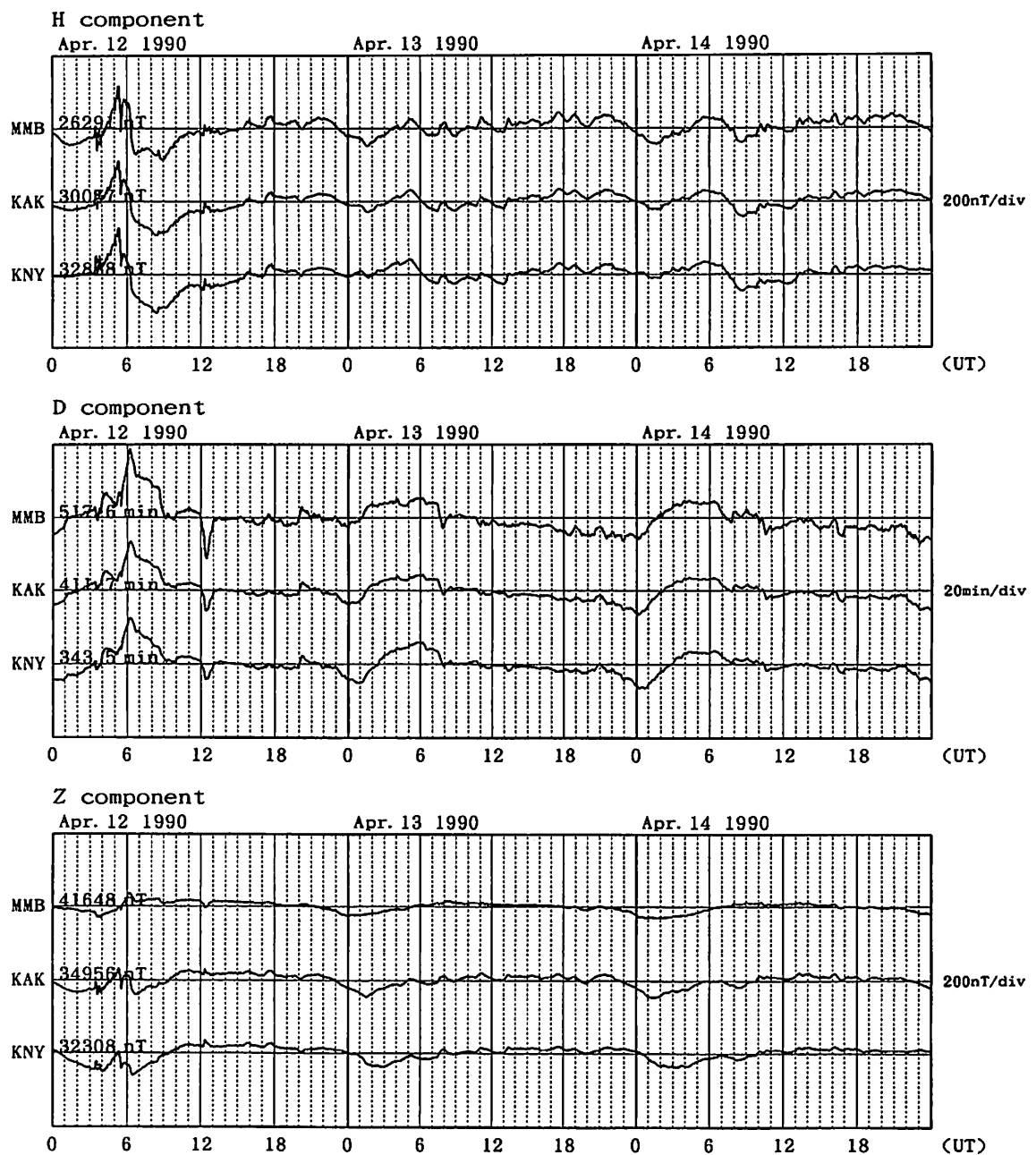


Fig. A-33 Magnetic records at MMB, KAK and KNY for the geomagnetic storm of April 12, 1990.

Magnetogram for 1990 Apr. 17-19

at Memambetsu(MMB), Kakioka(KAK), Kanoya(KNY), Chichijima(CBI)

Upward: increase(H), westward(D), downward(Z)

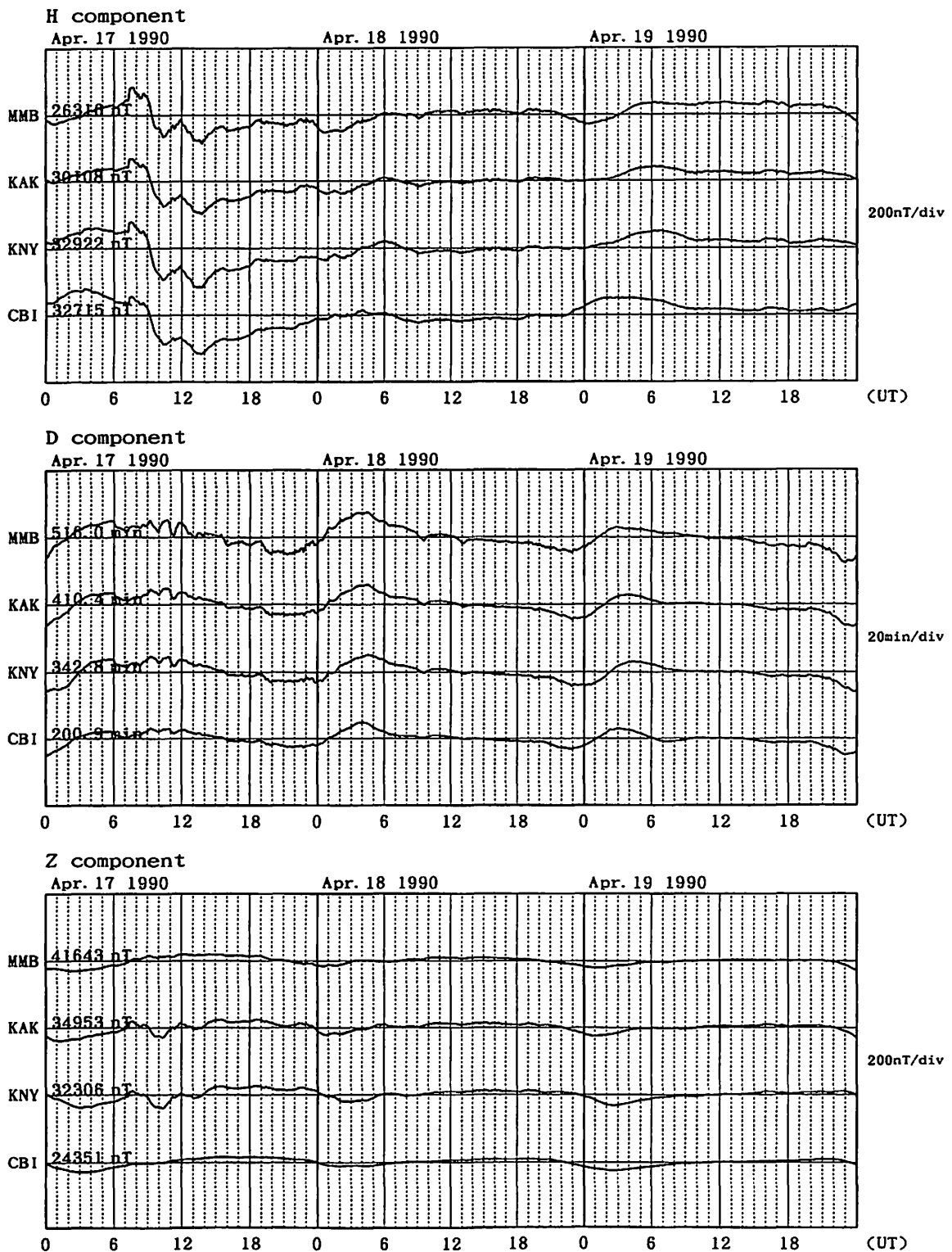


Fig. A-34 Magnetic records at MMB, KAK, KNY and CBI for the geomagnetic storm of April 17, 1990.

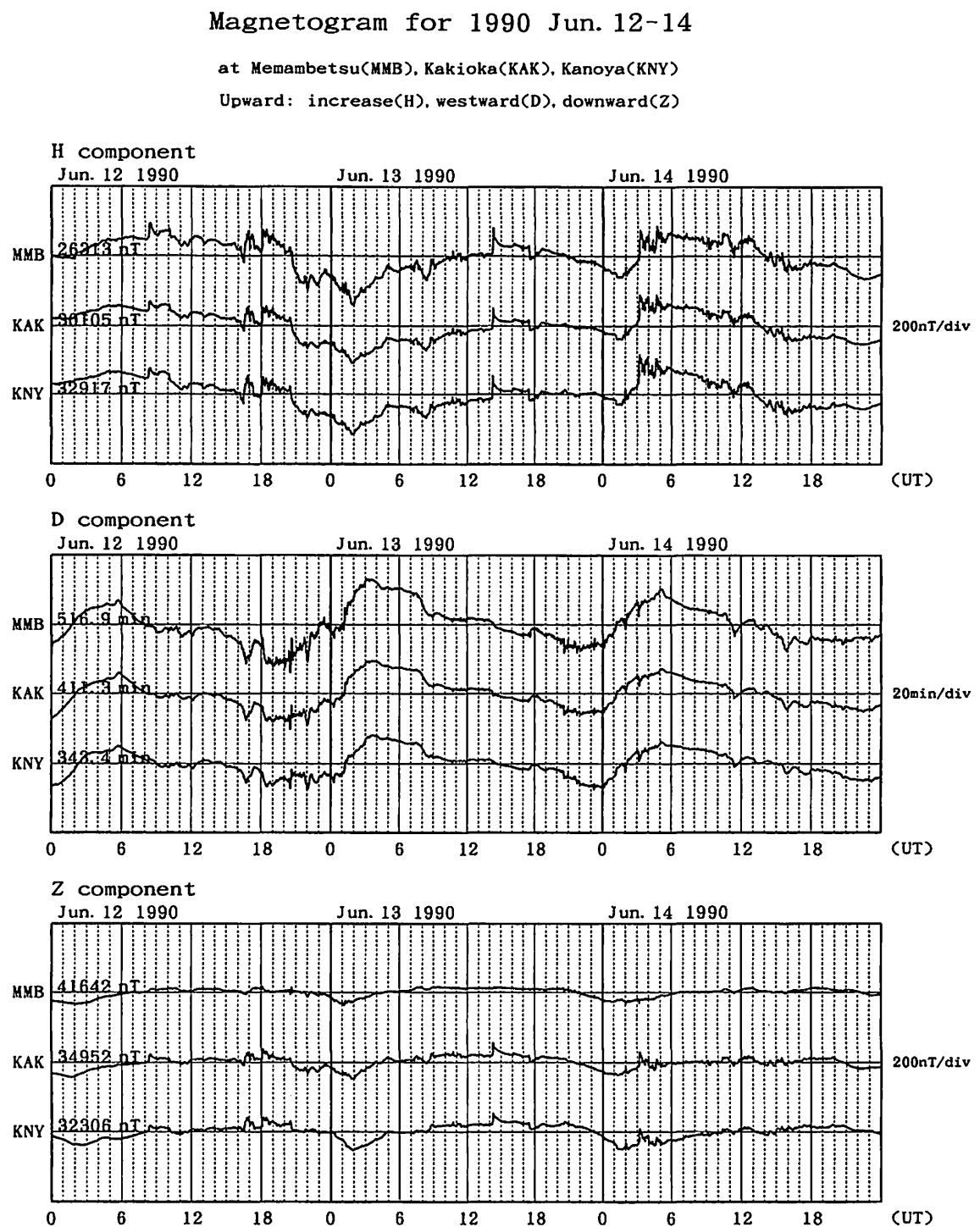


Fig. A-35 Magnetic records at MMB, KAK and KNY for the geomagnetic storm of June 12, 1990.

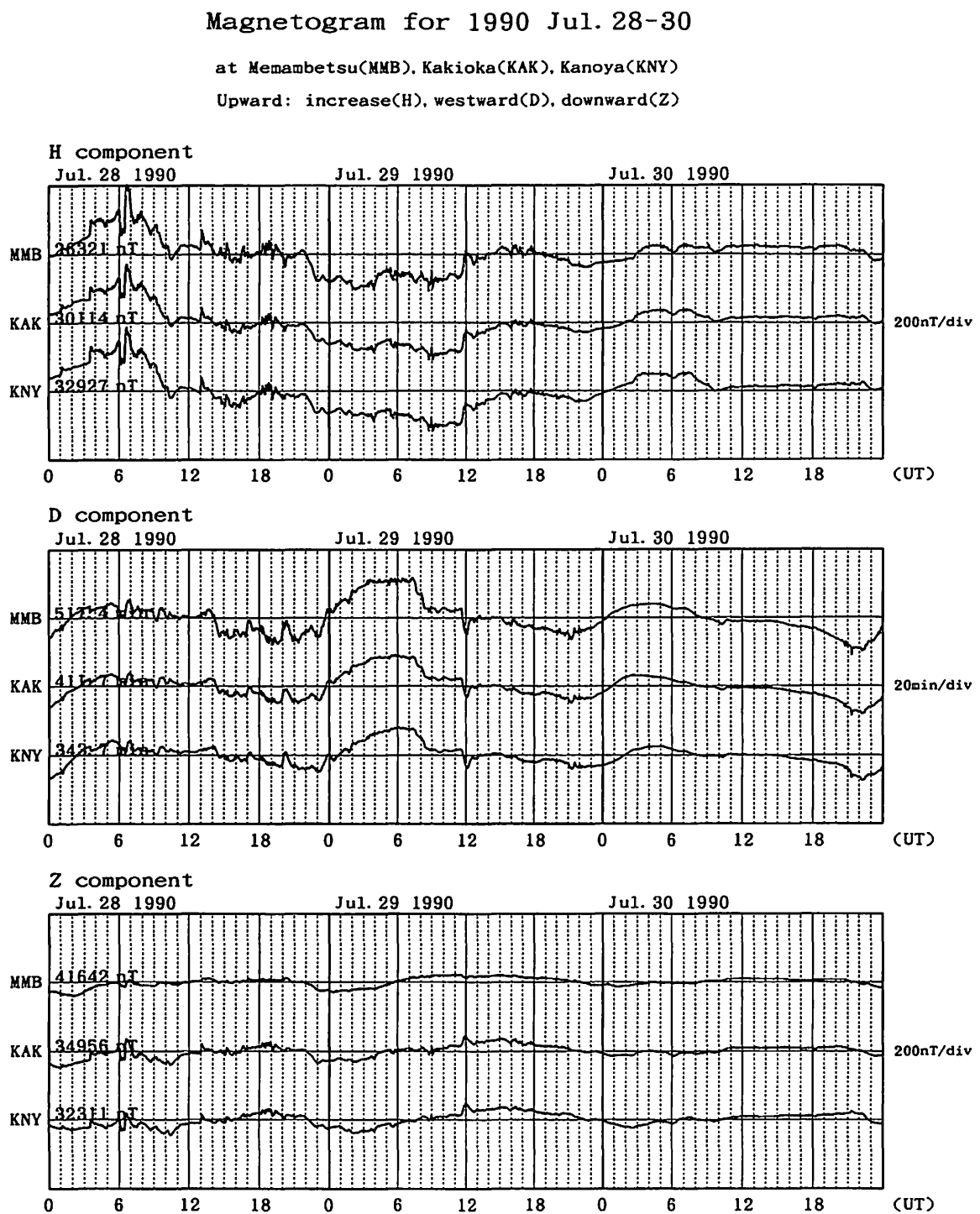


Fig. A-36 Magnetic records at MMB, KAK and KNY for the geomagnetic storm of July 28, 1990.

Magnetogram for 1990 Aug. 26-28

at Kakioka(KAK), Kanoya(KNY)

Upward: increase(H), westward(D), downward(Z)

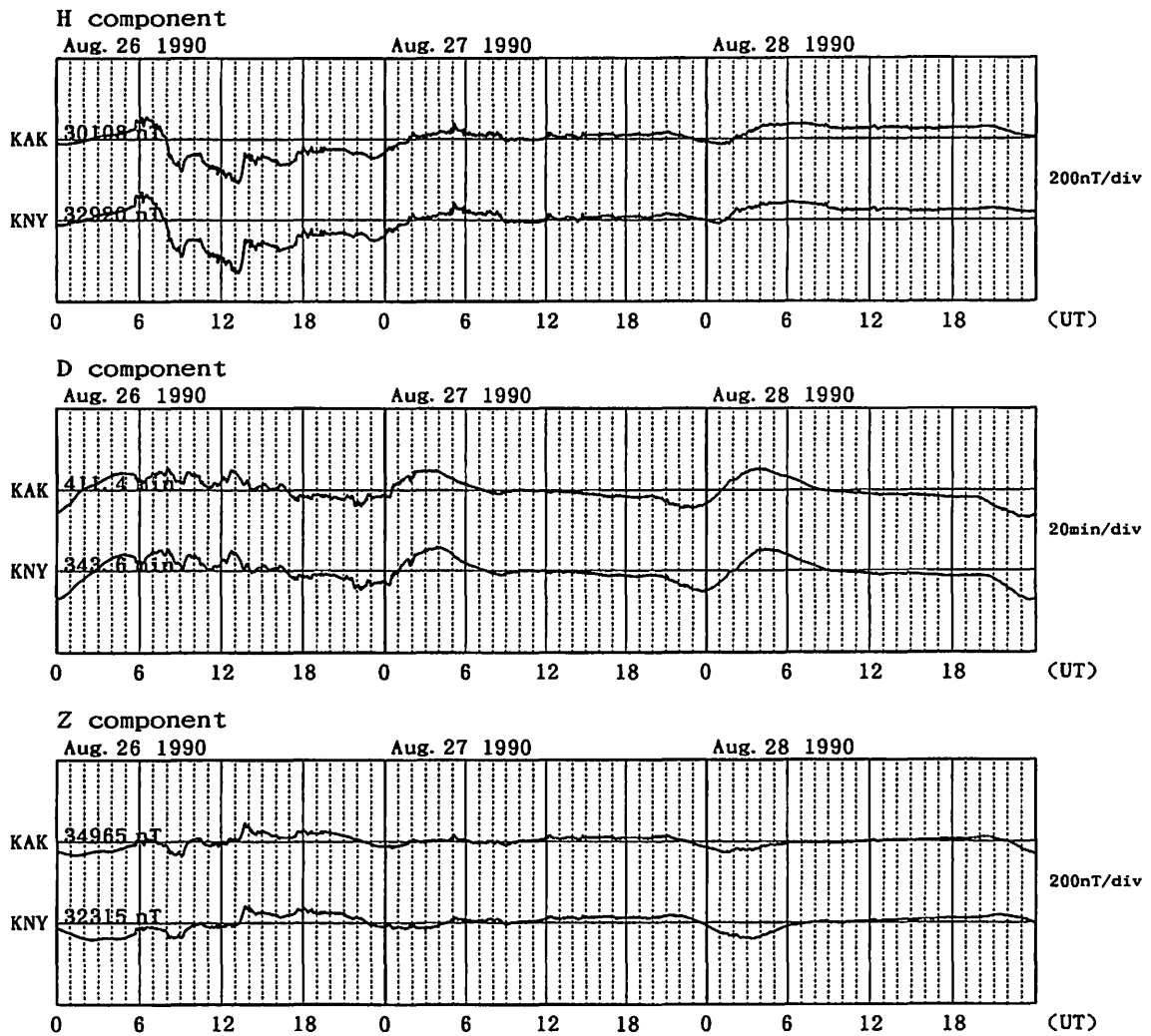


Fig. A-37 Magnetic records at KAK and KNY for the geomagnetic storm of August 26, 1990.

Magnetogram for 1990 Oct. 09-11

at Memambetsu(MMB), Kakioka(KAK), Kanoya(KNY), Chichijima(CBI)

Upward: increase(H), westward(D), downward(Z)

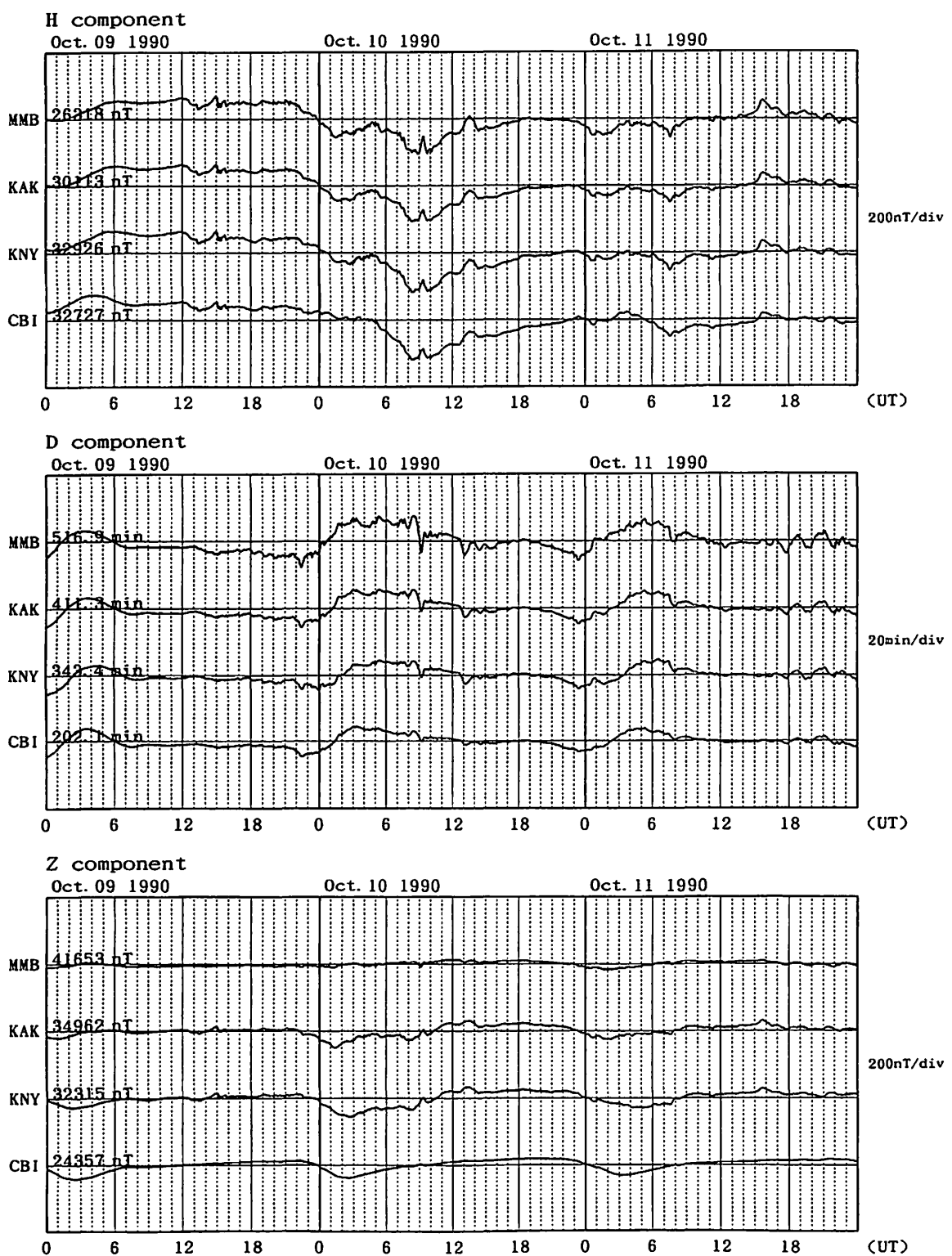


Fig. A-38 Magnetic records at MMB, KAK, KNY and CBI for the geomagnetic storm of October 17, 1990.

Magnetogram for 1991 Mar. 24-26

at Memambetsu(MMB), Kakioka(KAK), Kanoya(KNY)

Upward: increase(H), westward(D), downward(Z)

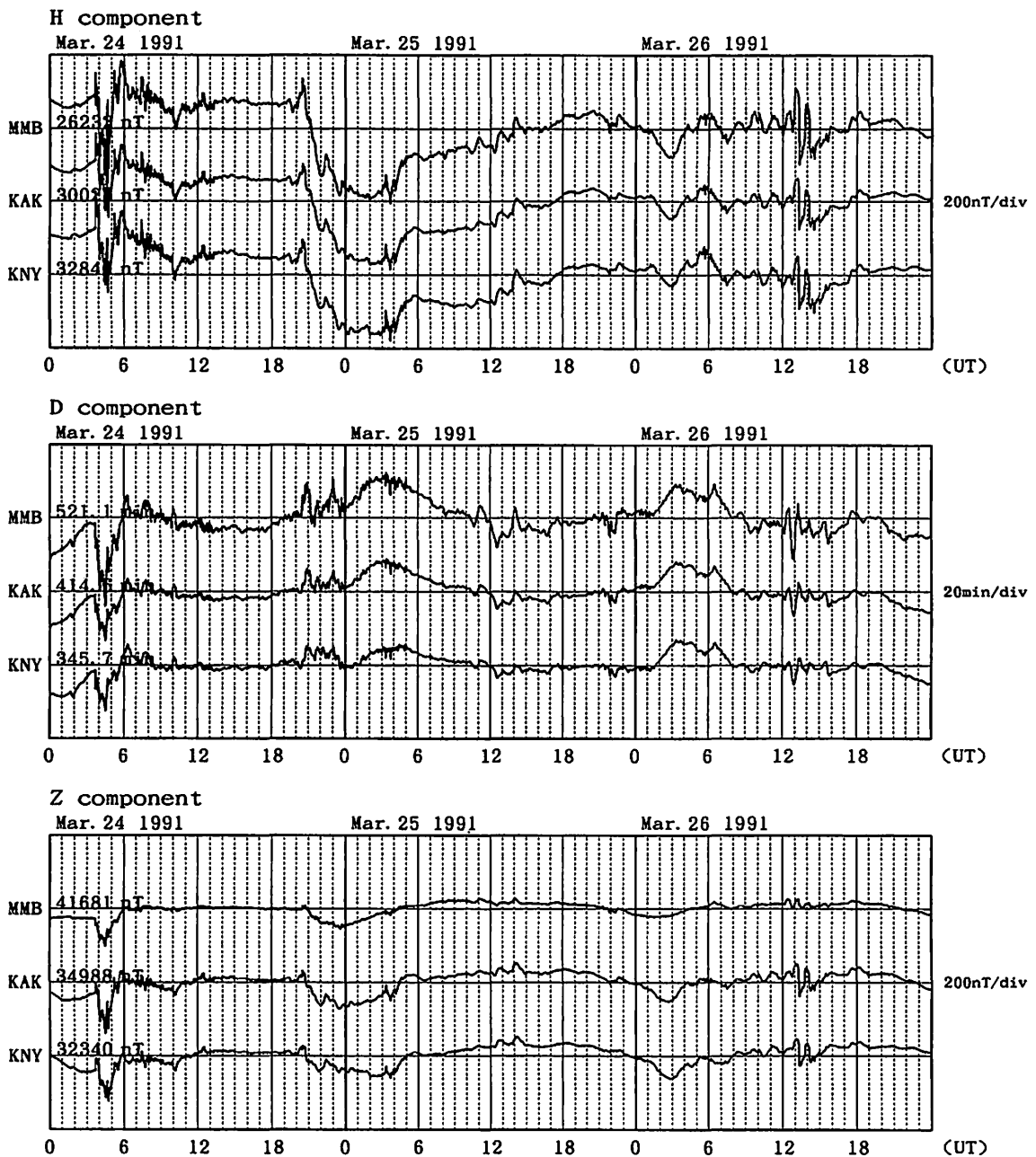


Fig. A-39(a) Magnetic records at MMB, KAK and KNY for the geomagnetic storm of March 24, 1991.

Magnetogram for 1991 Mar. 27-29

at Memambetsu(MMB), Kakioka(KAK), Kanoya(KNY)

Upward: increase(H), westward(D), downward(Z)

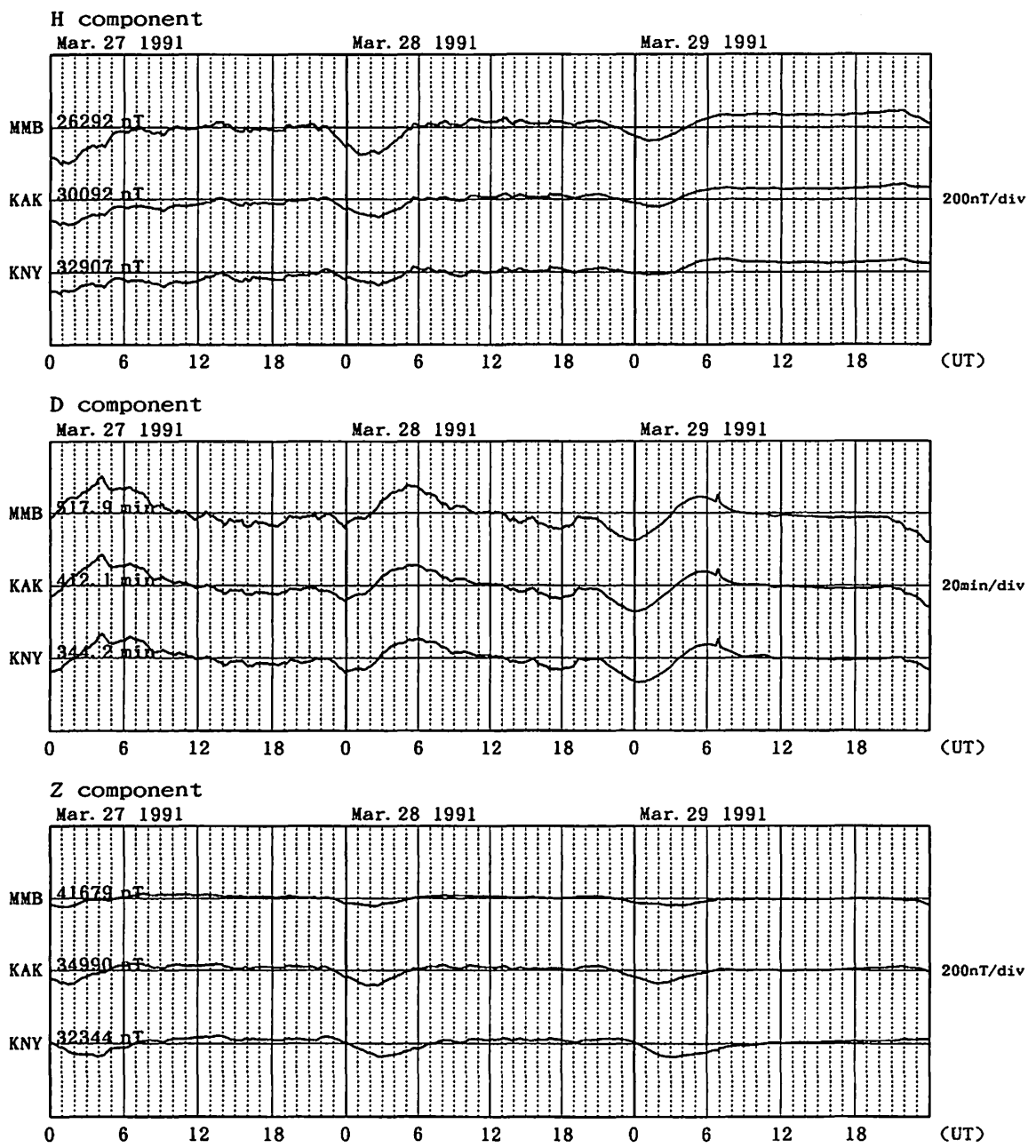


Fig. A-39(b) Magnetic records at MMB, KAK and KNY for the geomagnetic storm of March 24, 1991 (succeeding Fig. A-39(a)).

Magnetogram for 1991 Apr. 04-06

at Memambetsu(MMB), Kakioka(KAK), Kanoya(KNY), Chichijima(CBI)

Upward: increase(H), westward(D), downward(Z)

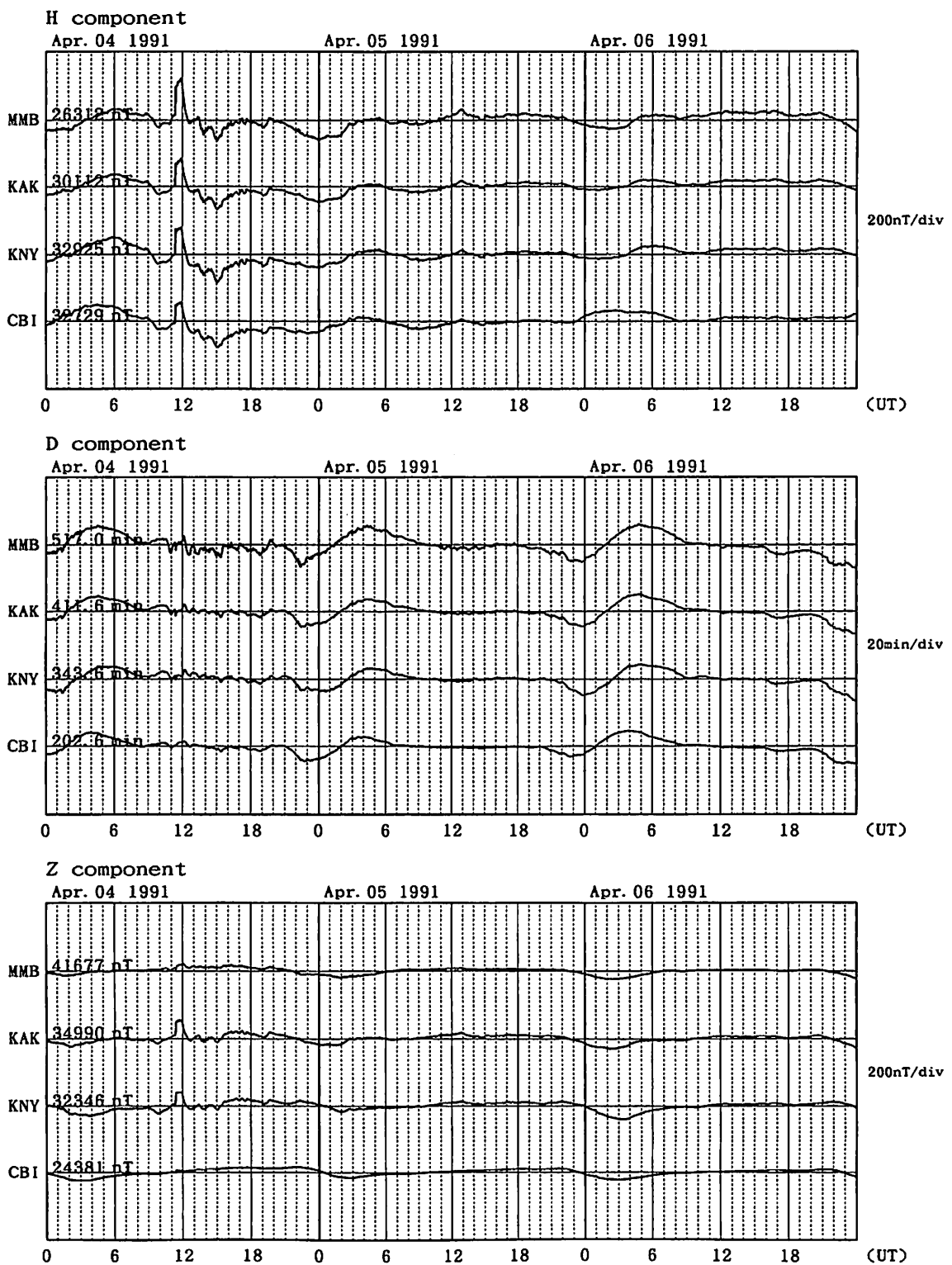


Fig. A-40 Magnetic records at MMB, KAK, KNY and CBI for the geomagnetic storm of April 4, 1991.

Magnetogram for 1991 May 16-18

at Memambetsu(MMB), Kakicka(KAK), Kanoya(KNY)

Upward: increase(H), westward(D), downward(Z)

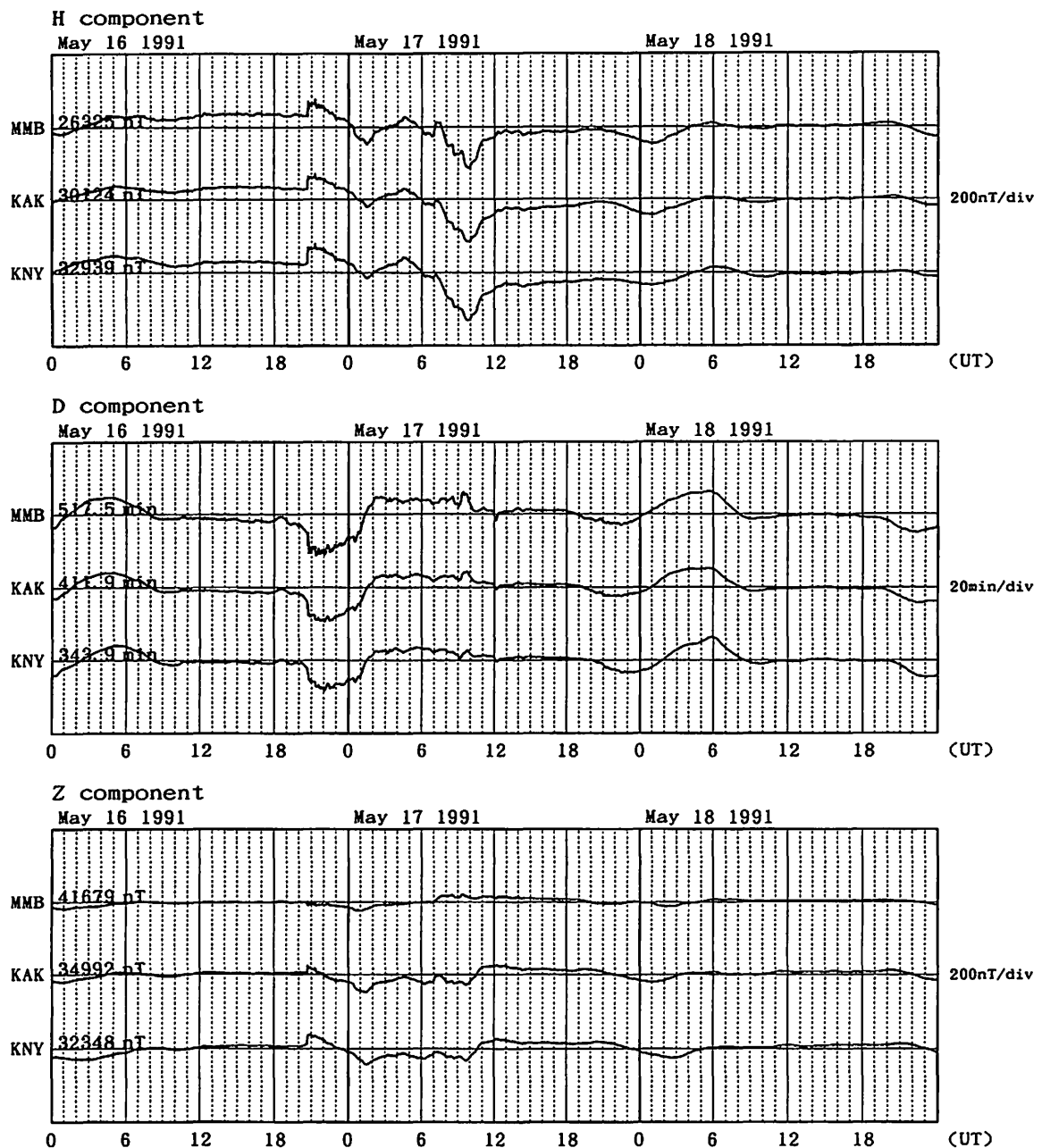


Fig. A-41 Magnetic records at MMB, KAK and KNY for the geomagnetic storm of May 16, 1991.

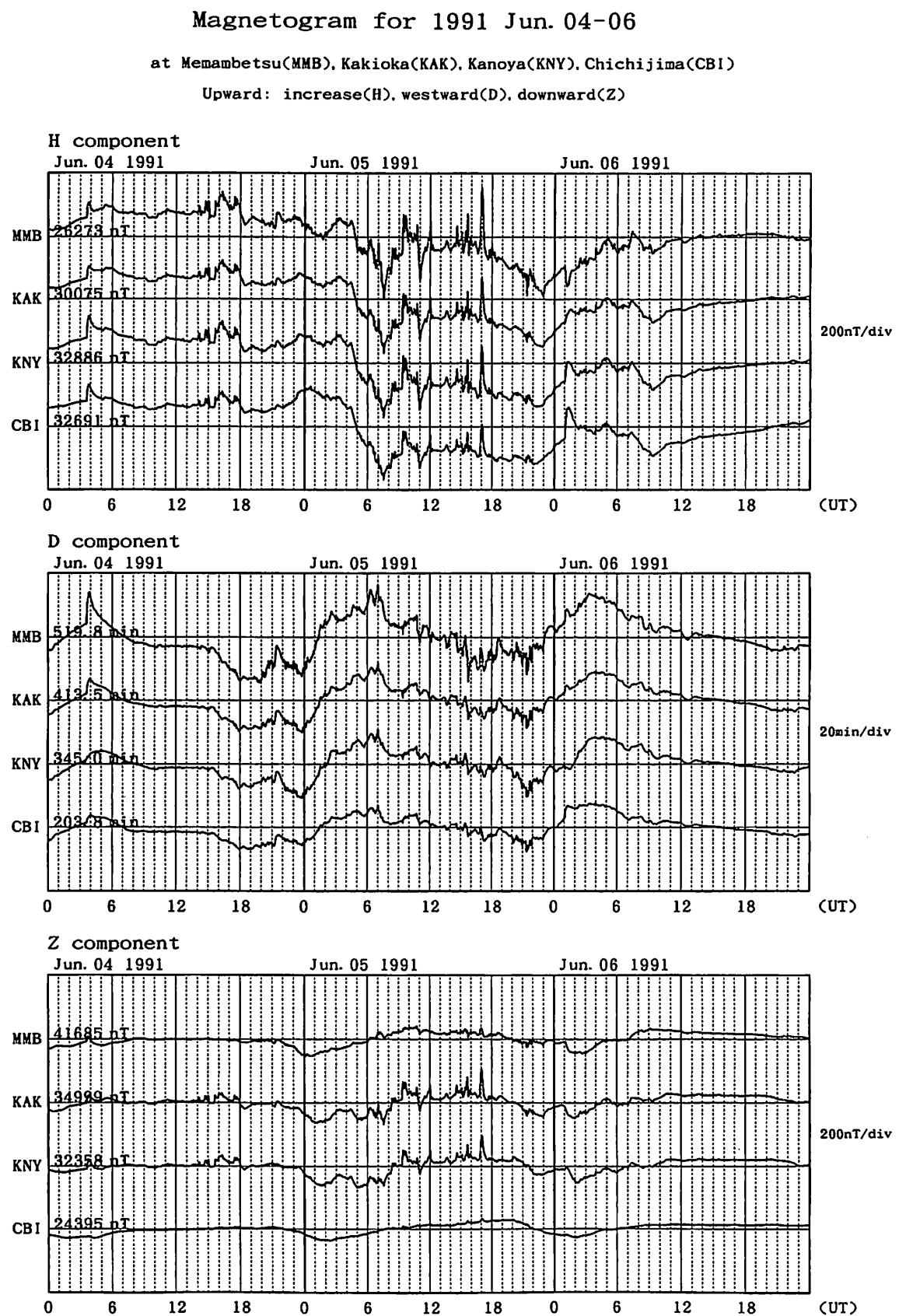


Fig. A-42 Magnetic records at MMB, KAK, KNY and CBI for the geomagnetic storm of June 4, 1991.

Magnetogram for 1991 Jun. 09-11

at Memambetsu(MMB), Kakioka(KAK), Kanoya(KNY)

Upward: increase(H), westward(D), downward(Z)

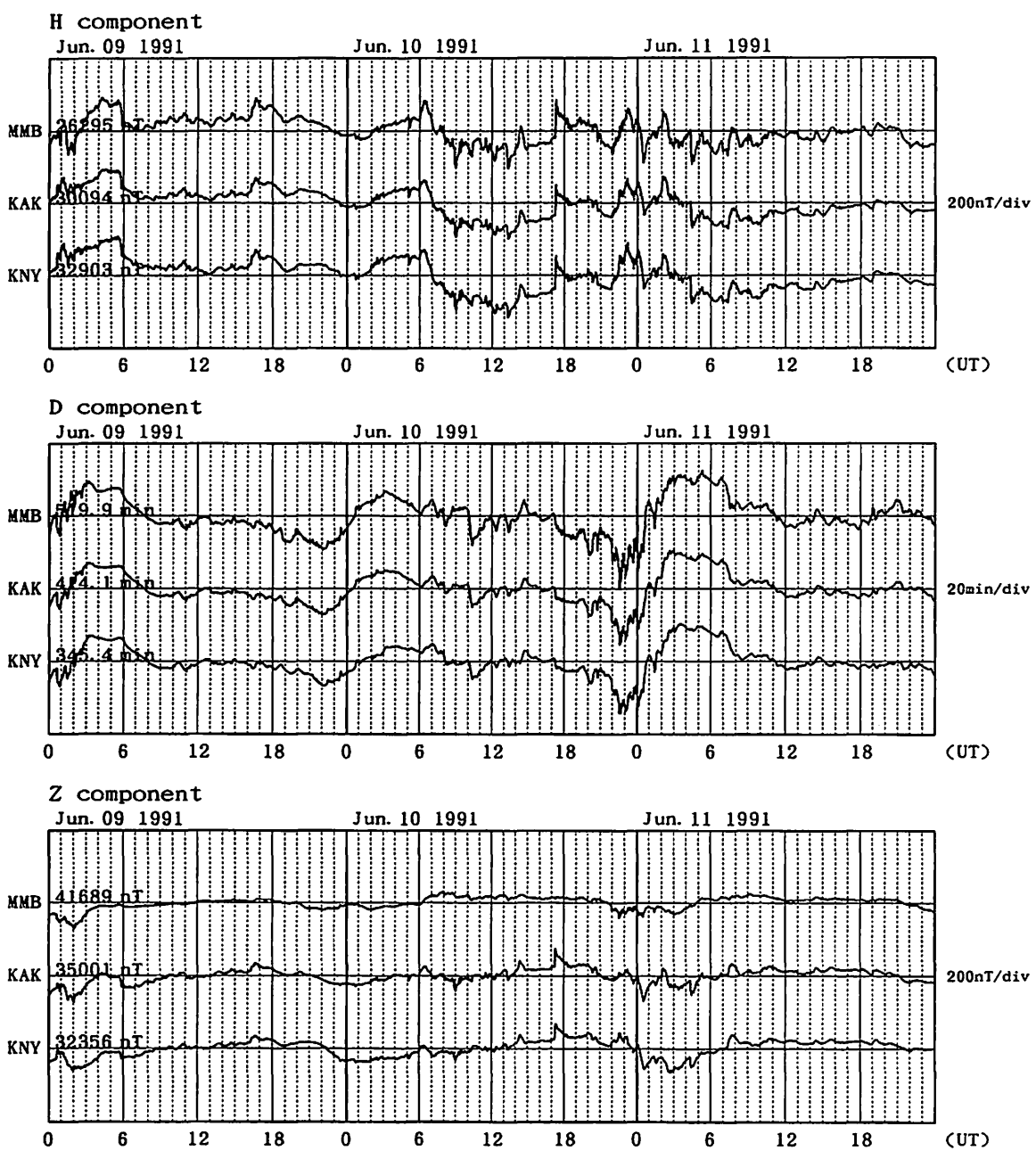


Fig. A-43 Magnetic records at MMB, KAK and KNY for the geomagnetic storm of June 9, 1991.

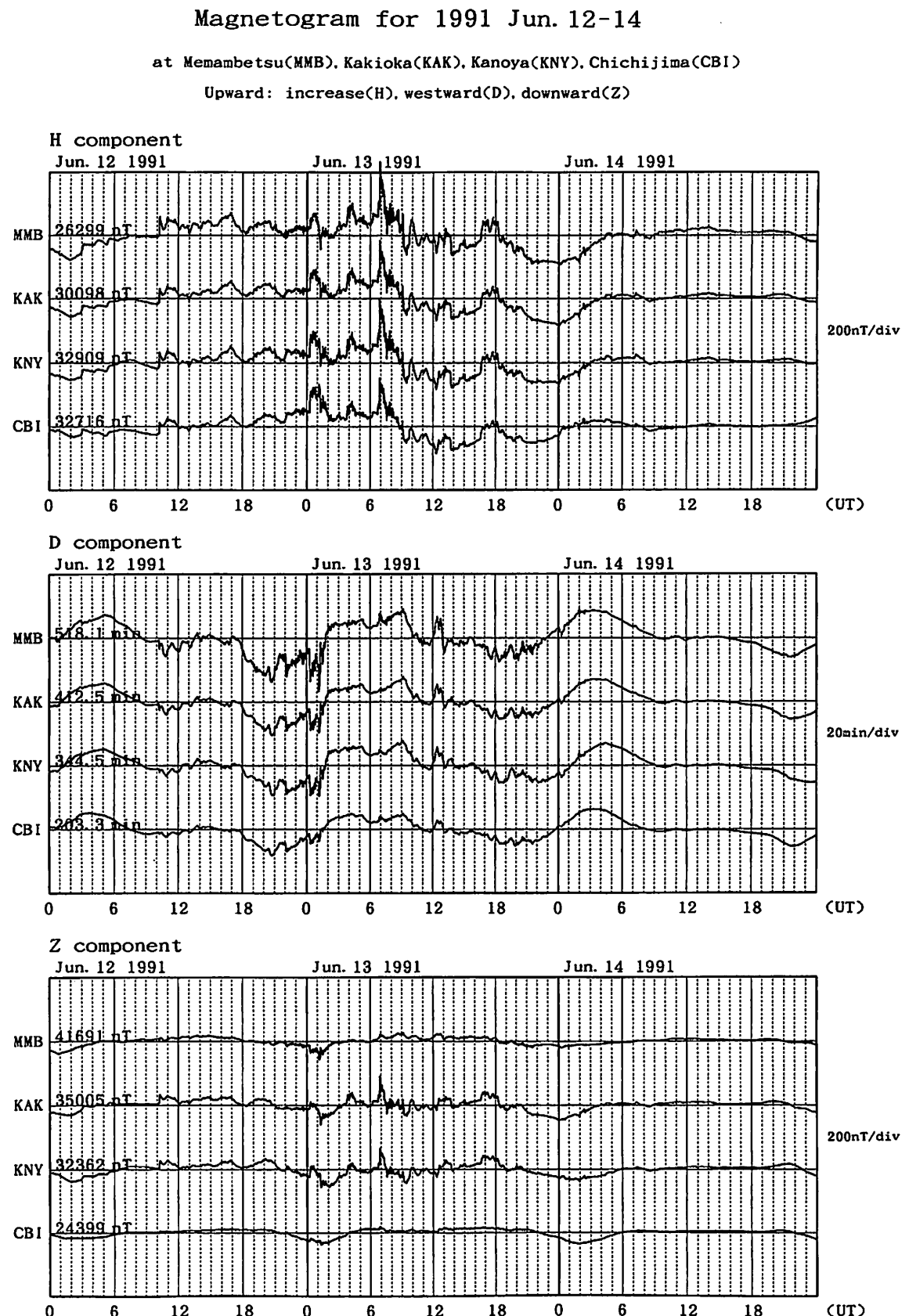


Fig. A-44 Magnetic records at MMB, KAK, KNY and CBI for the geomagnetic storm of June 12, 1991.

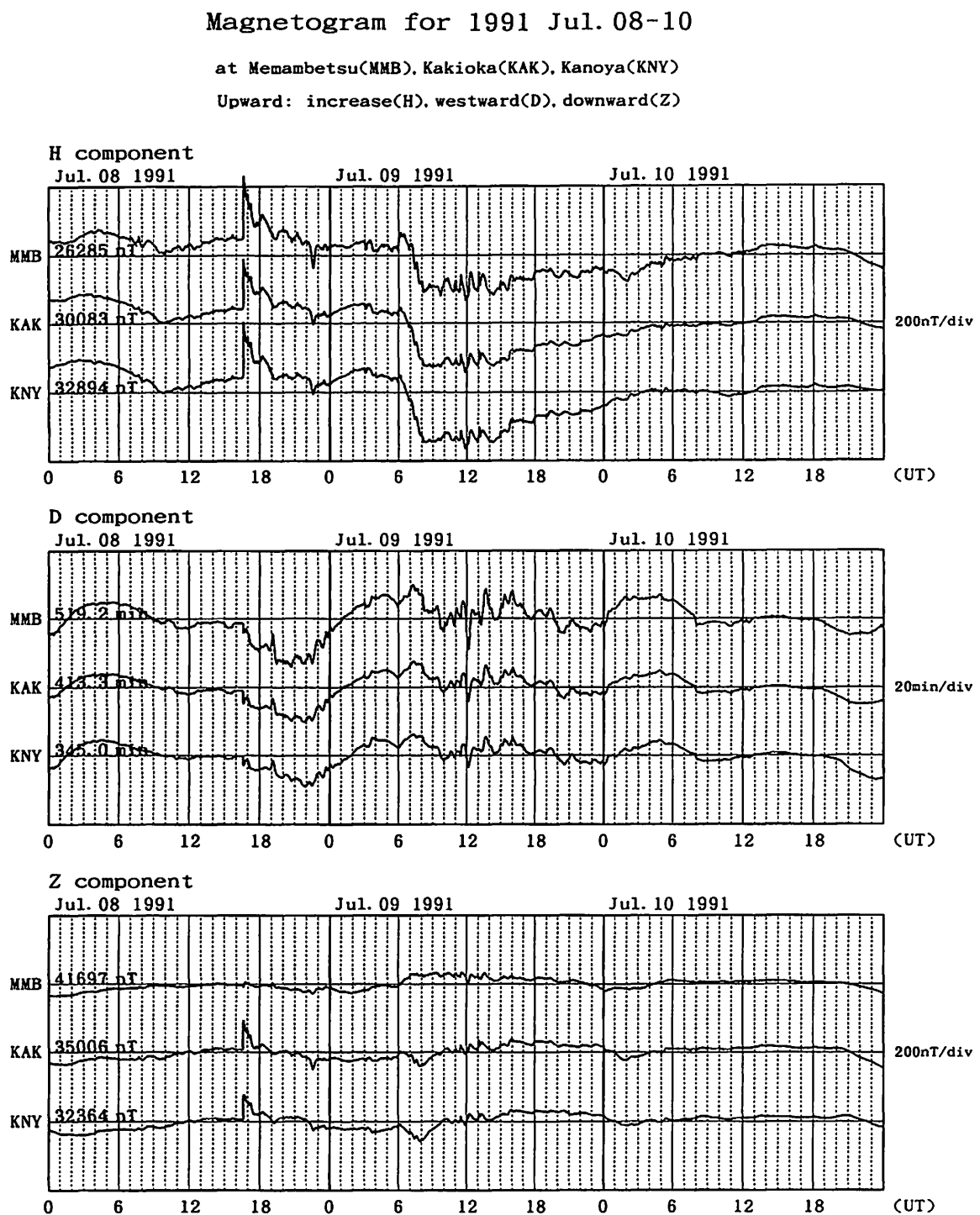


Fig. A-45 Magnetic records at MMB, KAK and KNY for the geomagnetic storm of July 8, 1991.

Magnetogram for 1991 Jul. 13-15

at Memambetsu(MMB), Kakioka(KAK), Kanoya(KNY)

Upward: increase(H), westward(D), downward(Z)

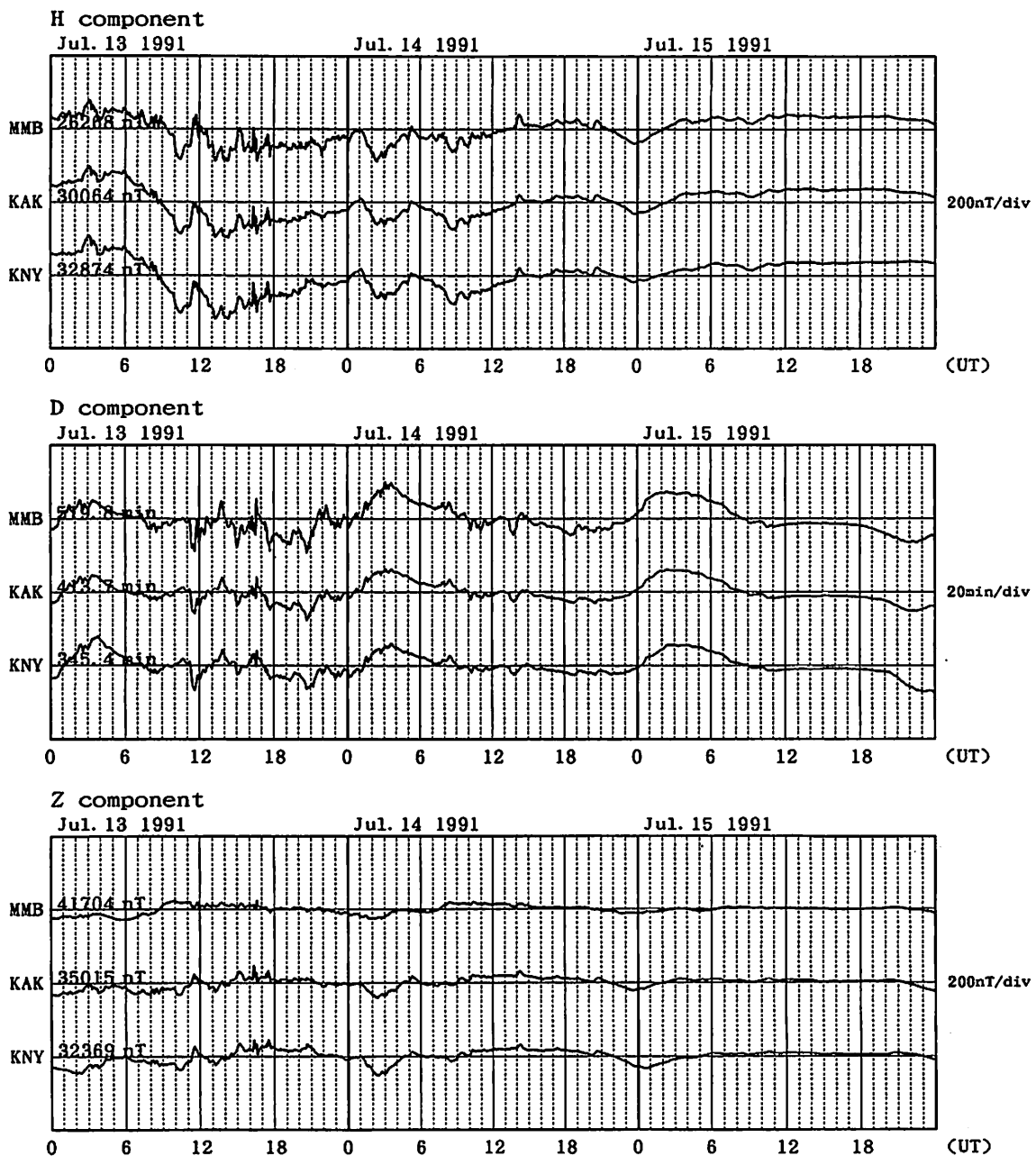


Fig. A-46 Magnetic records at MMB, KAK and KNY for the geomagnetic storm of July 13, 1991.

Magnetogram for 1991 Aug. 11-13

at Memambetsu(MMB), Kakioka(KAK), Kanoya(KNY)

Upward: increase(H), westward(D), downward(Z)

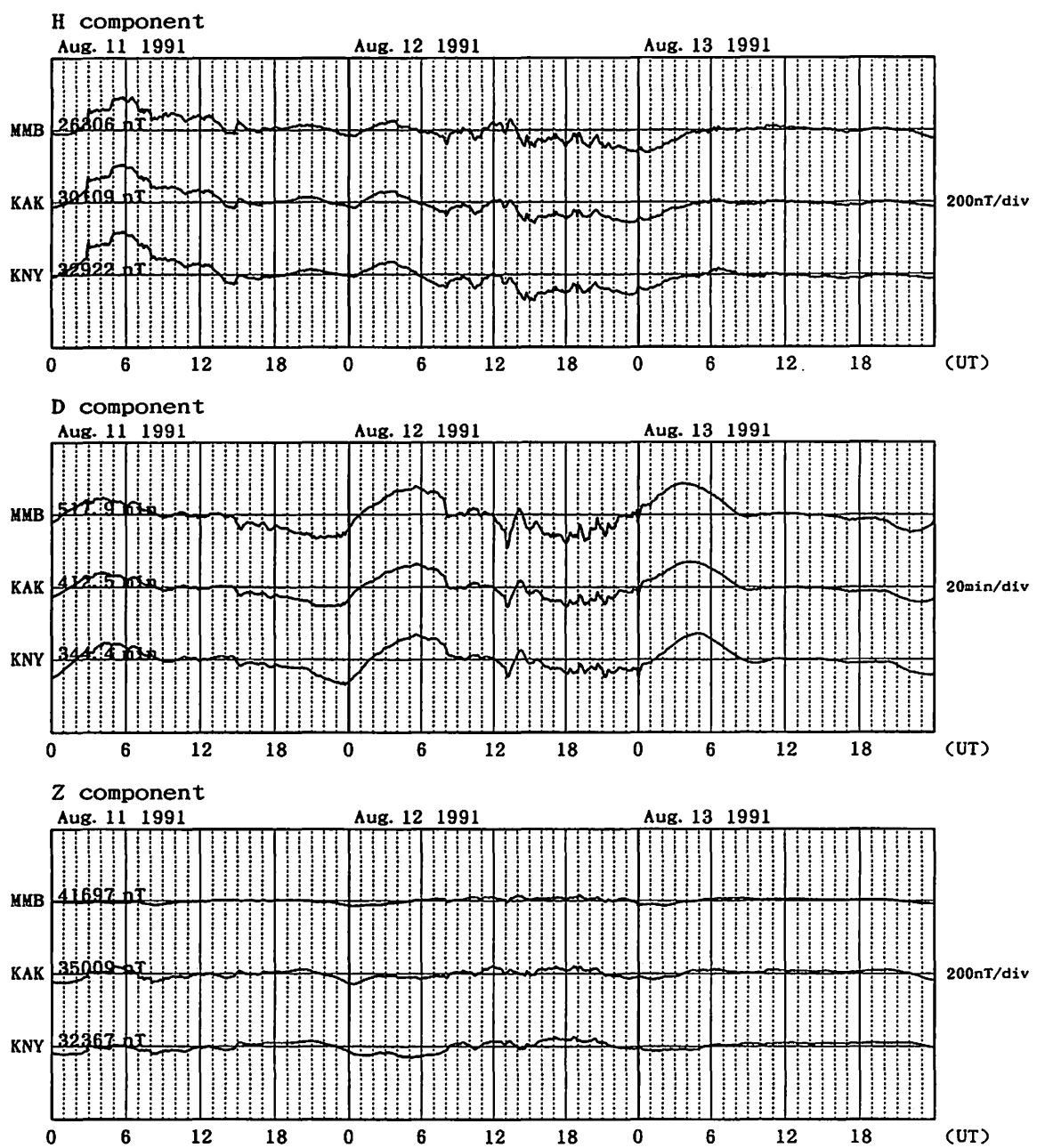


Fig. A-47 Magnetic records at MMB, KAK and KNY for the geomagnetic storm of August 11, 1991.

Magnetogram for 1991 Aug. 18-20

at Memambetsu(MMB), Kakioka(KAK), Kanoya(KNY)

Upward: increase(H), westward(D), downward(Z)

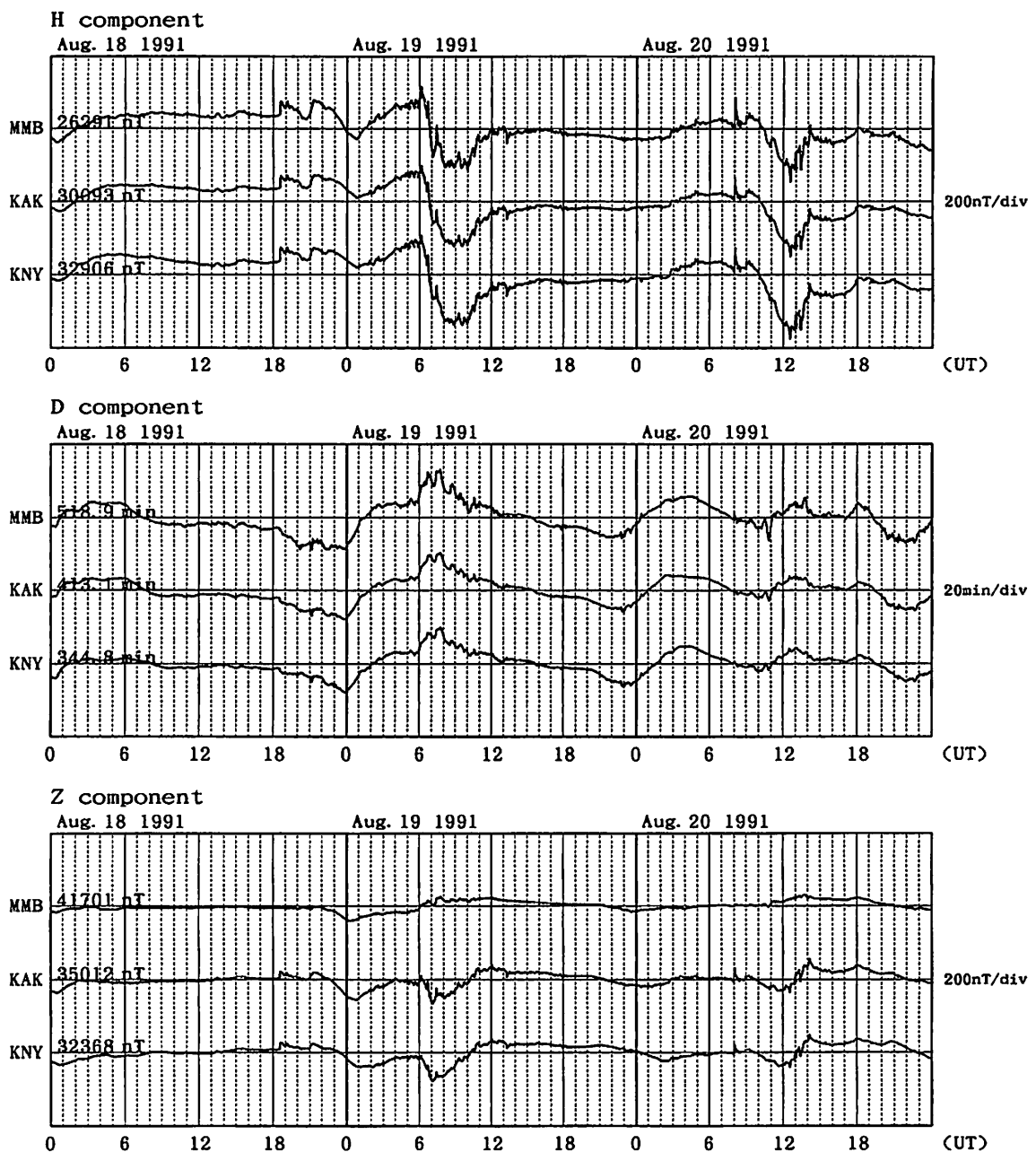


Fig. A-48 Magnetic records at MMB, KAK and KNY for the geomagnetic storm of August 18, 1991.

Magnetogram for 1991 Aug. 20-22

at Memambetsu(MMB), Kakioka(KAK), Kanoya(KNY)

Upward: increase(H), westward(D), downward(Z)

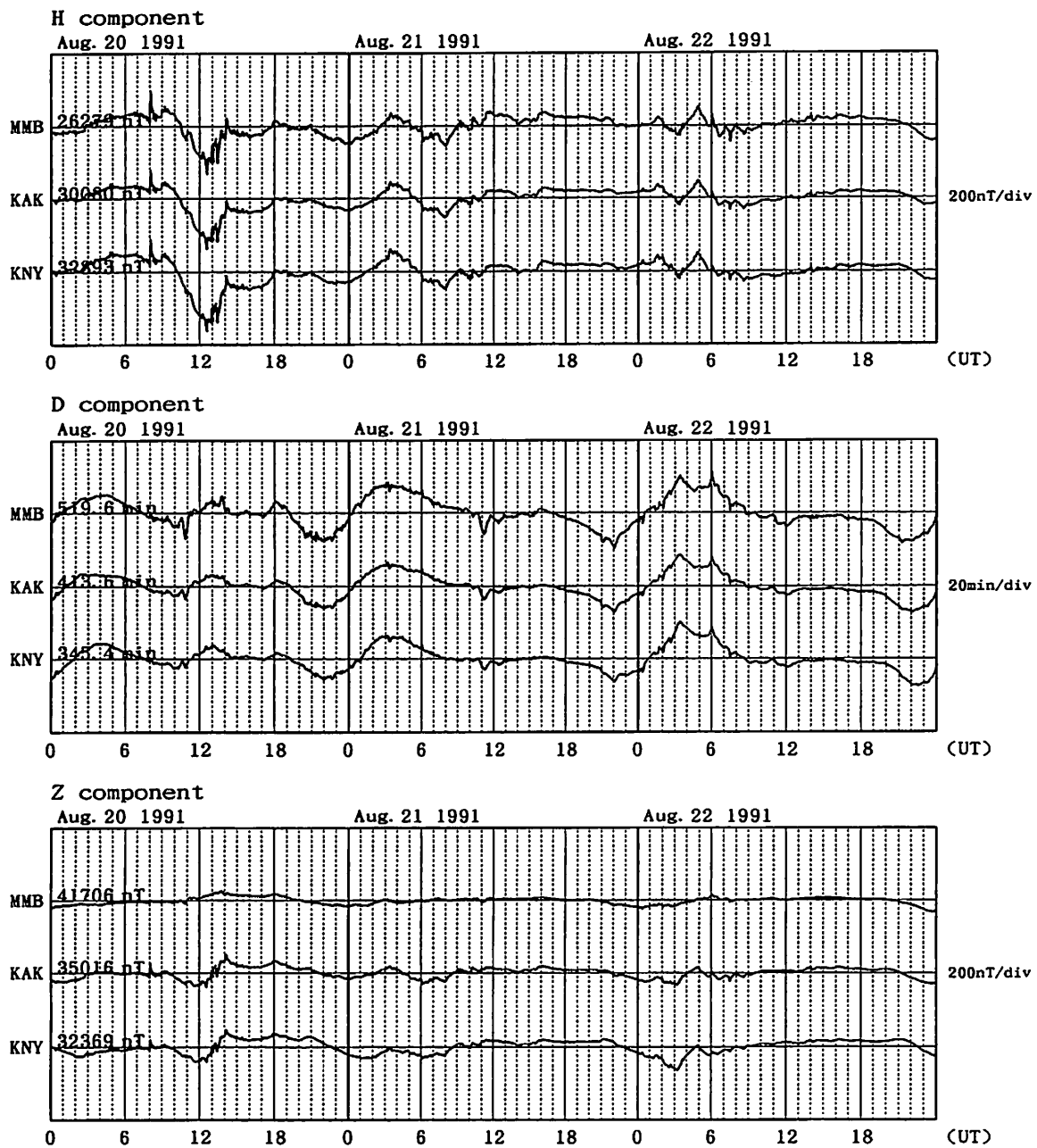


Fig. A-49 Magnetic records at MMB, KAK and KNY for the geomagnetic storm of August 20, 1991.

Magnetogram for 1991 Oct. 01-03

at Memambetsu(MMB), Kakioka(KAK), Kanoya(KNY)

Upward: increase(H), westward(D), downward(Z)

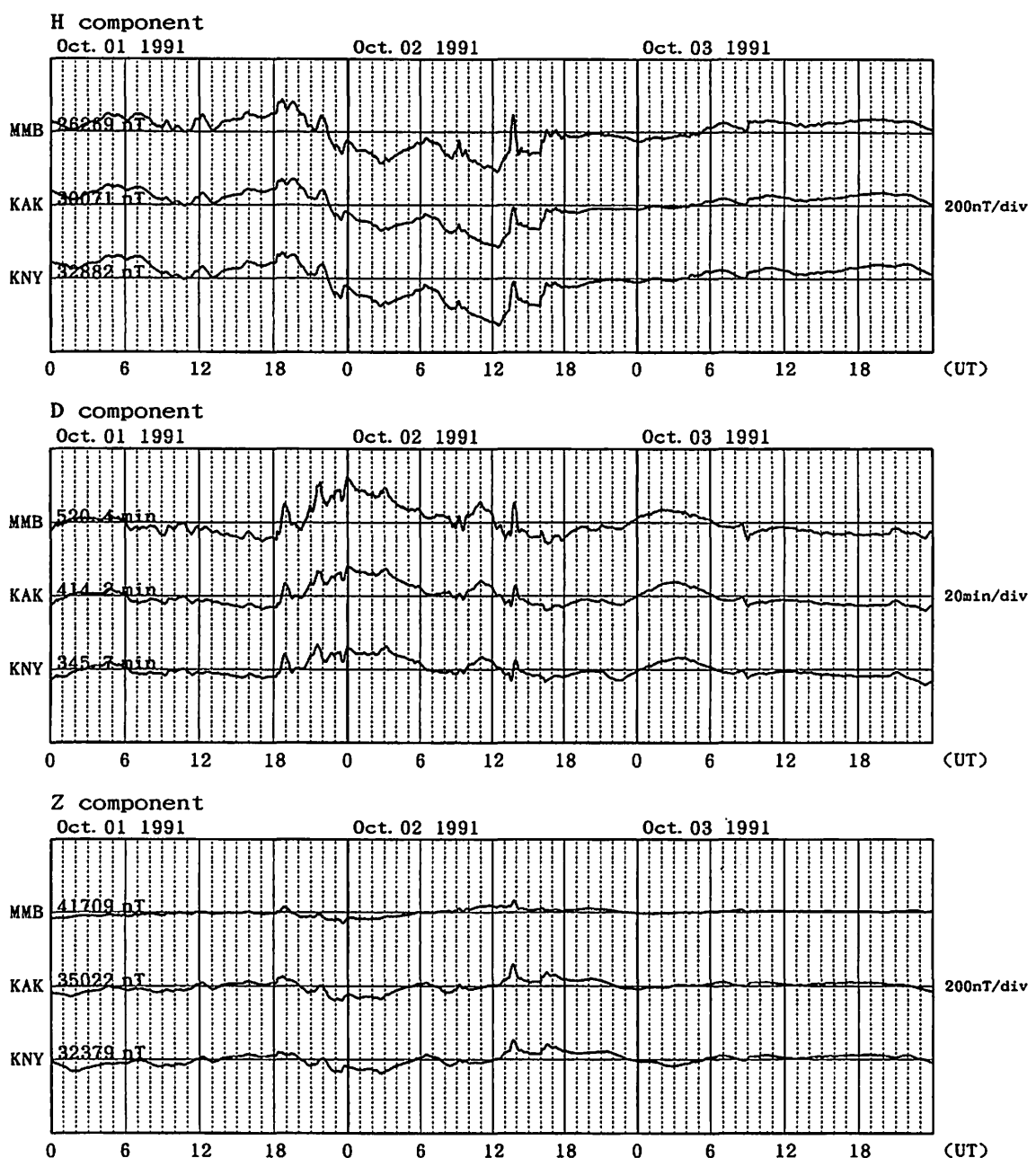


Fig. A-50 Magnetic records at MMB, KAK and KNY for the geomagnetic storm of October 1, 1991.

Magnetogram for 1991 Oct. 28-30

at Memambetsu(MMB), Kakioka(KAK), Kanoya(KNY)

Upward: increase(H), westward(D), downward(Z)

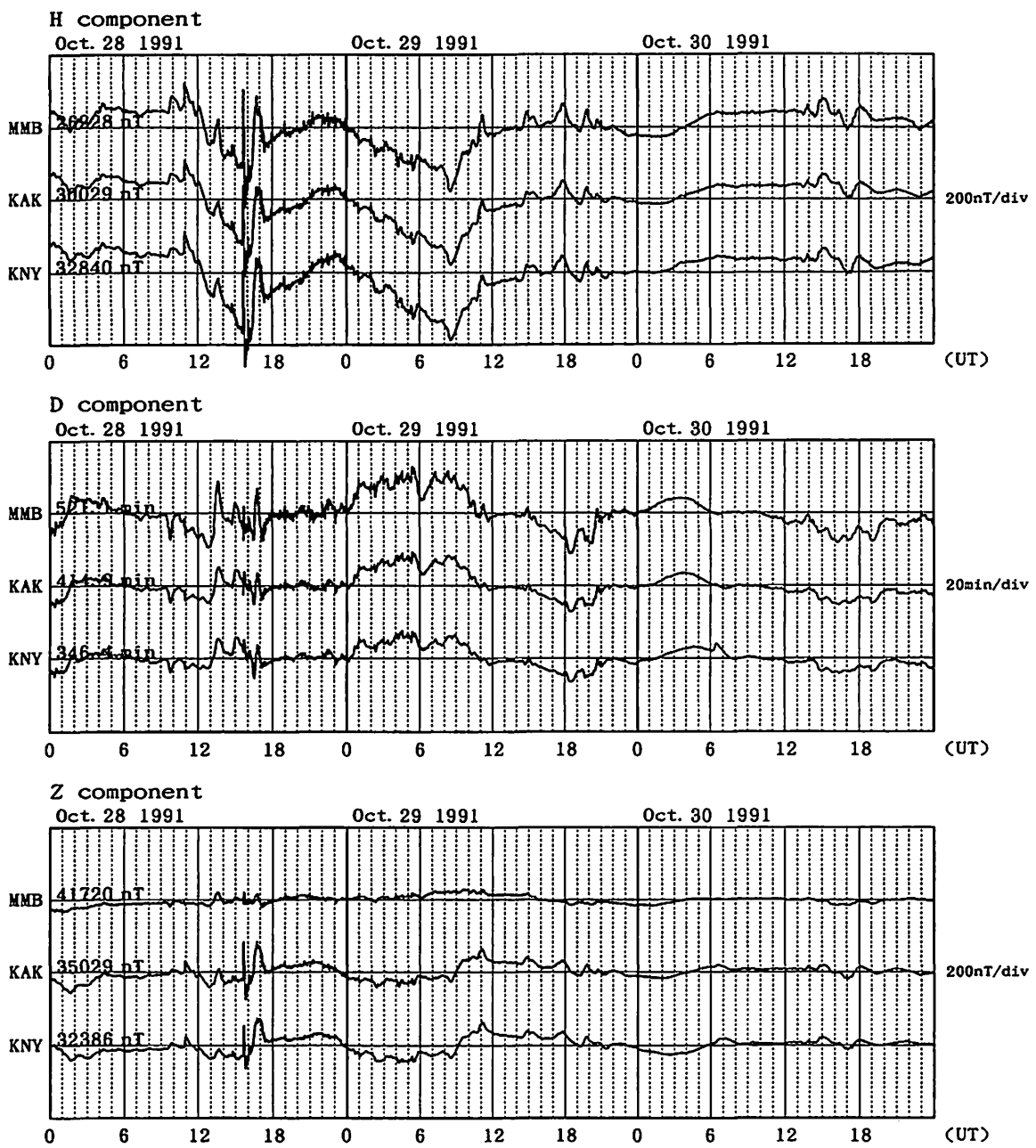


Fig. A-51 Magnetic records at MMB, KAK and KNY for the geomagnetic storm of October 28, 1991.

Magnetogram for 1991 Oct. 31-Nov. 02

at Memambetsu(MMB), Kakioka(KAK), Kanoya(KNY)

Upward: increase(H), westward(D), downward(Z)

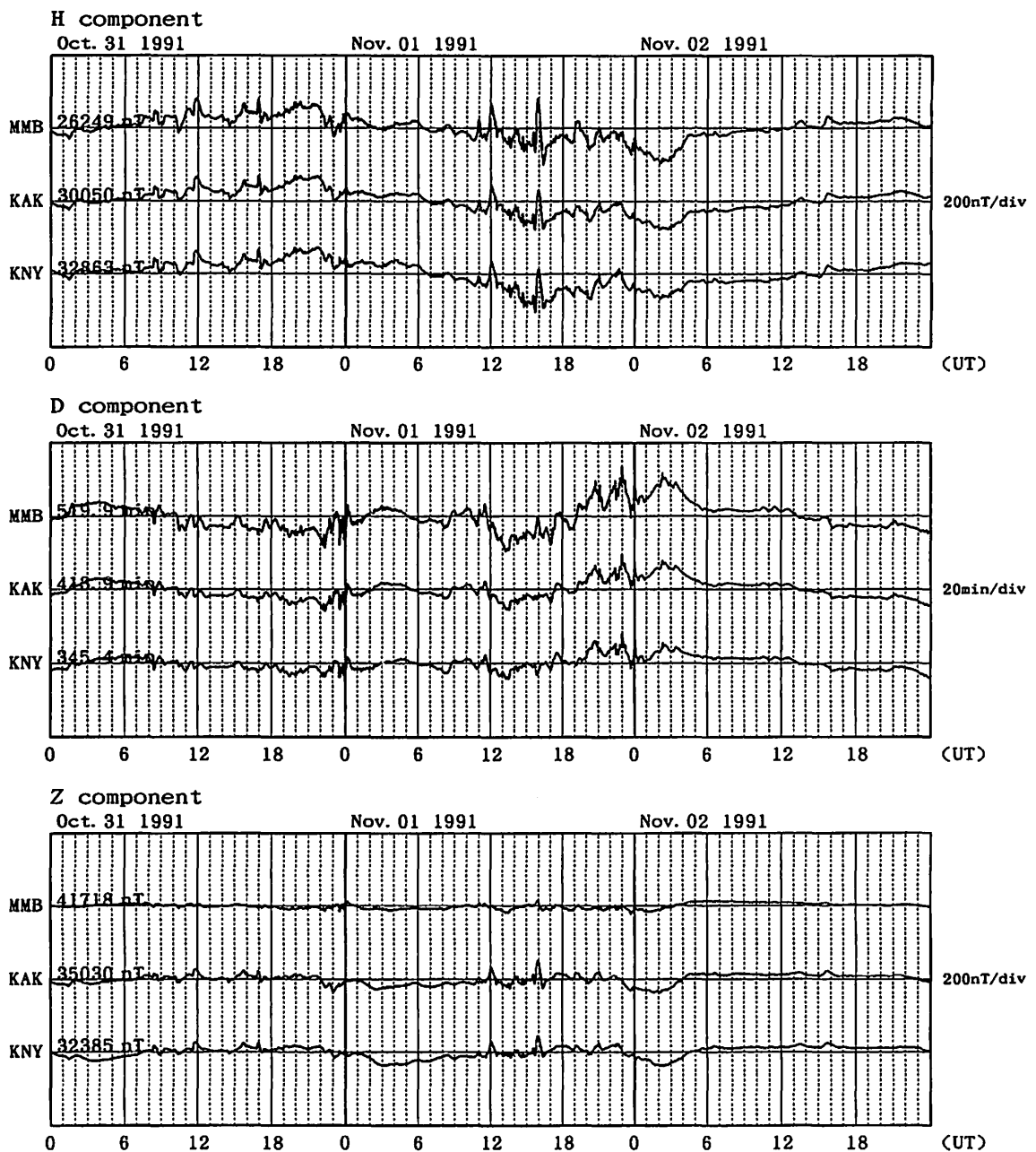


Fig. A-52 Magnetic records at MMB, KAK and KNY for the geomagnetic storm of October 31, 1991.

Magnetogram for 1991 Nov. 08-10

at Memambetsu(MMB), Kakioka(KAK), Kanoya(KNY)

Upward: increase(H), westward(D), downward(Z)

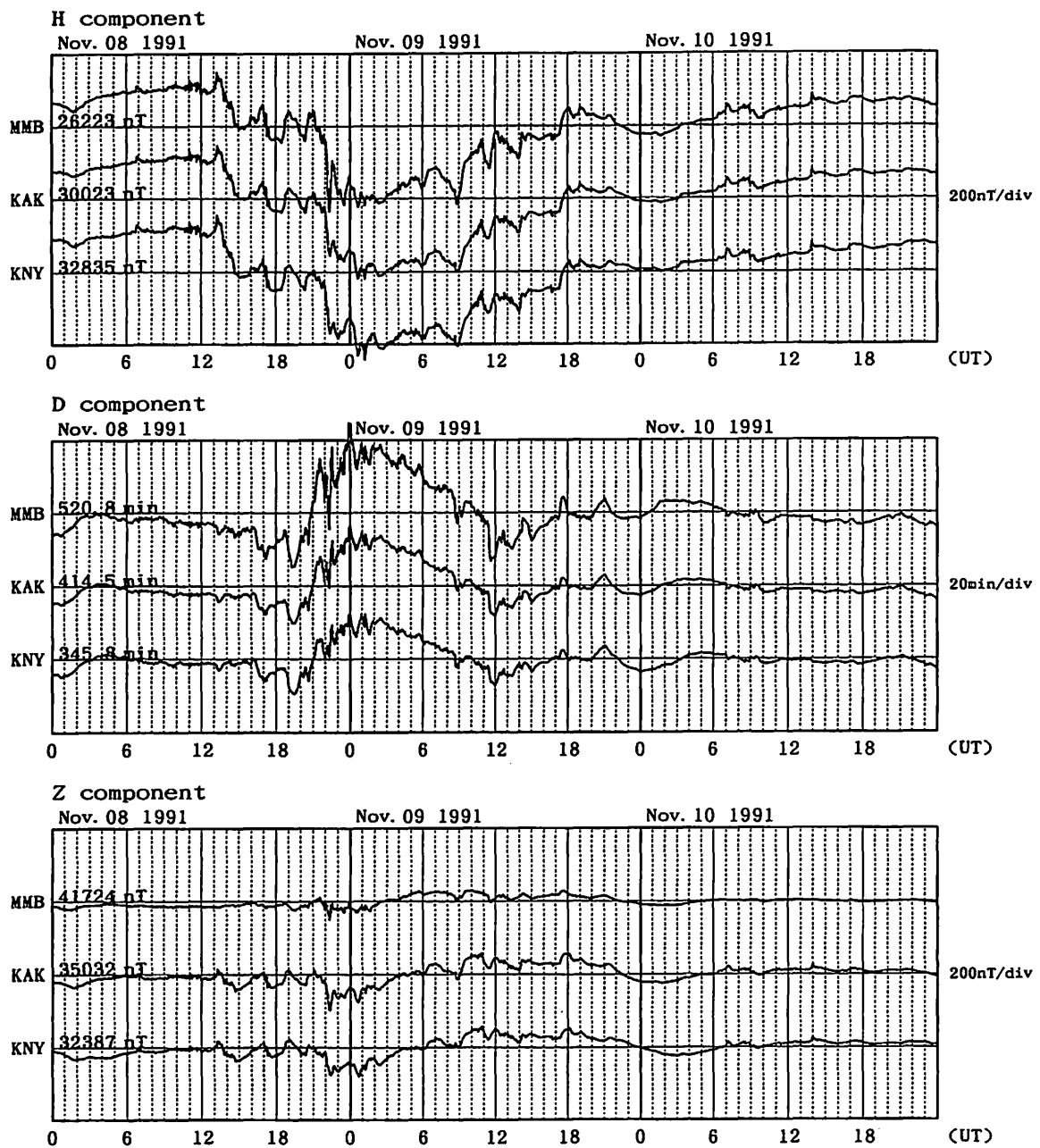


Fig. A-53 Magnetic records at MMB, KAK and KNY for the geomagnetic storm of November 8, 1991.

Magnetogram for 1992 Feb. 02-04

at Memambetsu(MMB), Kakioka(KAK), Kanoya(KNY)

Upward: increase(H), westward(D), downward(Z)

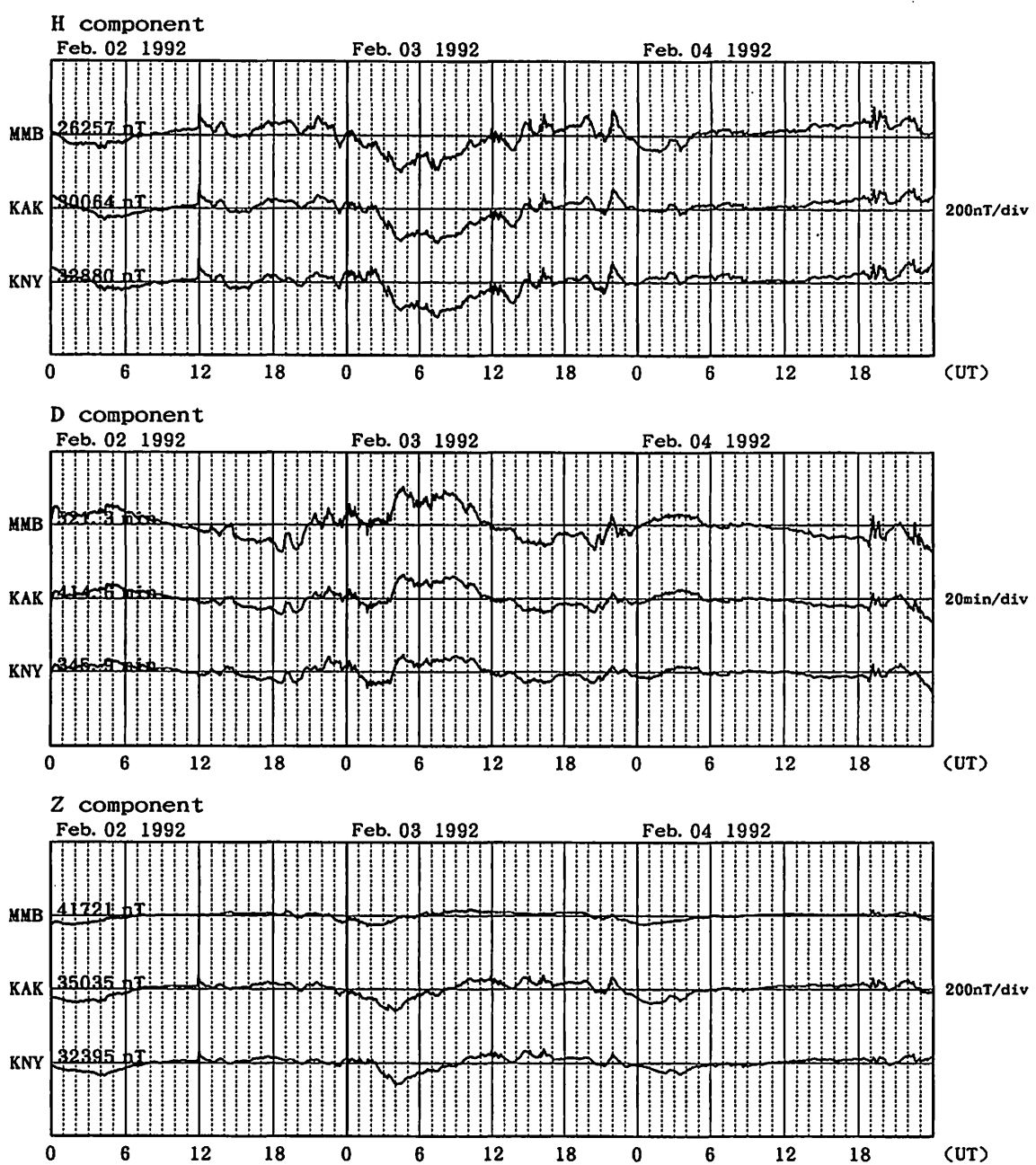


Fig. A-54(a) Magnetic records at MMB, KAK and KNY for the geomagnetic storm of February 2, 1992.

Magnetogram for 1992 Feb. 05-07

at Memambetsu(MMB), Kakioka(KAK), Kanoya(KNY)

Upward: increase(H), westward(D), downward(Z)

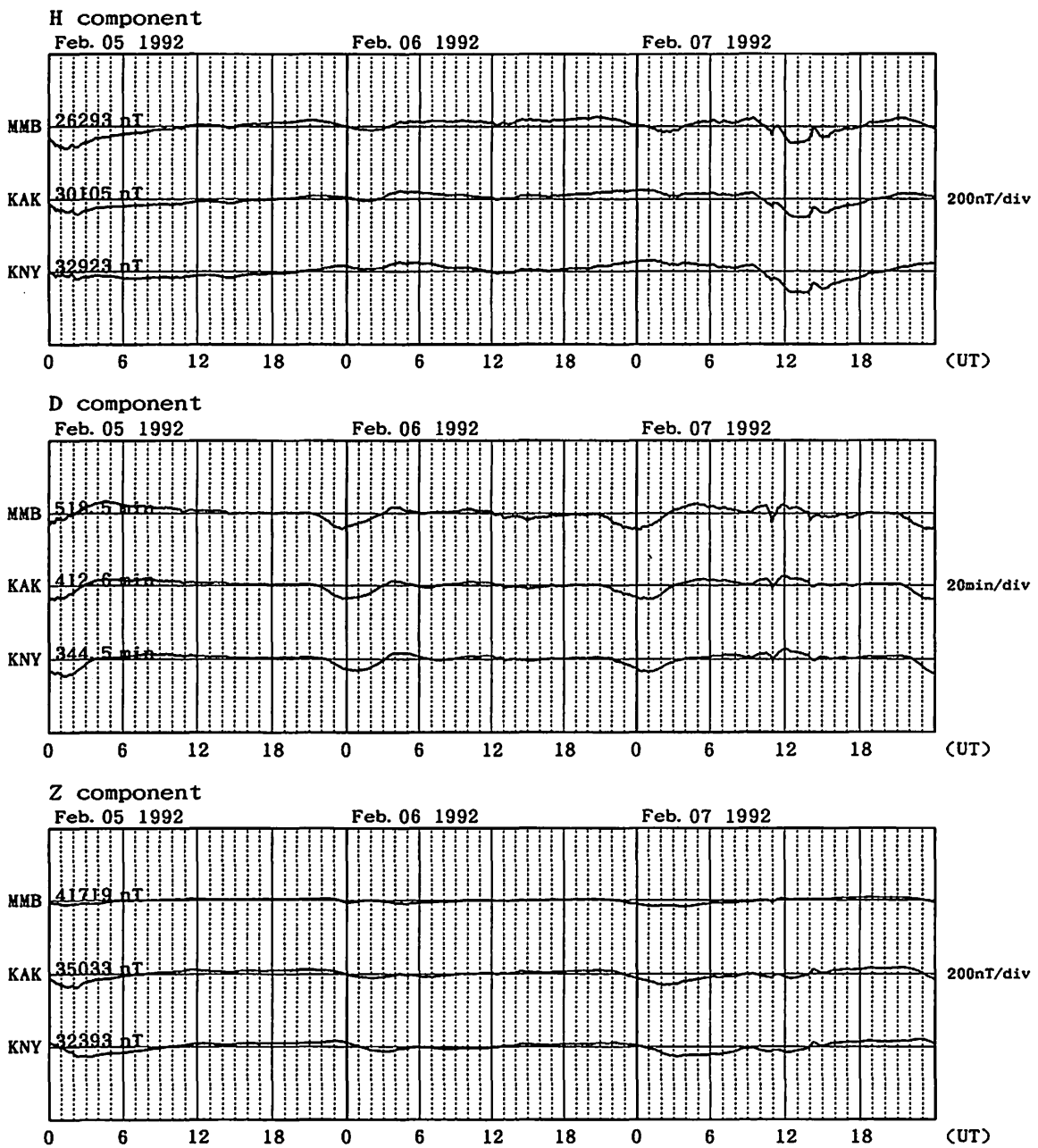


Fig. A-54(b) Magnetic records at MMB, KAK and KNY for the geomagnetic storm of February 2, 1992 (succeeding Fig. A-54(a)).

Magnetogram for 1992 Feb. 08-10

at Memambetsu(MMB), Kakioka(KAK), Kanoya(KNY)

Upward: increase(H), westward(D), downward(Z)

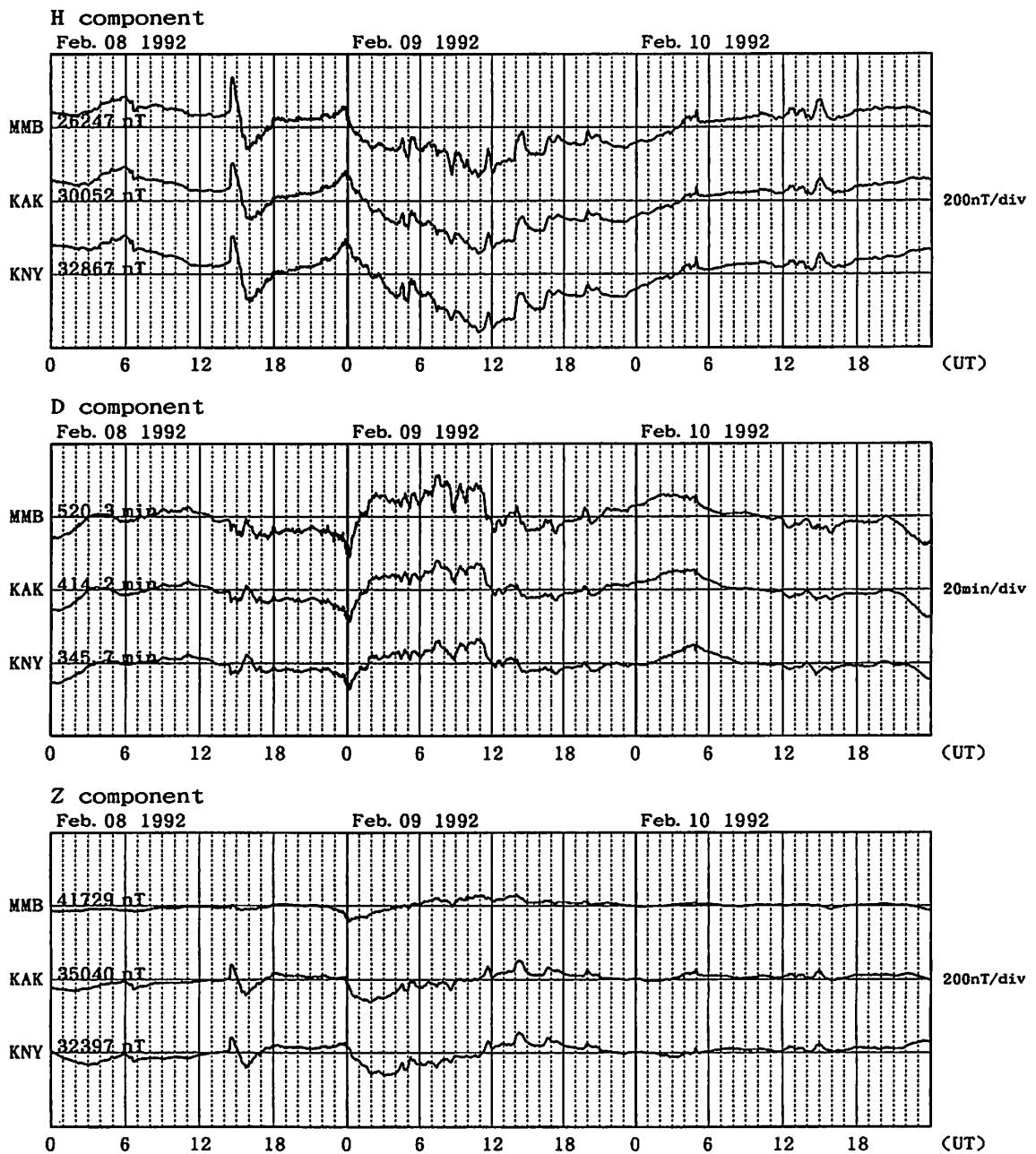


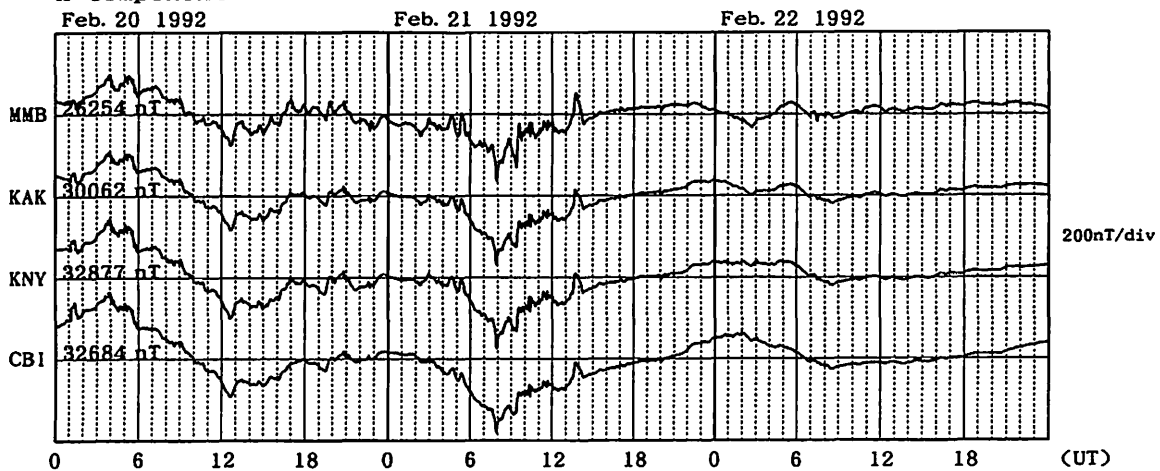
Fig. A-55 Magnetic records at MMB, KAK and KNY for the geomagnetic storm of February 8, 1992.

Magnetogram for 1992 Feb. 20-22

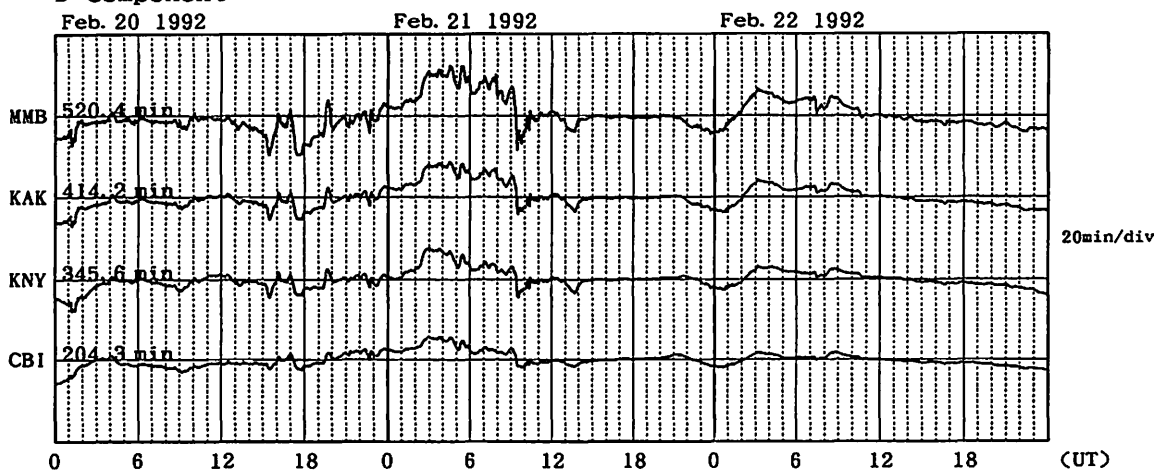
at Memambetsu(MMB), Kakioka(KAK), Kanoya(KNY), Chichijima(CBI)

Upward: increase(H), westward(D), downward(Z)

H component



D component



Z component

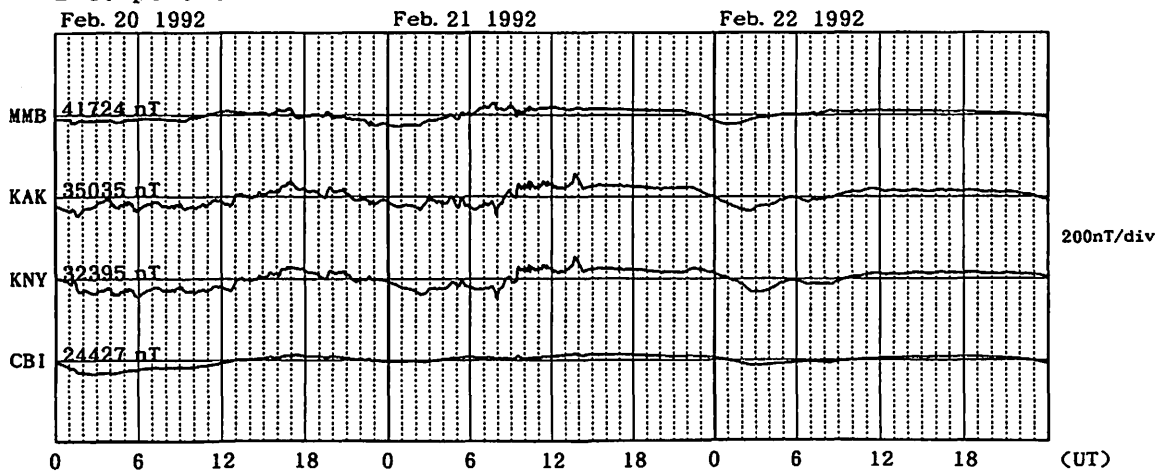


Fig. A-56 Magnetic records at MMB, KAK, KNY and CBI for the geomagnetic storm of February 20, 1992.

Magnetogram for 1992 Feb. 26-28

at Memambetsu(MMB), Kakioka(KAK), Kanoya(KNY)

Upward: increase(H), westward(D), downward(Z)

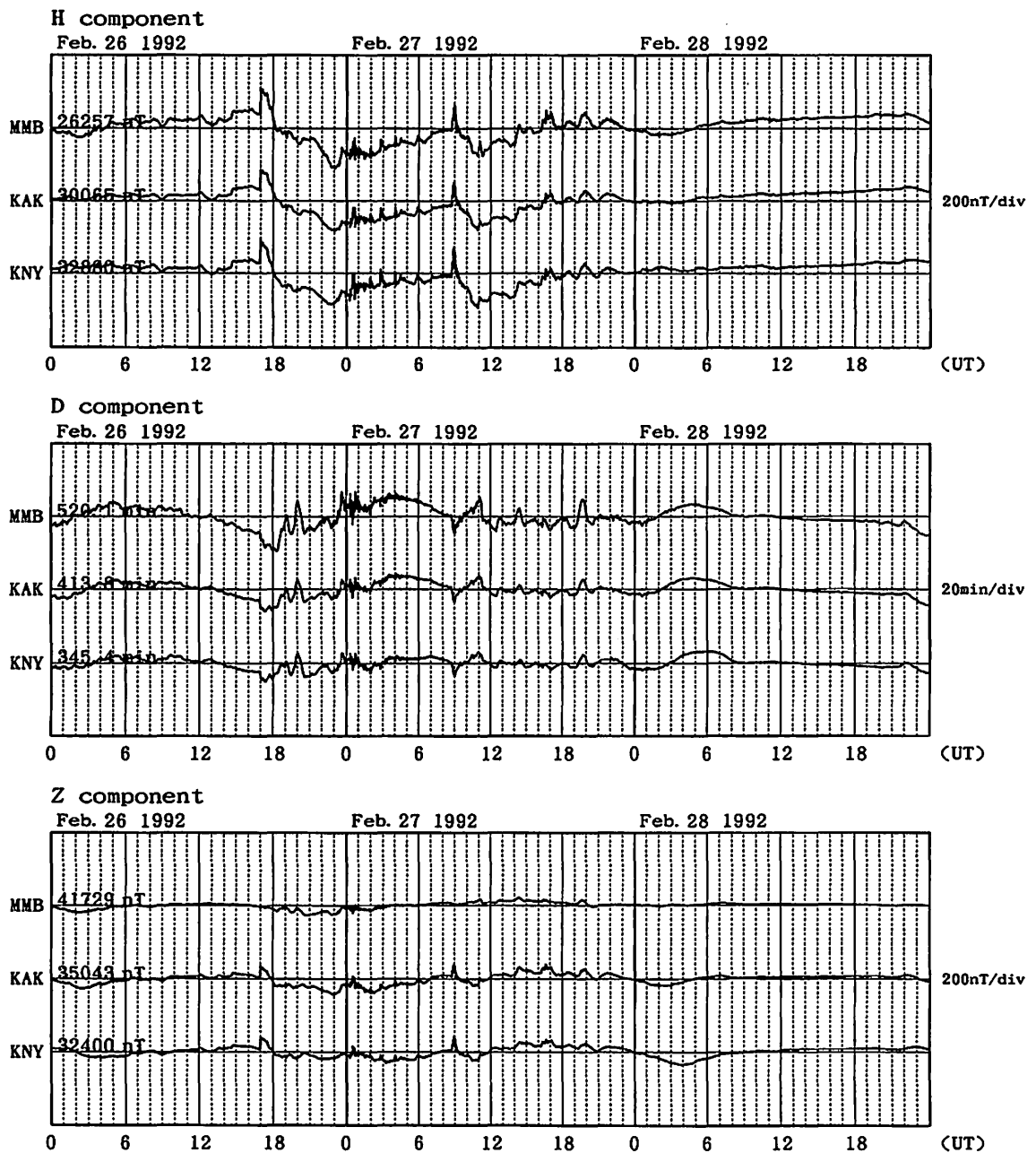


Fig. A-57 Magnetic records at MMB, KAK and KNY for the geomagnetic storm of February 26, 1992.

Magnetogram for 1992 May 09-11

at Memambetsu(MMB), Kakioka(KAK), Kanoya(KNY), Chichijima(CBI)

Upward: increase(H), westward(D), downward(Z)

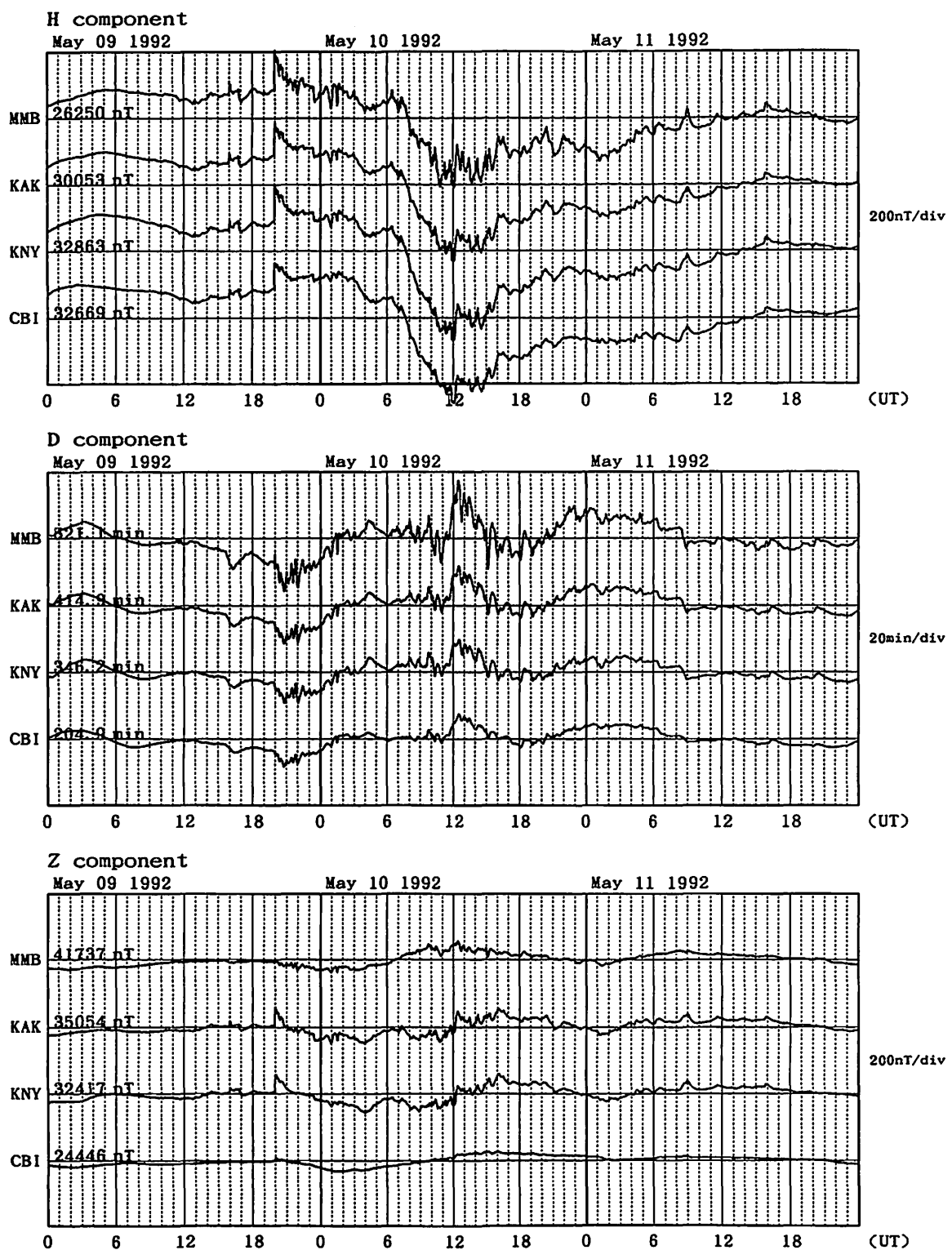


Fig. A-58(a) Magnetic records at MMB, KAK, KNY and CBI for the geomagnetic storm of May 9, 1992.

Magnetogram for 1992 May 12-14

at Memambetsu(MMB), Kakioka(KAK), Kanoya(KNY), Chichijima(CBI)

Upward: increase(H), westward(D), downward(Z)

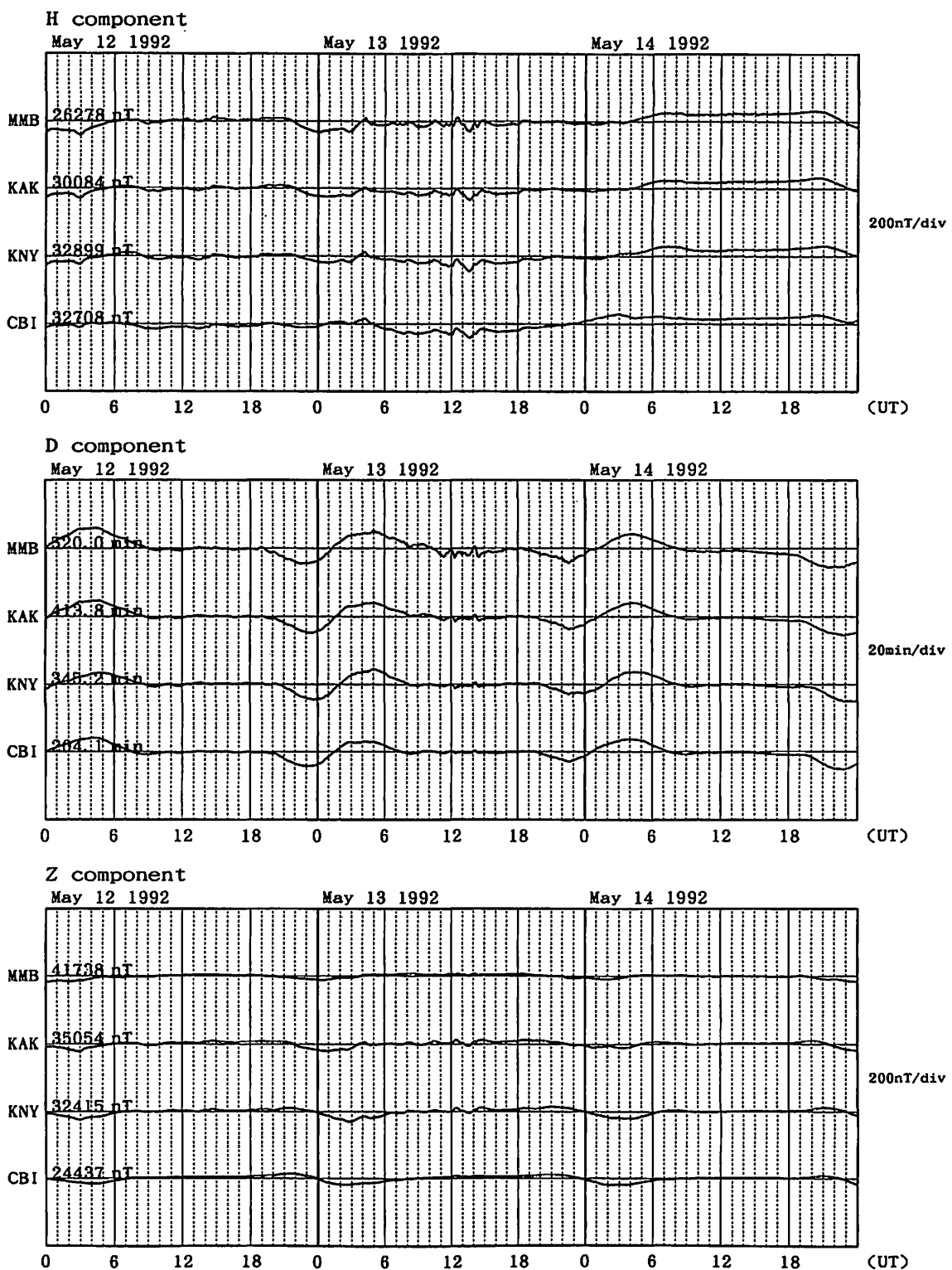


Fig. A-58(b) Magnetic records at MMB, KAK, KNY and CBI for the geomagnetic storm of May 9, 1992 (succeeding Fig. A-58(a)).

Magnetogram for 1992 Sep. 09-11

at Memambetsu(MMB), Kakioka(KAK), Kanoya(KNY)

Upward: increase(H), westward(D), downward(Z)

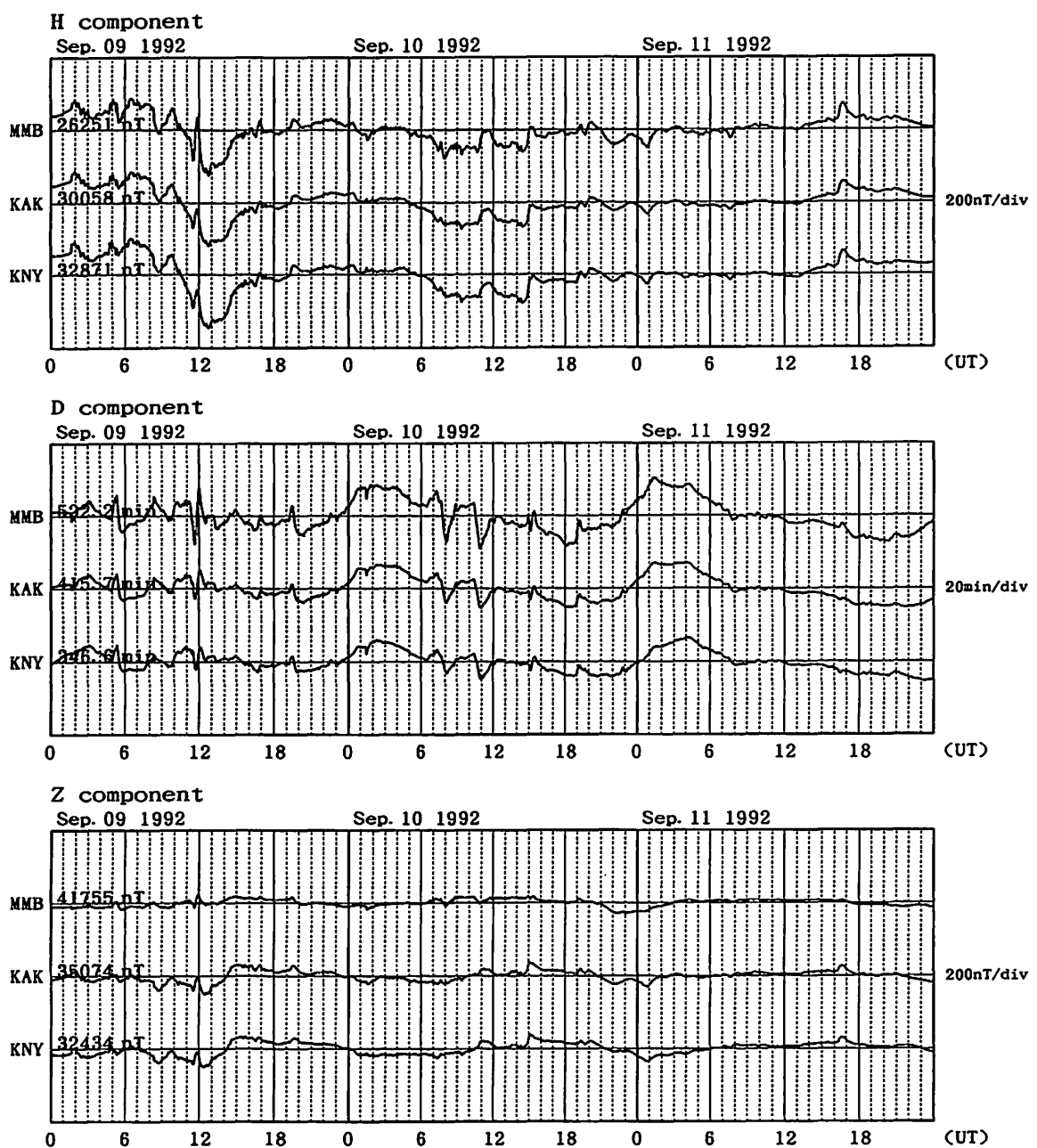


Fig. A-59 Magnetic records at MMB, KAK and KNY for the geomagnetic storm of September 9, 1992.

Magnetogram for 1992 Sep. 17-19

at Memambetsu(MMB), Kakioka(KAK), Kanoya(KNY), Chichijima(CBI)

Upward: increase(H), westward(D), downward(Z)

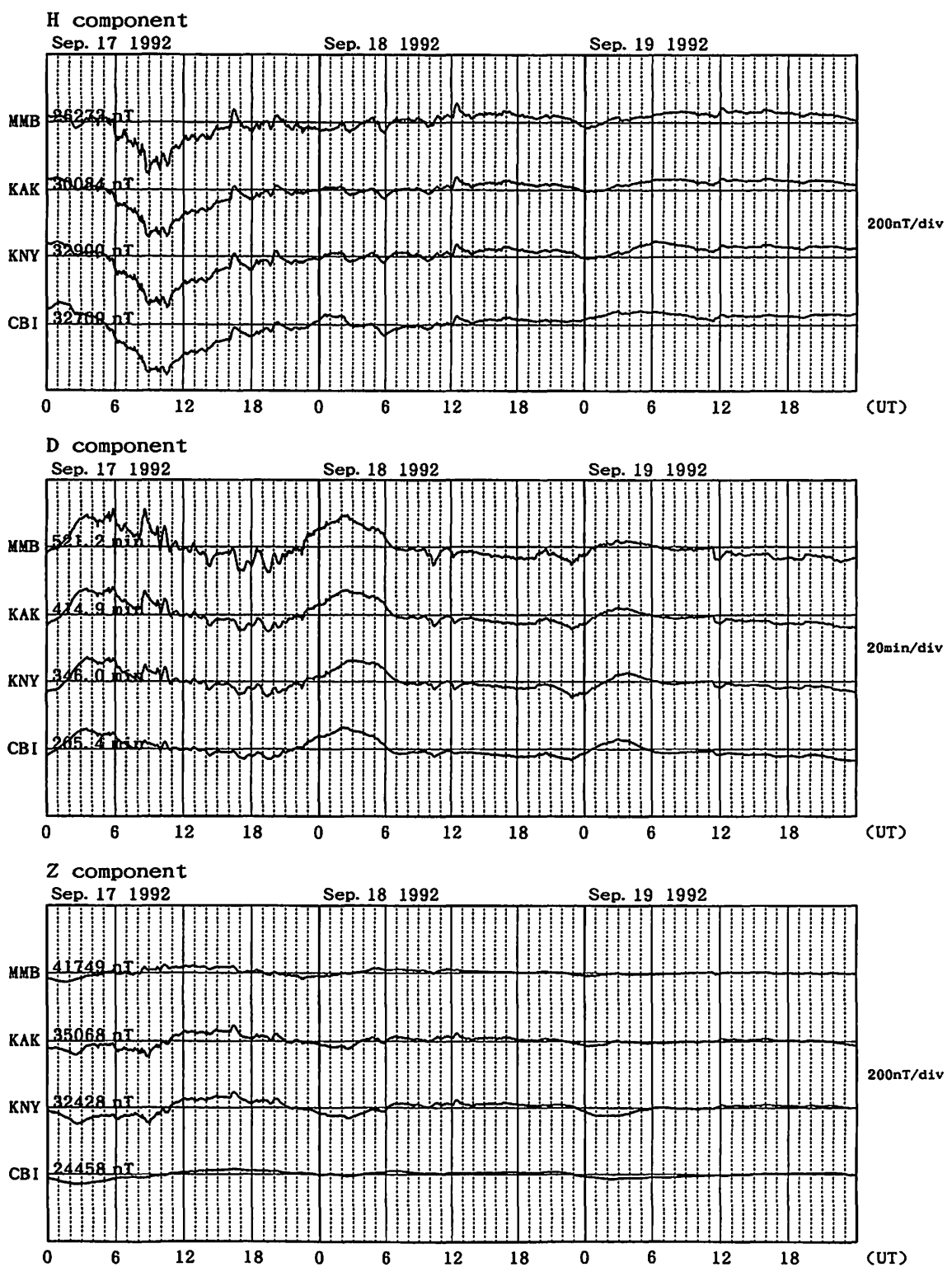


Fig. A-60 Magnetic records at MMB, KAK, KNY and CBI for the geomagnetic storm of September 17, 1992.

Magnetogram for 1992 Sep. 28-30

at Memambetsu(MMB), Kakioka(KAK), Kanoya(KNY)

Upward: increase(H), westward(D), downward(Z)

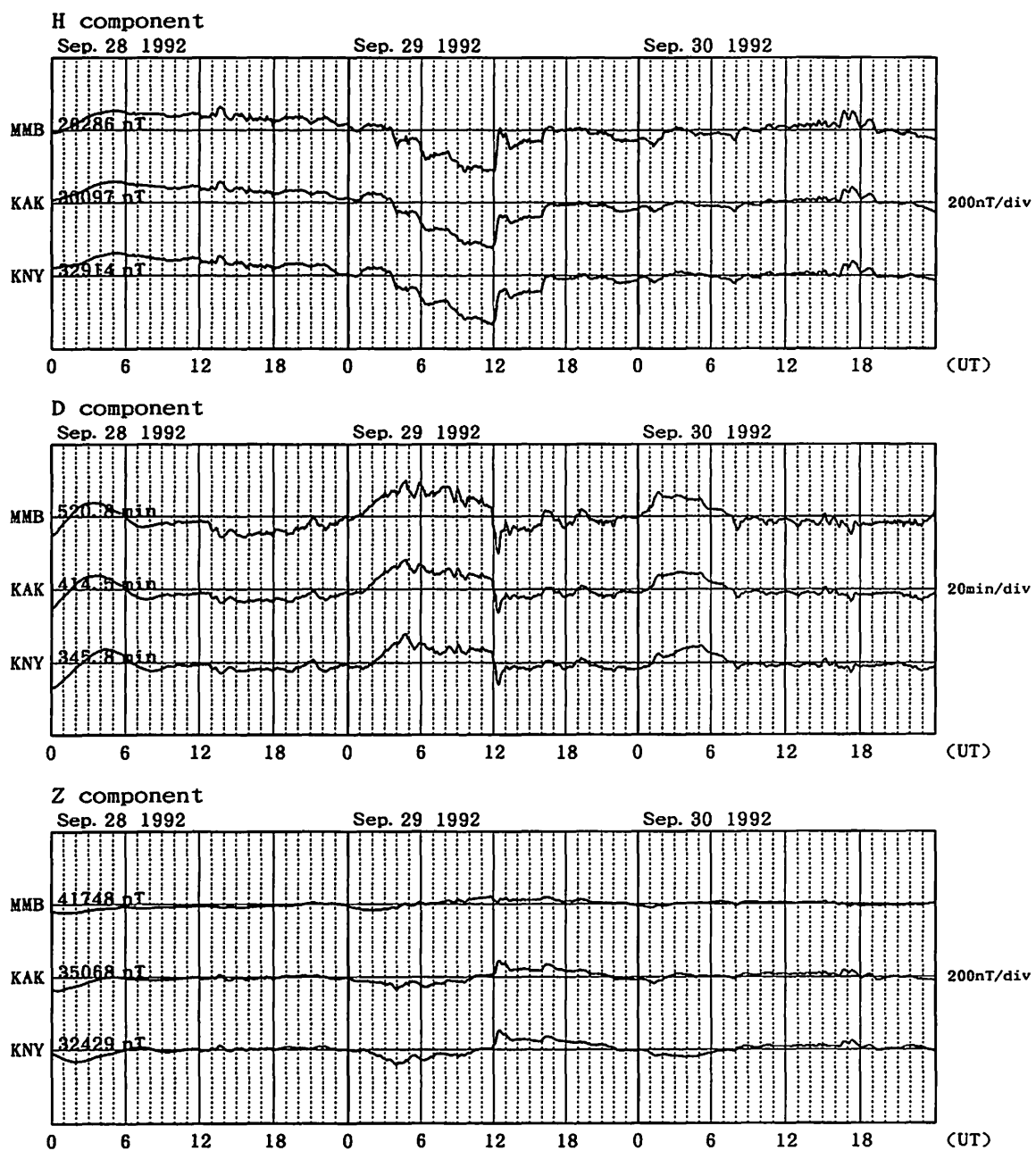


Fig. A-61(a) Magnetic records at MMB, KAK and KNY for the geomagnetic storm of September 28, 1992.

Magnetogram for 1992 Oct. 01-03

at Memambetsu(MMB), Kakioka(KAK), Kanoya(KNY)

Upward: increase(H), westward(D), downward(Z)

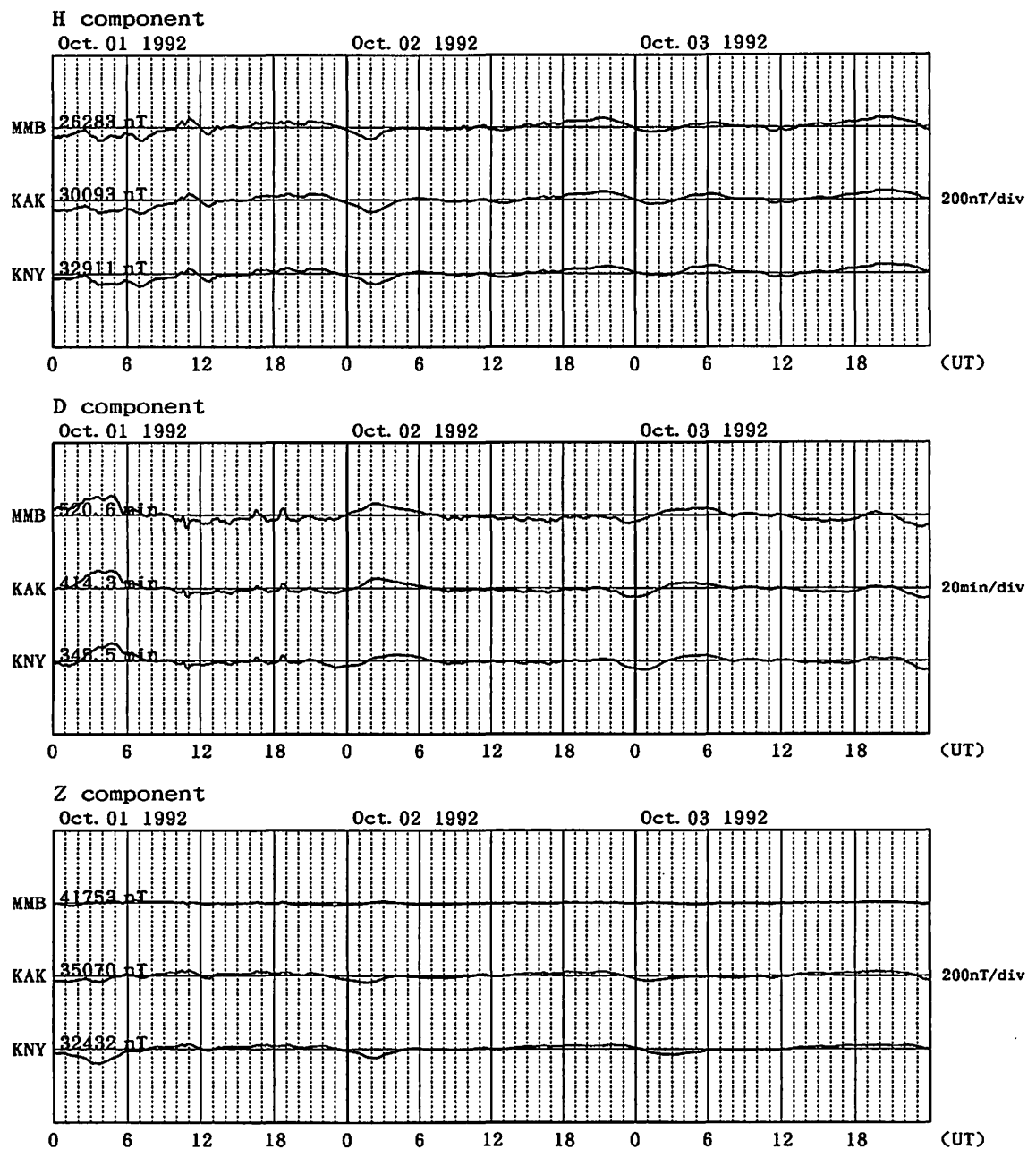


Fig. A-61(b) Magnetic records at MMB, KAK and KNY for the geomagnetic storm of September 28, 1992 (succeeding Fig. A-61(a)).

Magnetogram for 1992 Oct. 08-10

at Memambetsu(MMB), Kakioka(KAK), Kanoya(KNY)

Upward: increase(H), westward(D), downward(Z)

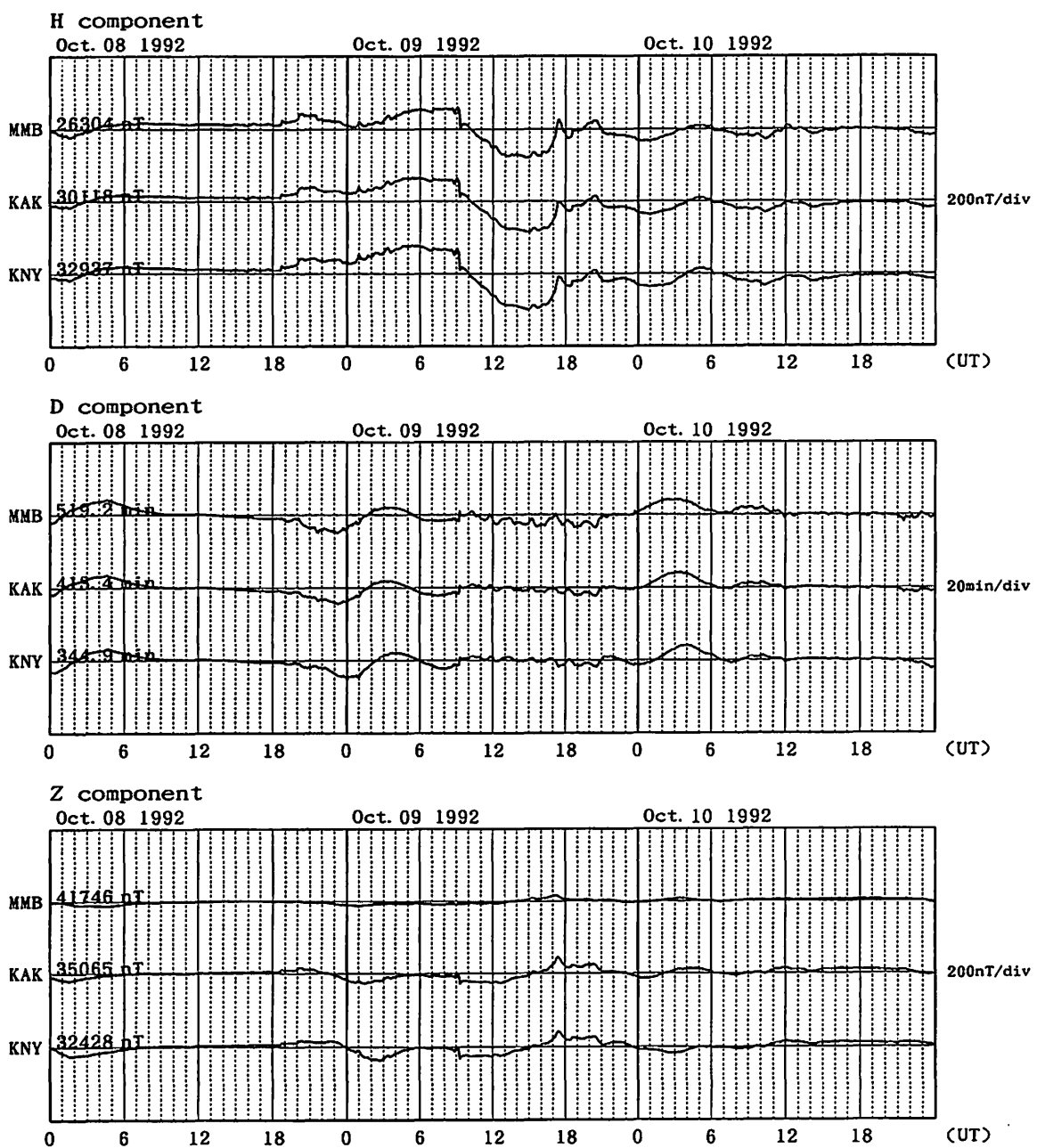


Fig. A-62 Magnetic records at MMB, KAK and KNY for the geomagnetic storm of October 8, 1992.

Magnetogram for 1992 Nov. 09-11

at Memambetsu(MMB), Kakioka(KAK), Kanoya(KNY)

Upward: increase(H), westward(D), downward(Z)

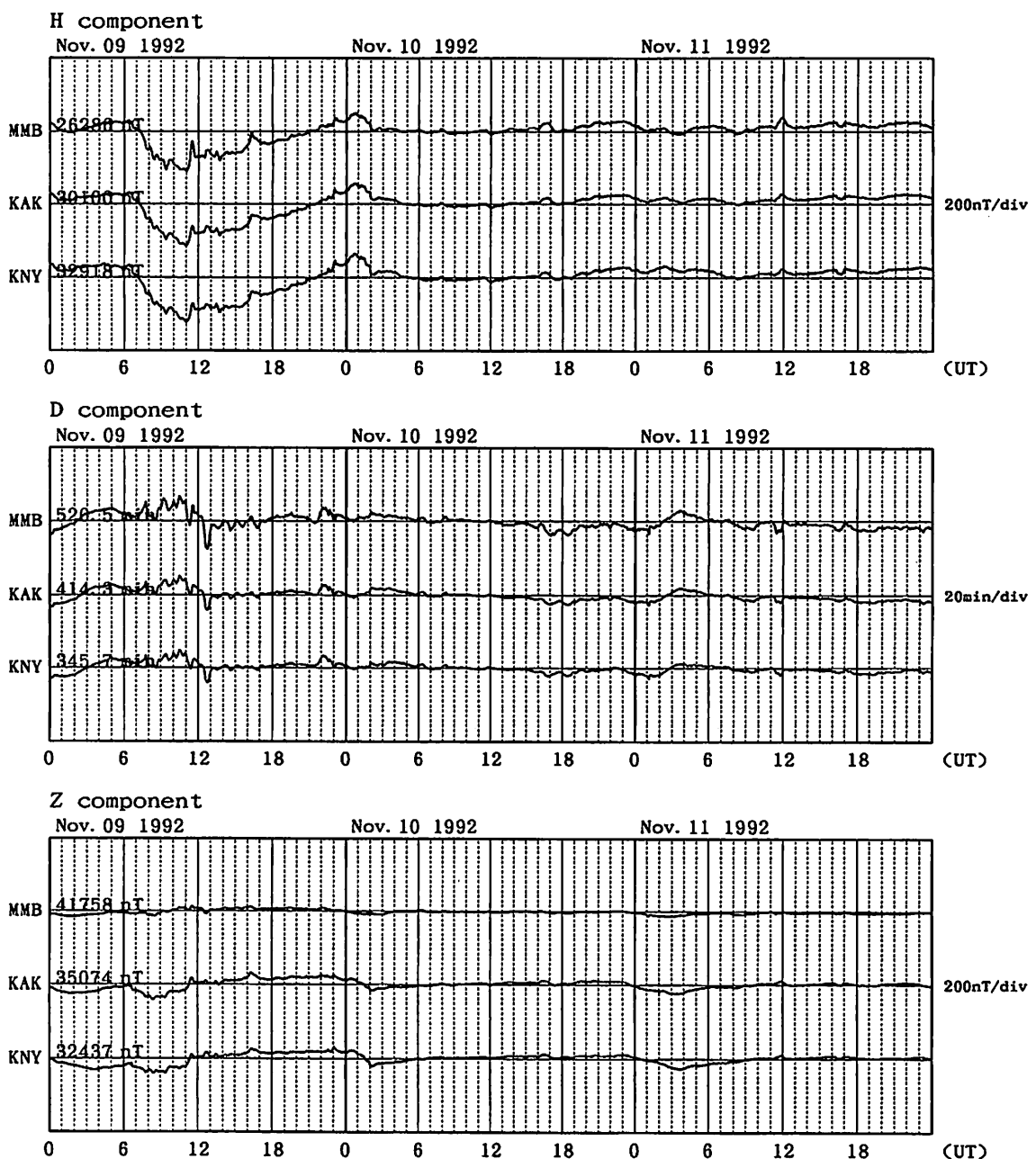


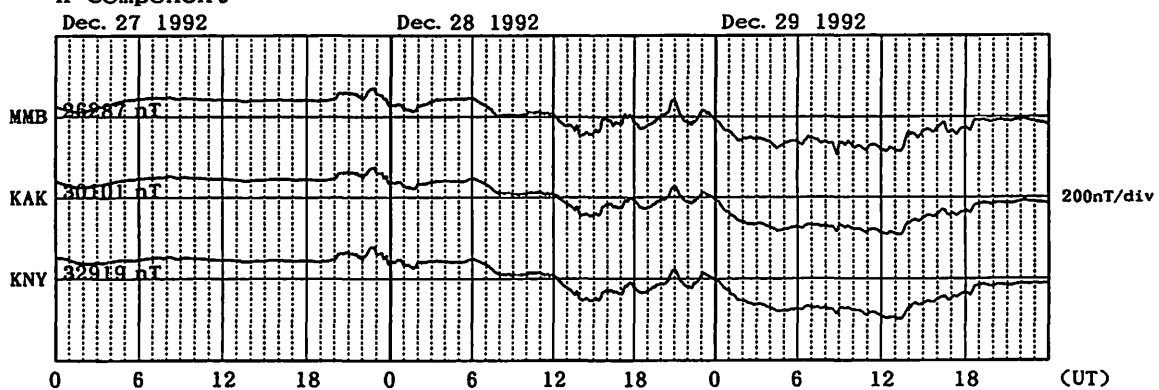
Fig. A-63 Magnetic records at MMB, KAK and KNY for the geomagnetic storm of November 9, 1992.

Magnetogram for 1992 Dec. 27-29

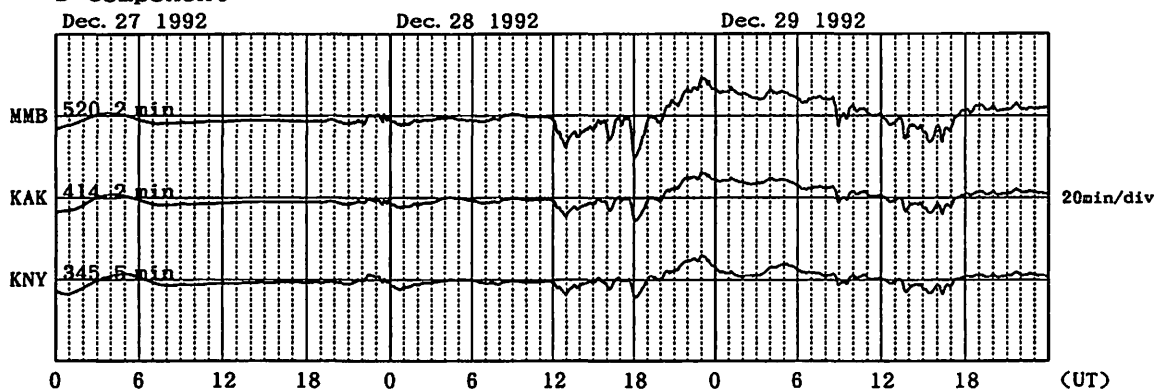
at Memambetsu(MMB), Kakioka(KAK), Kanoya(KNY)

Upward: increase(H), westward(D), downward(Z)

H component



D component



Z component

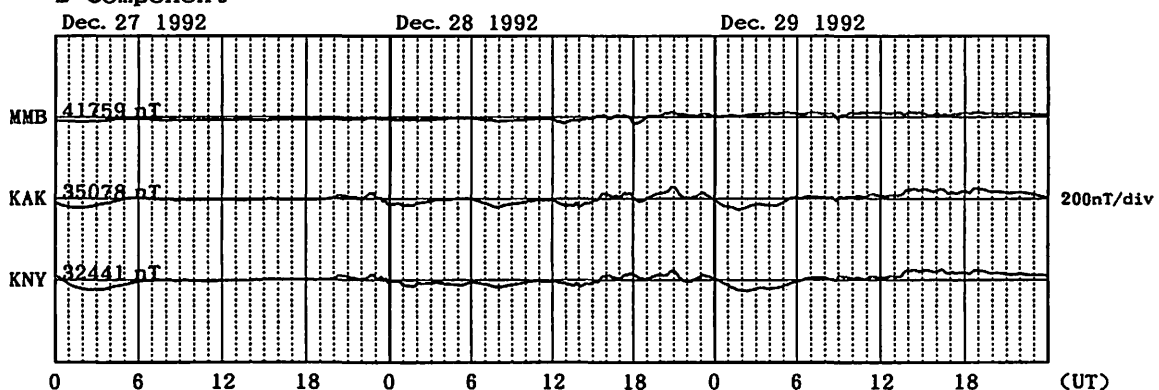


Fig. A-64(a) Magnetic records at MMB, KAK and KNY for the geomagnetic storm of December 27, 1992.

Magnetogram for 1992 Dec. 30-1993 Jan. 01

at Memambetsu(MMB), Kakioka(KAK), Kanoya(KNY)

Upward: increase(H), westward(D), downward(Z)

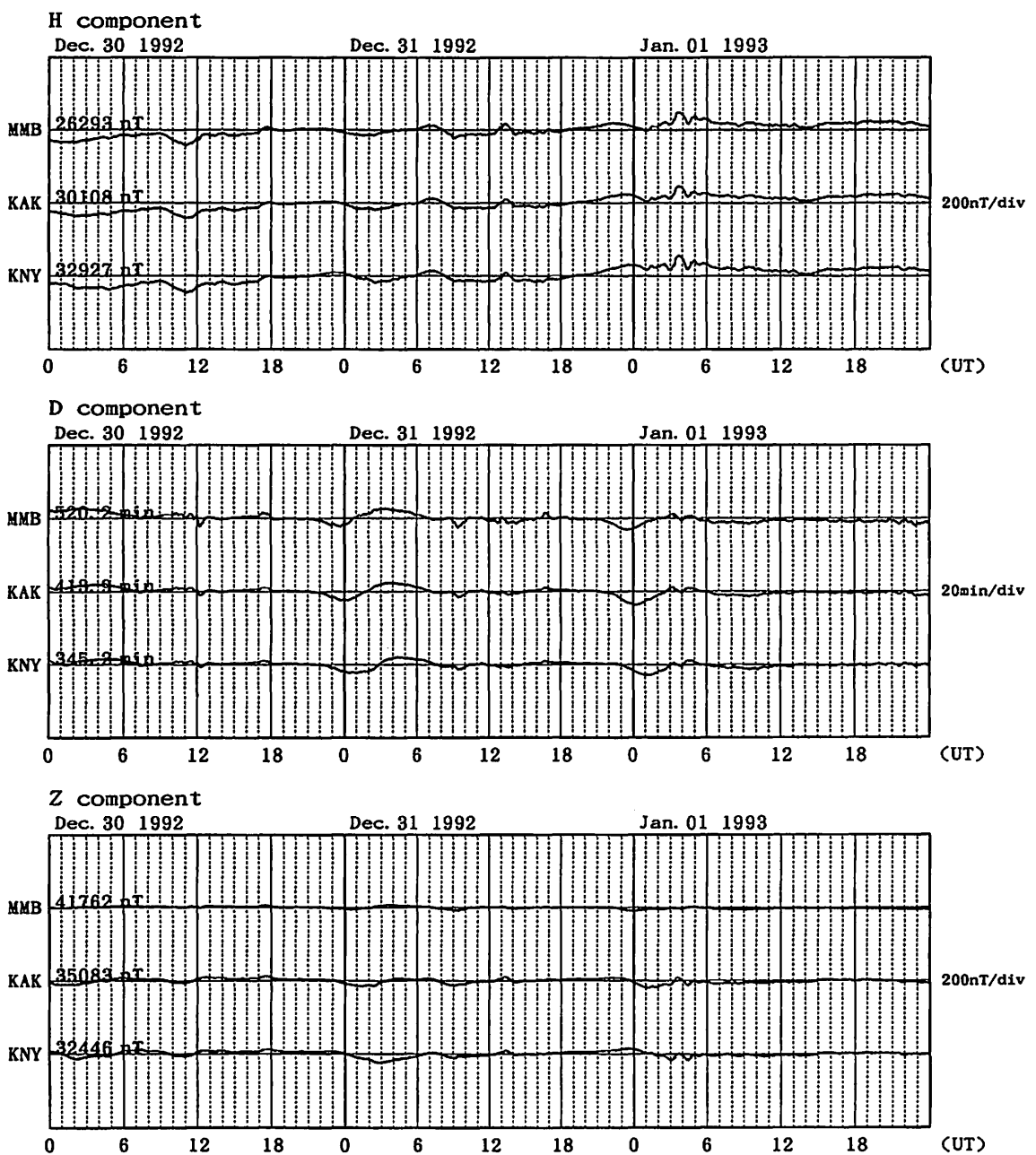


Fig. A-64(b) Magnetic records at MMB, KAK and KNY for the geomagnetic storm of December 27, 1992 (succeeding Fig. A-64(a)).

Magnetogram for 1993 Feb. 17-19

at Memambetsu(MMB), Kakioka(KAK), Kanoya(KNY)

Upward: increase(H), westward(D), downward(Z)

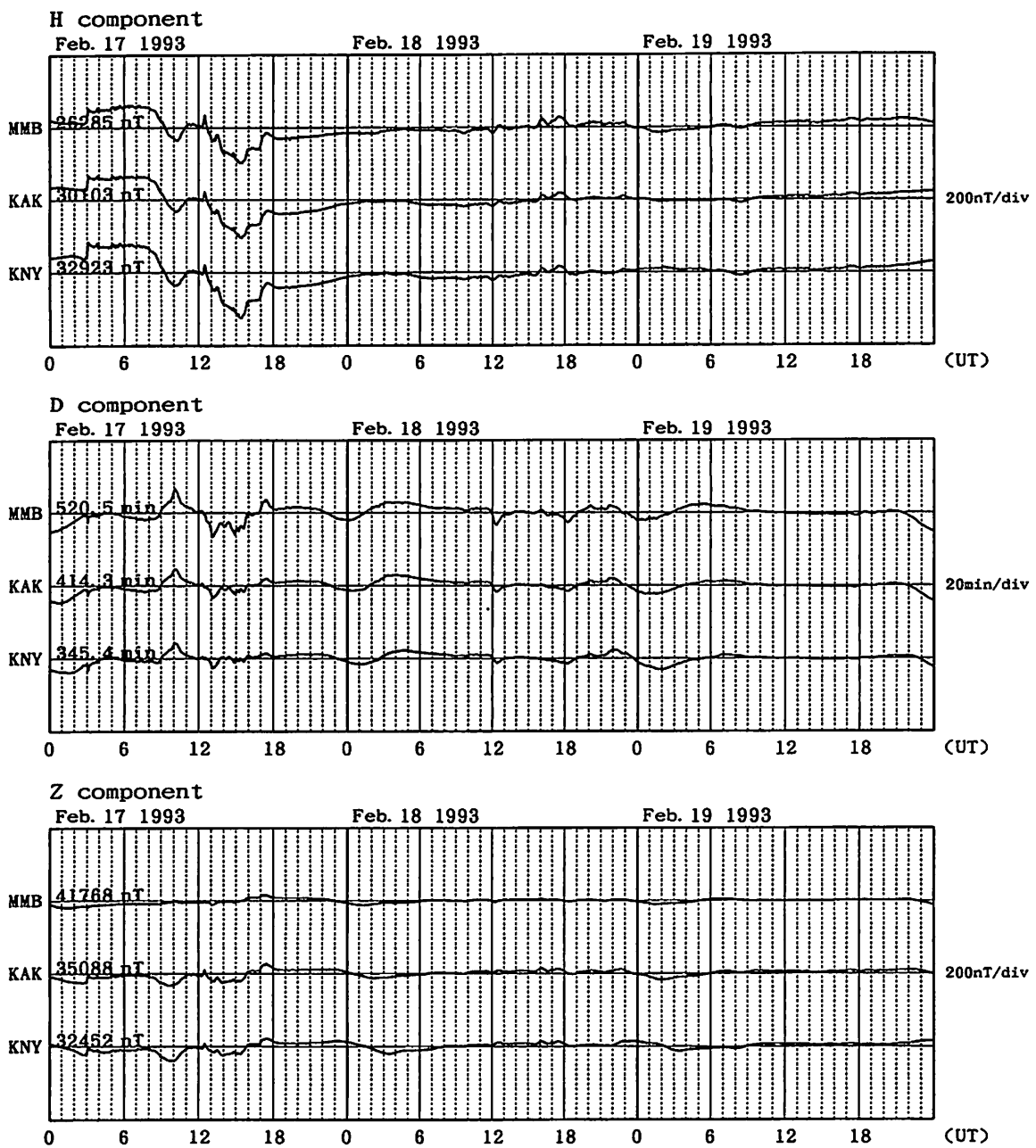


Fig. A-65 Magnetic records at MMB, KAK and KNY for the geomagnetic storm of February 17, 1993.

Magnetogram for 1993 Mar. 08-10

at Memambetsu(MMB), Kakioka(KAK), Kanoya(KNY), Chichijima(CBI)

Upward: increase(H), westward(D), downward(Z)

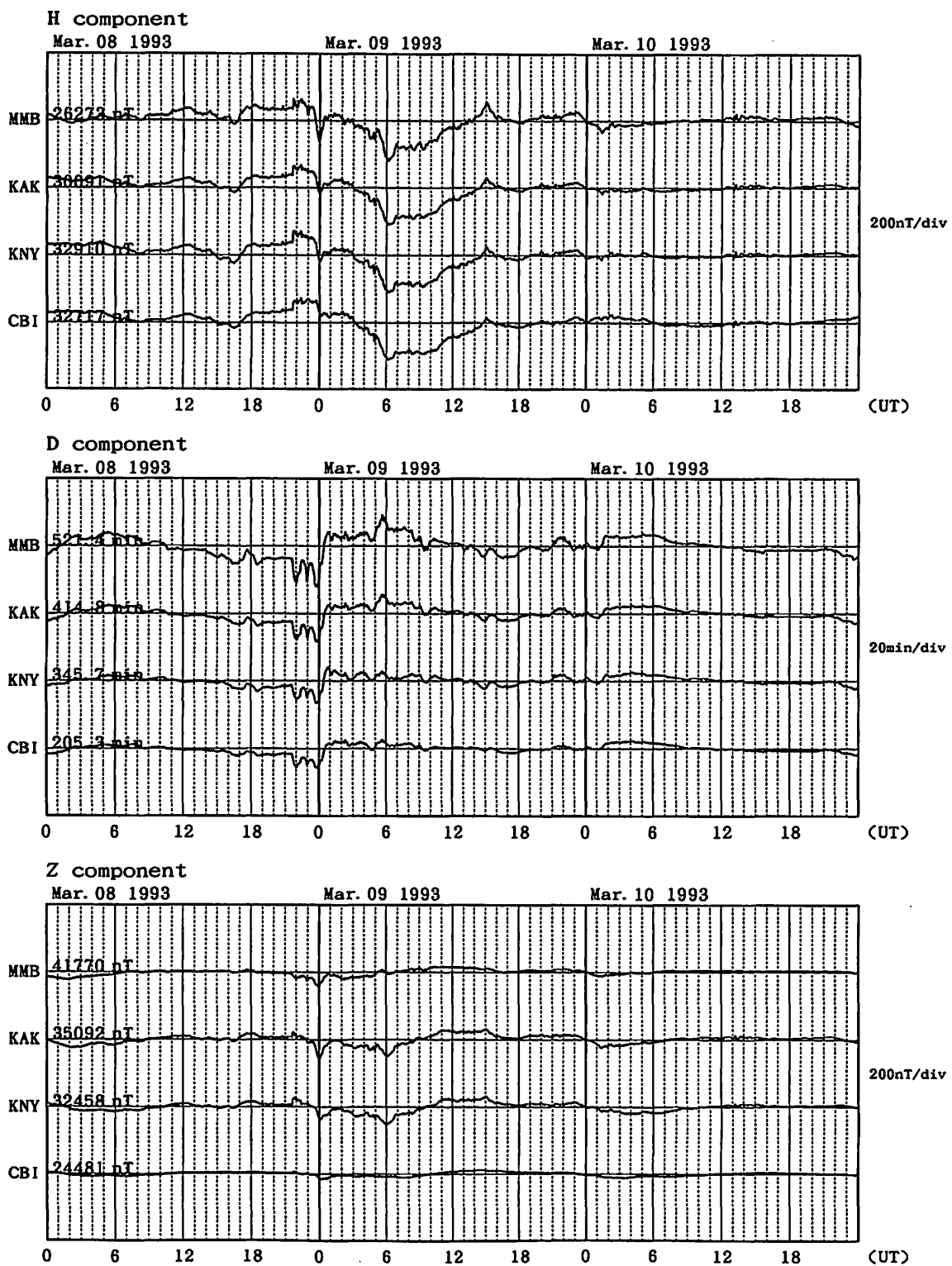


Fig. A-66 Magnetic records at MMB, KAK, KNY and CBI for the geomagnetic storm of March 8, 1993.

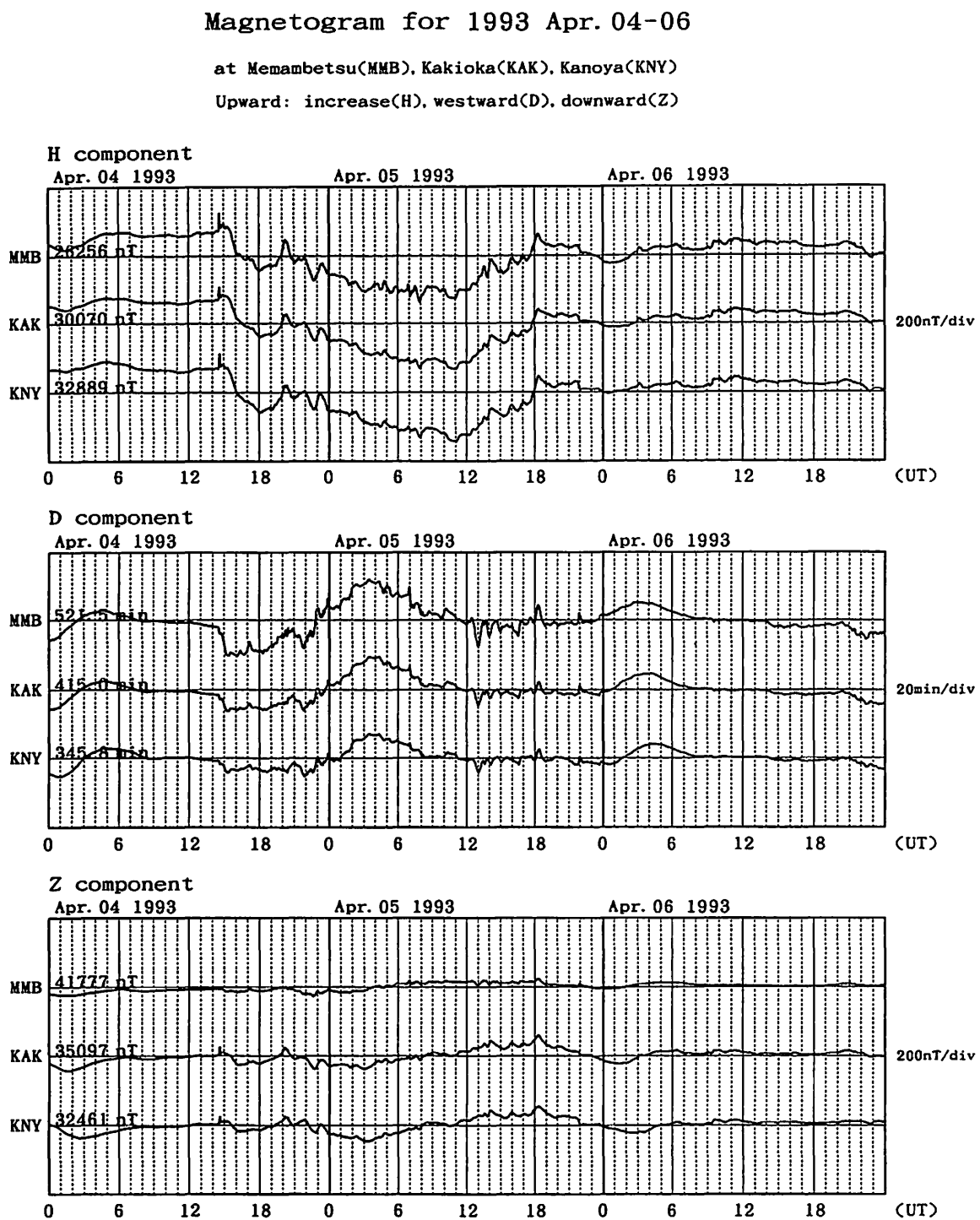


Fig. A-67 Magnetic records at MMB, KAK and KNY for the geomagnetic storm of April 4, 1993.

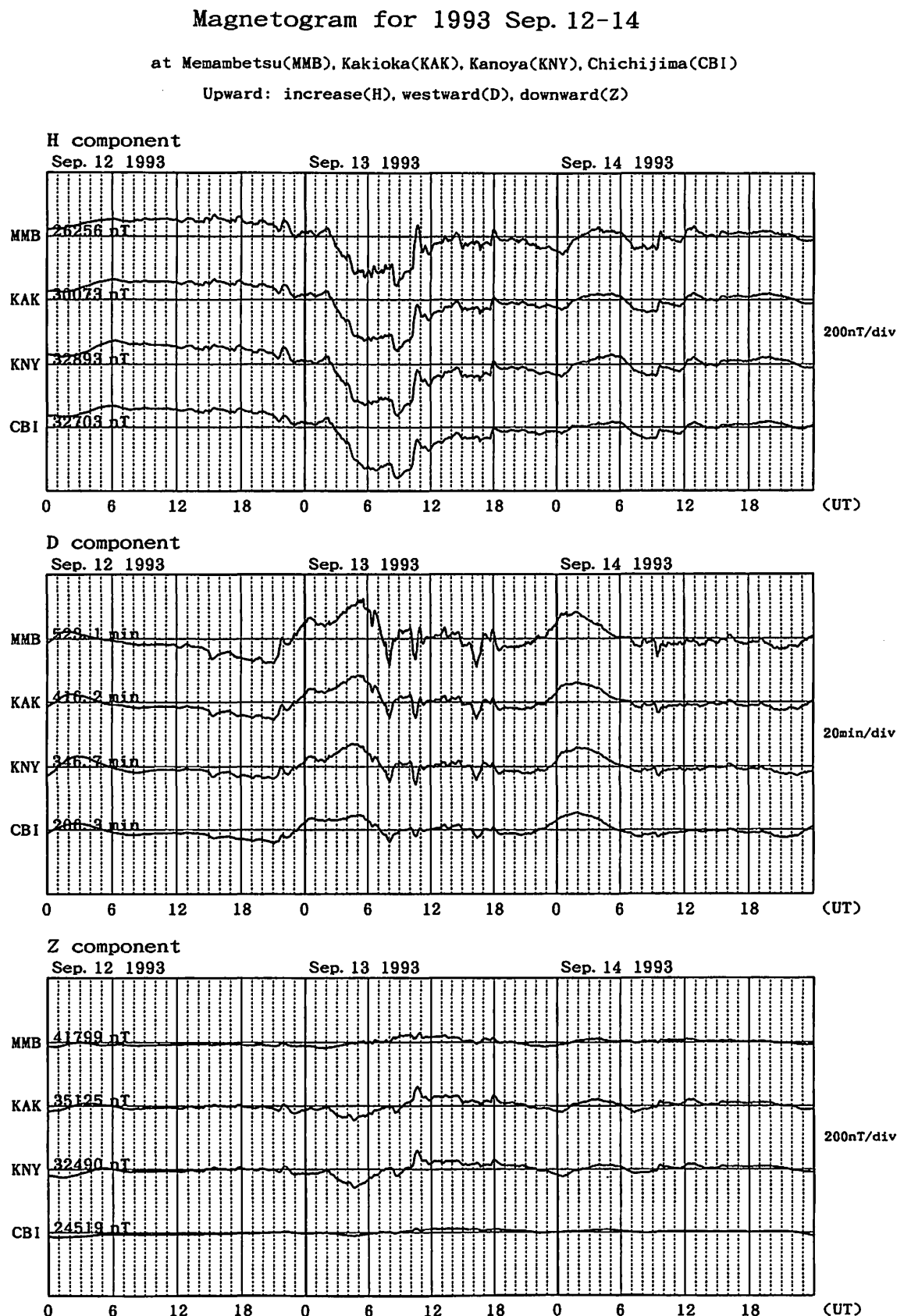


Fig. A-68 Magnetic records at MMB, KAK, KNY and CBI for the geomagnetic storm of September 12, 1993.

Magnetogram for 1993 Oct. 08-10

at Memambetsu(MMB), Kakioka(KAK), Kanoya(KNY)

Upward: increase(H), westward(D), downward(Z)

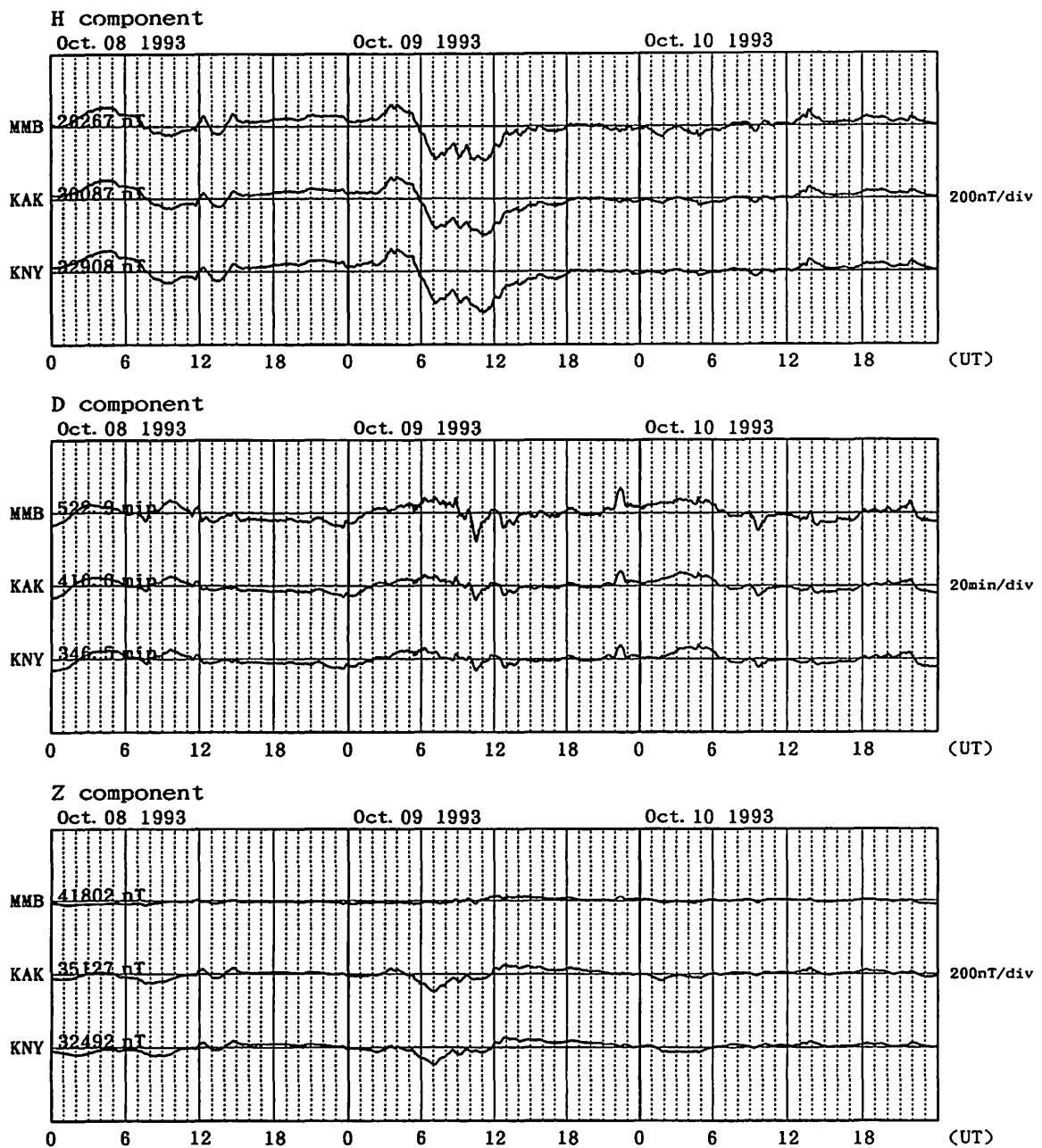


Fig. A-69(a) Magnetic records at MMB, KAK and KNY for the geomagnetic storm of October 8, 1993.

Magnetogram for 1993 Oct. 11-13

at Memambetsu(MMB), Kakioka(KAK), Kanoya(KNY)

Upward: increase(H), westward(D), downward(Z)

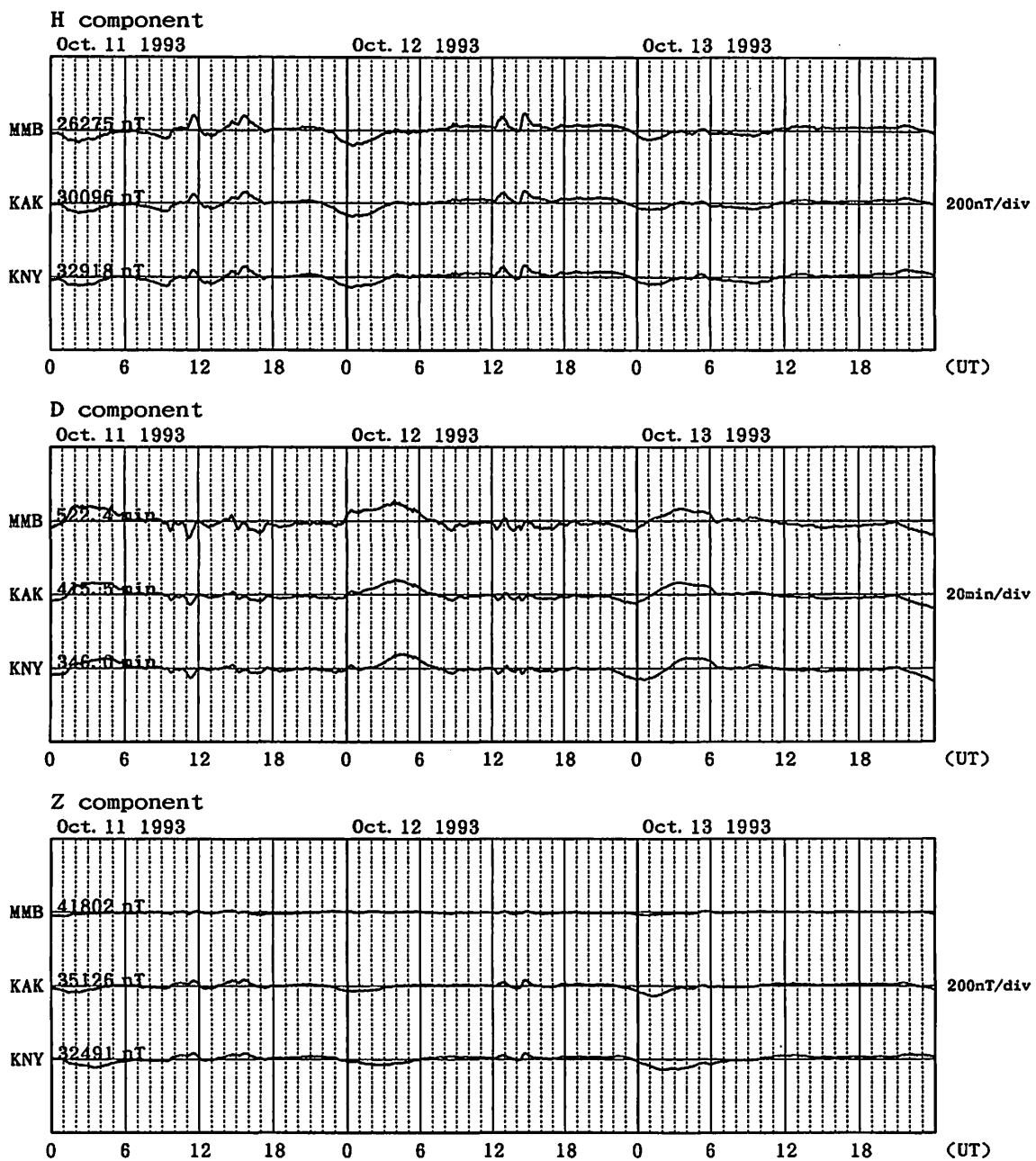


Fig. A-69(b) Magnetic records at MMB, KAK and KNY for the geomagnetic storm of October 8, 1993 (succeding Fig. A-69(a)).

Magnetogram for 1993 Nov. 03-05

at Memambetsu(MMB), Kakioka(KAK), Kanoya(KNY), Chichijima(CBI)

Upward: increase(H), westward(D), downward(Z)

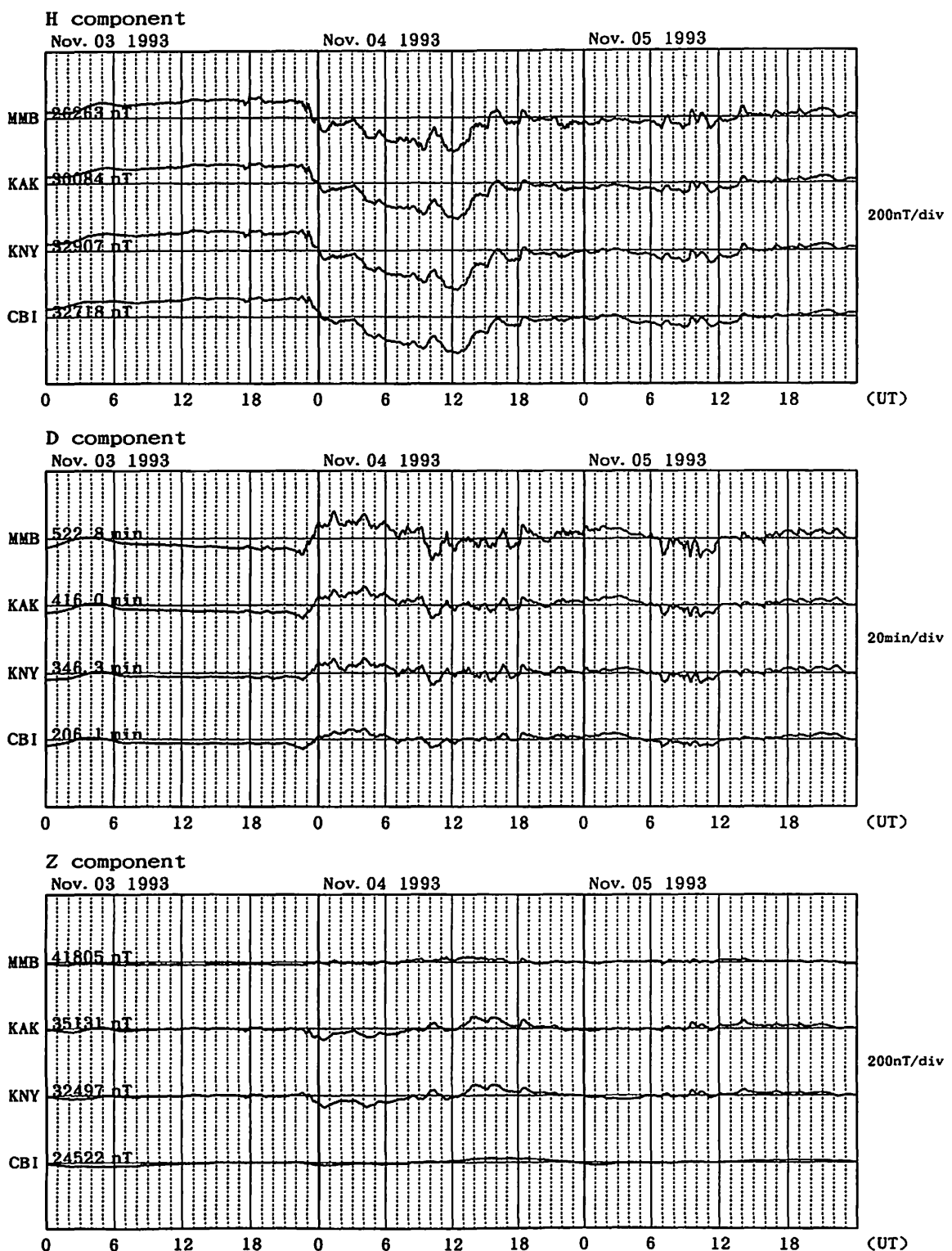


Fig. A-70 Magnetic records at MMB, KAK, KNY and CBI for the geomagnetic storm of November 3, 1993.

Magnetogram for 1994 Feb. 21-23

at Memambetsu(MMB), Kakioka(KAK), Kanoya(KNY), Chichijima(CBI)

Upward: increase(H), westward(D), downward(Z)

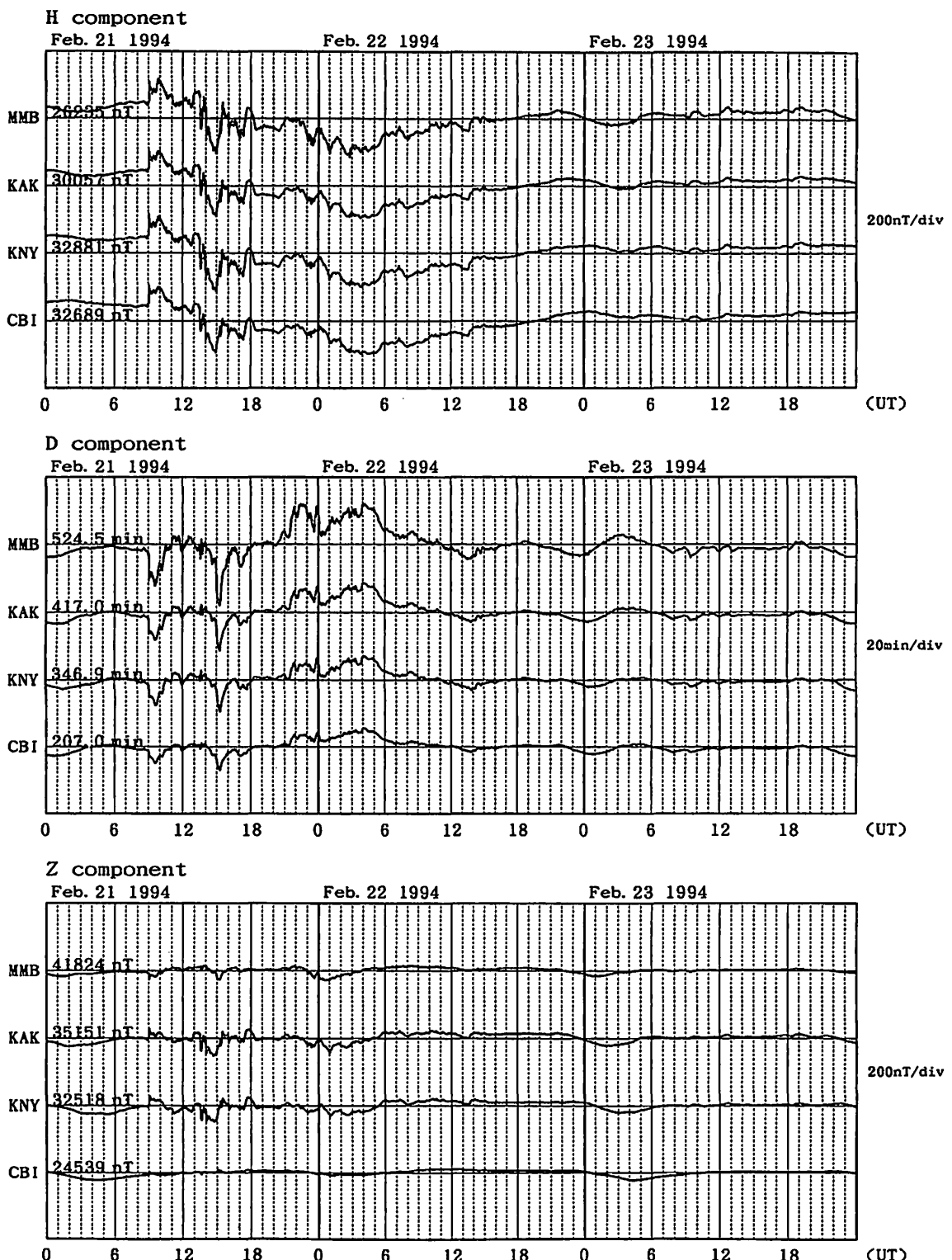


Fig. A-71 Magnetic records at MMB, KAK, KNY and CBI for the geomagnetic storm of February 21, 1994.

Magnetogram for 1994 Apr. 16-18

at Memambetsu(MMB), Kakioka(KAK), Kanoya(KNY)

Upward: increase(H), westward(D), downward(Z)

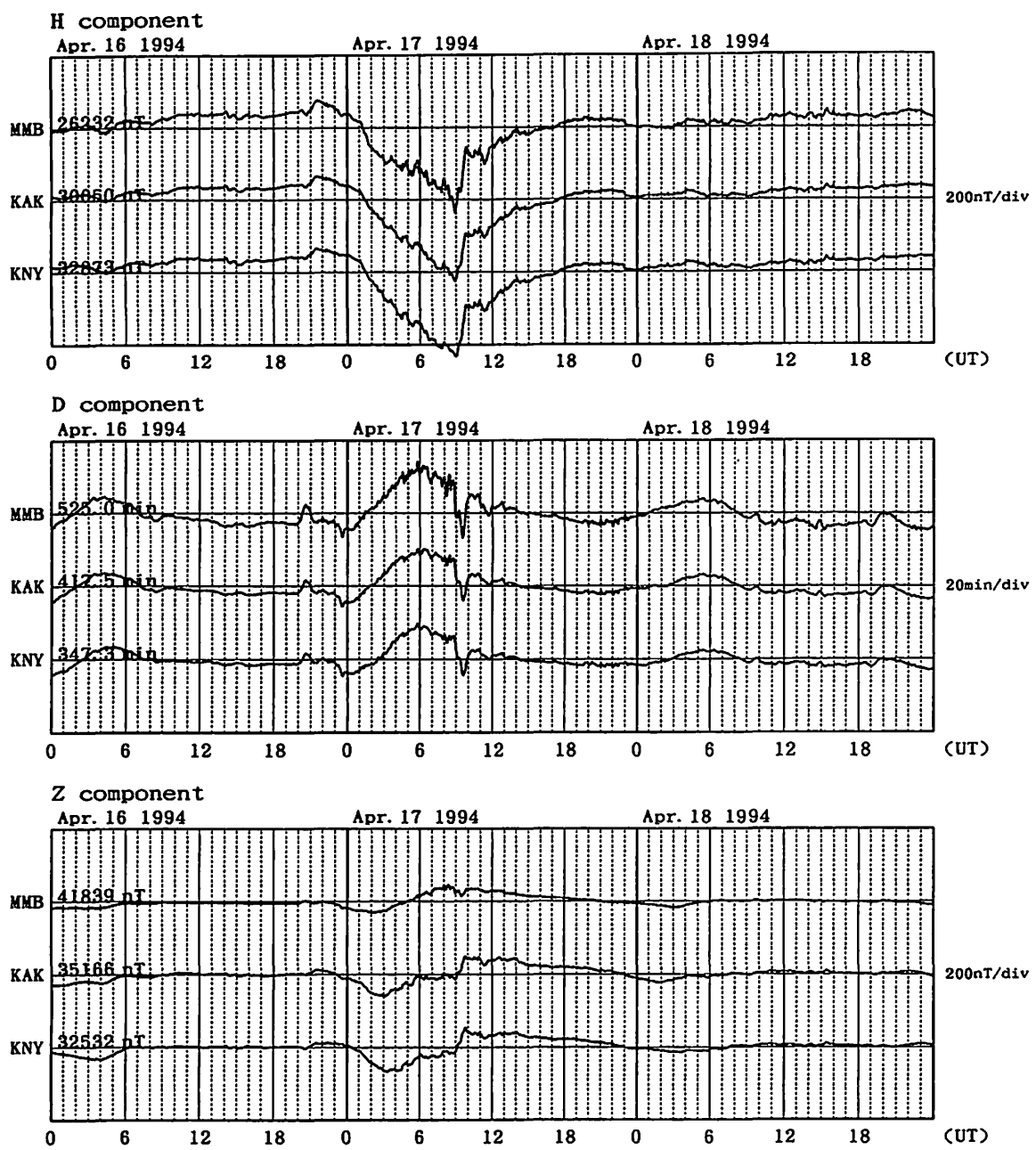


Fig. A-72 Magnetic records at MMB, KAK and KNY for the geomagnetic storm of April 16, 1994.

Magnetogram for 1994 Oct. 02-04

at Memambetsu(MMB), Kakioka(KAK), Kanoya(KNY)

Upward: increase(H), westward(D), downward(Z)

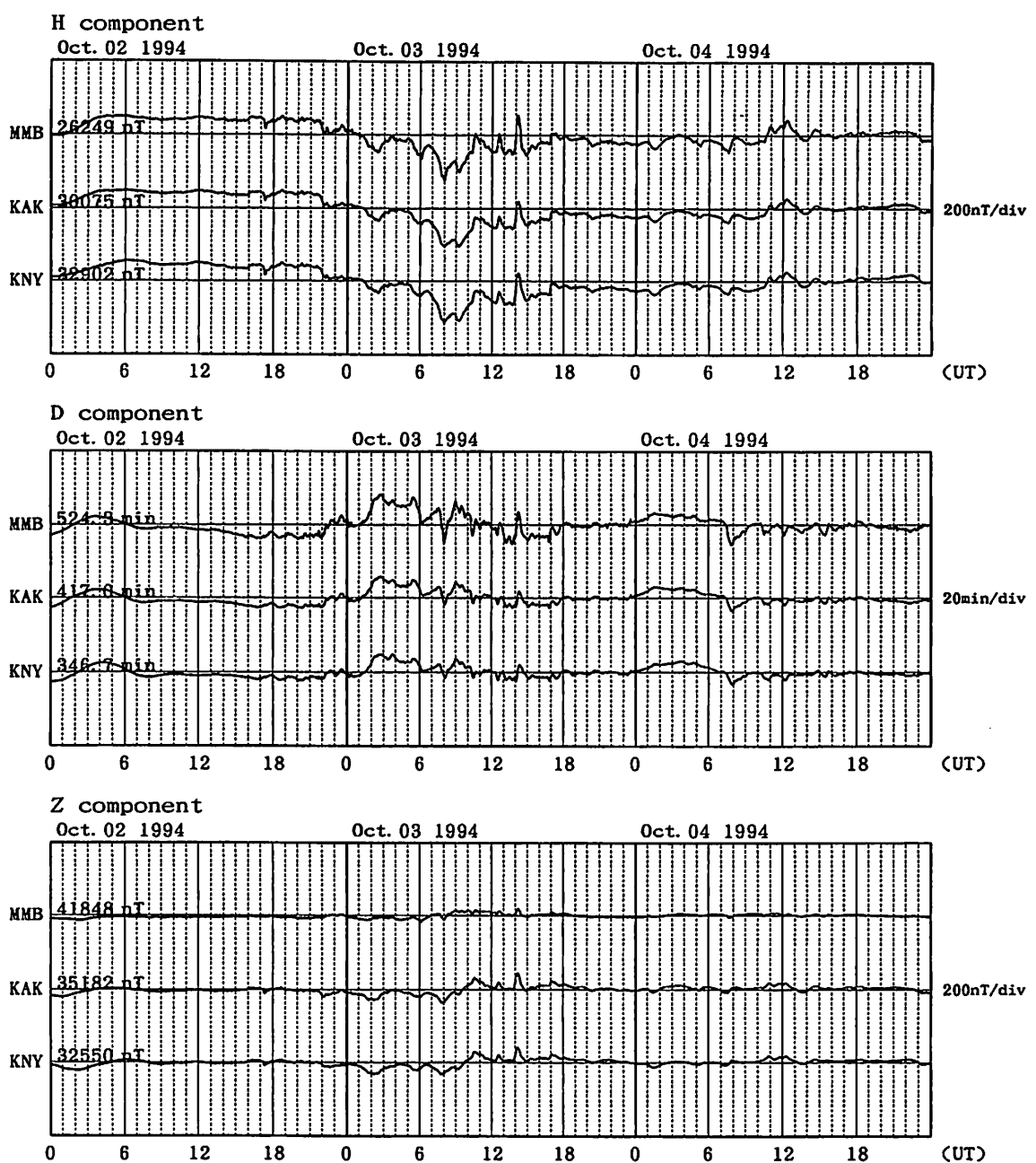


Fig. A-73 Magnetic records at MMB, KAK and KNY for the geomagnetic storm of October 2, 1994.

Magnetogram for 1994 Oct. 29-31

at Memambetsu(MMB), Kakioka(KAK), Kanoya(KNY), Chichijima(CBI)

Upward: increase(H), westward(D), downward(Z)

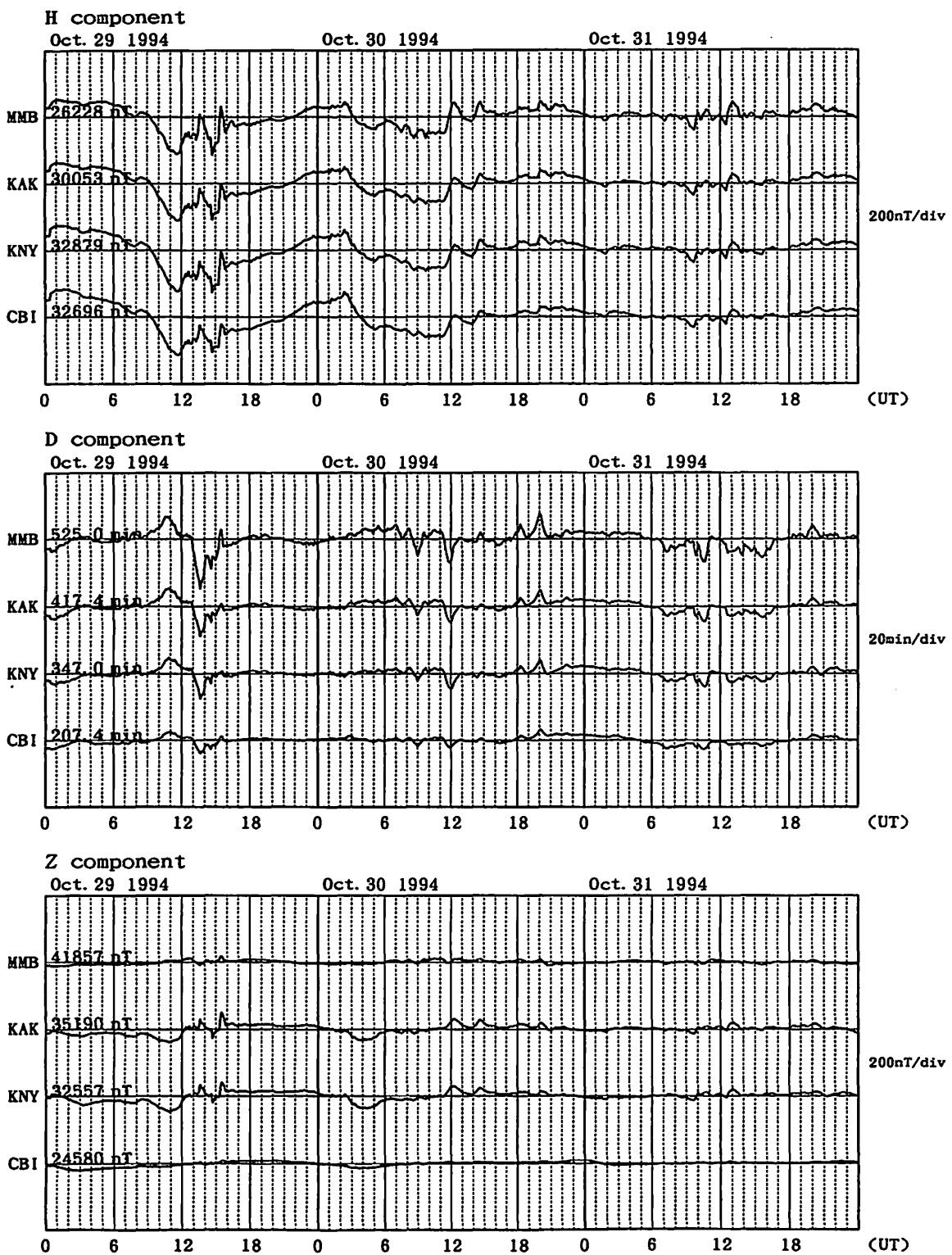


Fig. A-74 Magnetic records at MMB, KAK, KNY and CBI for the geomagnetic storm of October 29, 1994.

Magnetogram for 1994 Nov. 26-28

at Memambetsu(MMB), Kakioka(KAK), Kanoya(KNY), Chichijima(CBI)

Upward: increase(H), westward(D), downward(Z)

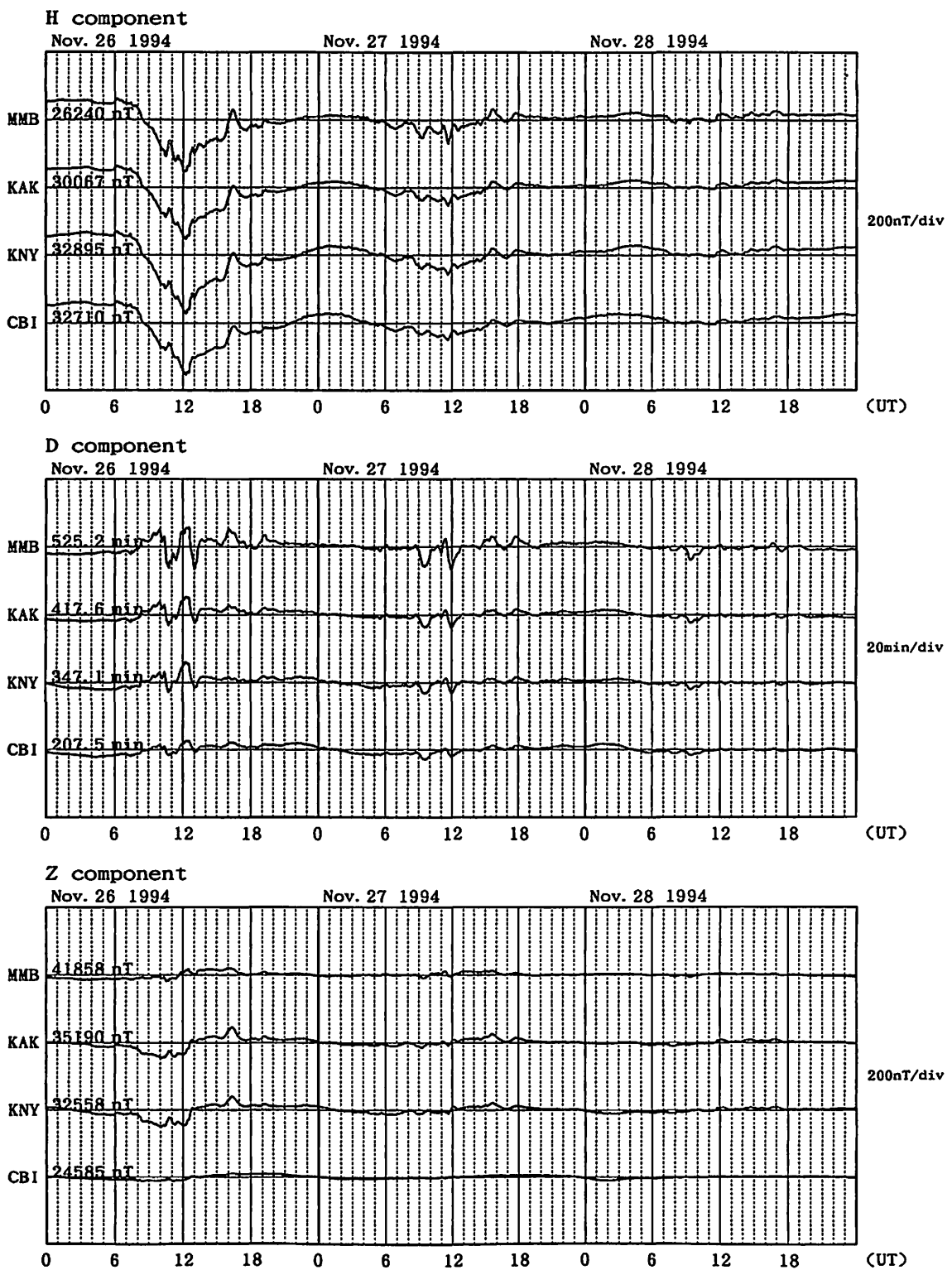


Fig. A-75 Magnetic records at MMB, KAK, KNY and CBI for the geomagnetic storm of November 26, 1994.

Magnetogram for 1995 Mar. 26-28

at Memambetsu(MMB), Kakioka(KAK), Kanoya(KNY)

Upward: increase(H), westward(D), downward(Z)

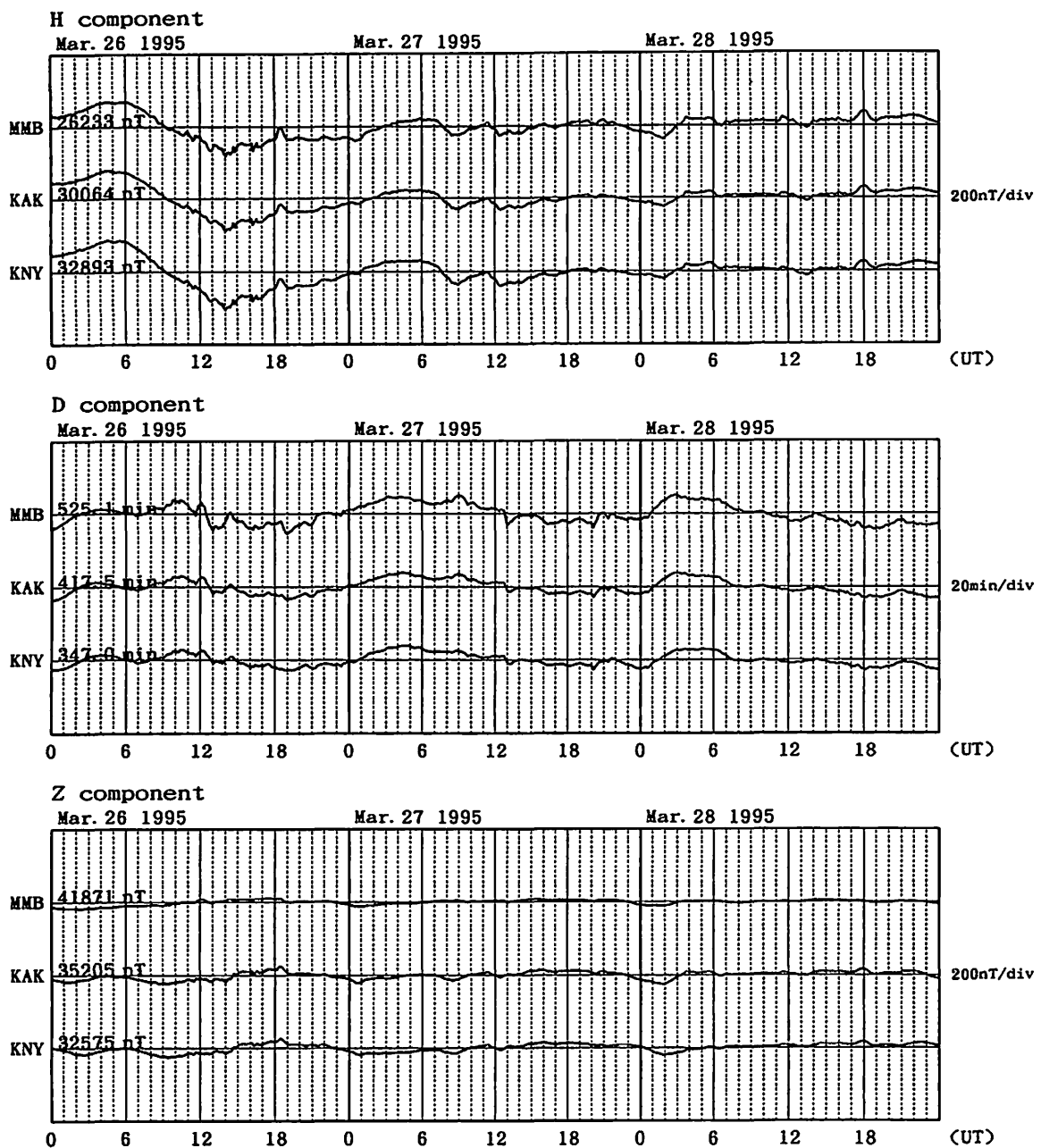


Fig. A-76 Magnetic records at MMB, KAK and KNY for the geomagnetic storm of March 26, 1995.

Magnetogram for 1997 Jan. 10-12

at Memambetsu(MMB), Kakioka(KAK), Kanoya(KNY), Chichijima(CBI)

Upward: increase(H), westward(D), downward(Z)

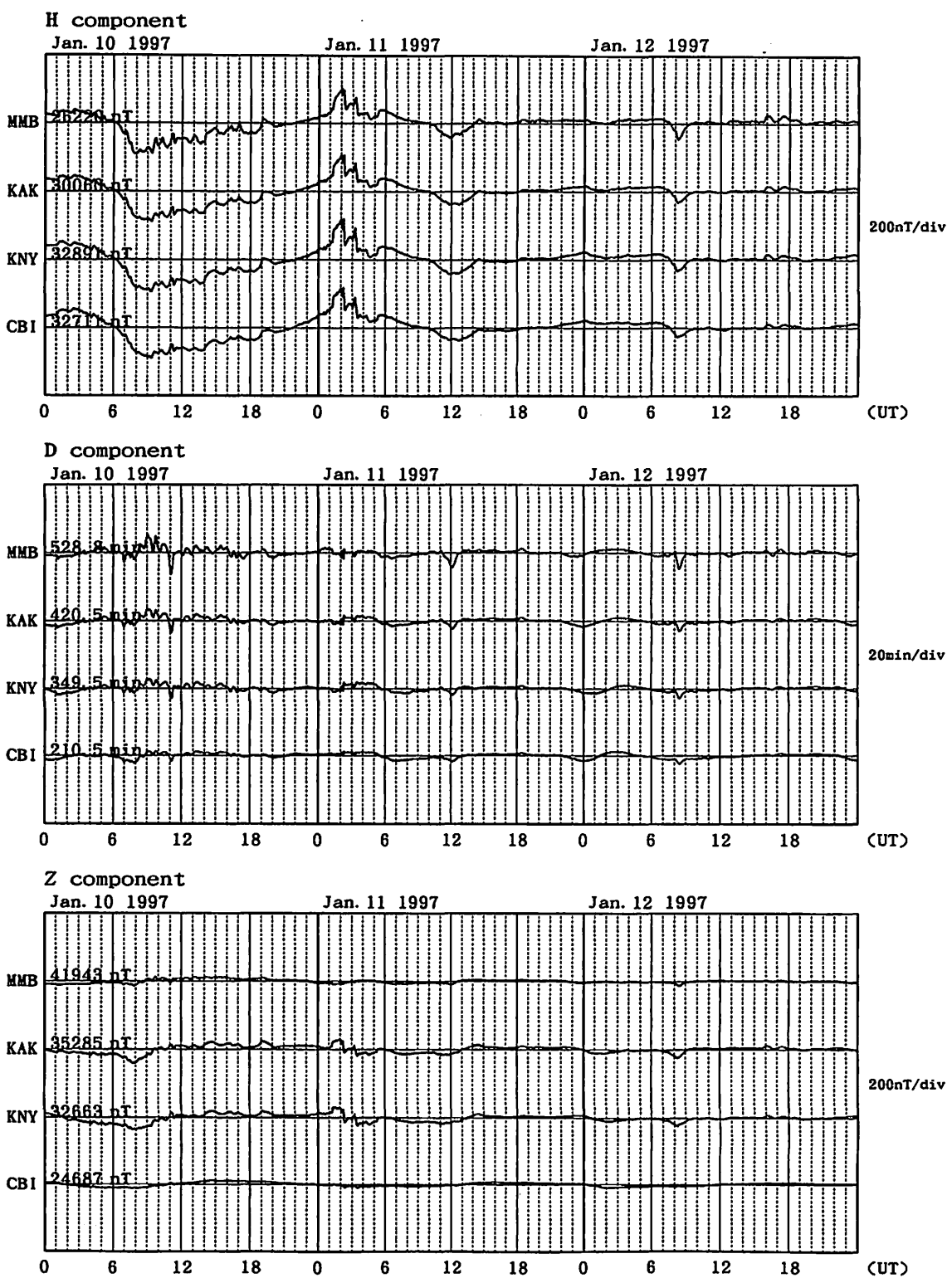


Fig. A-77 Magnetic records at MMB, KAK, KNY and CBI for the geomagnetic storm of January 10, 1997.

Magnetogram for 1997 May 15-17

at Memambetsu(MMB), Kakioka(KAK), Kanoya(KNY), Chichijima(CBI)

Upward: increase(H), westward(D), downward(Z)

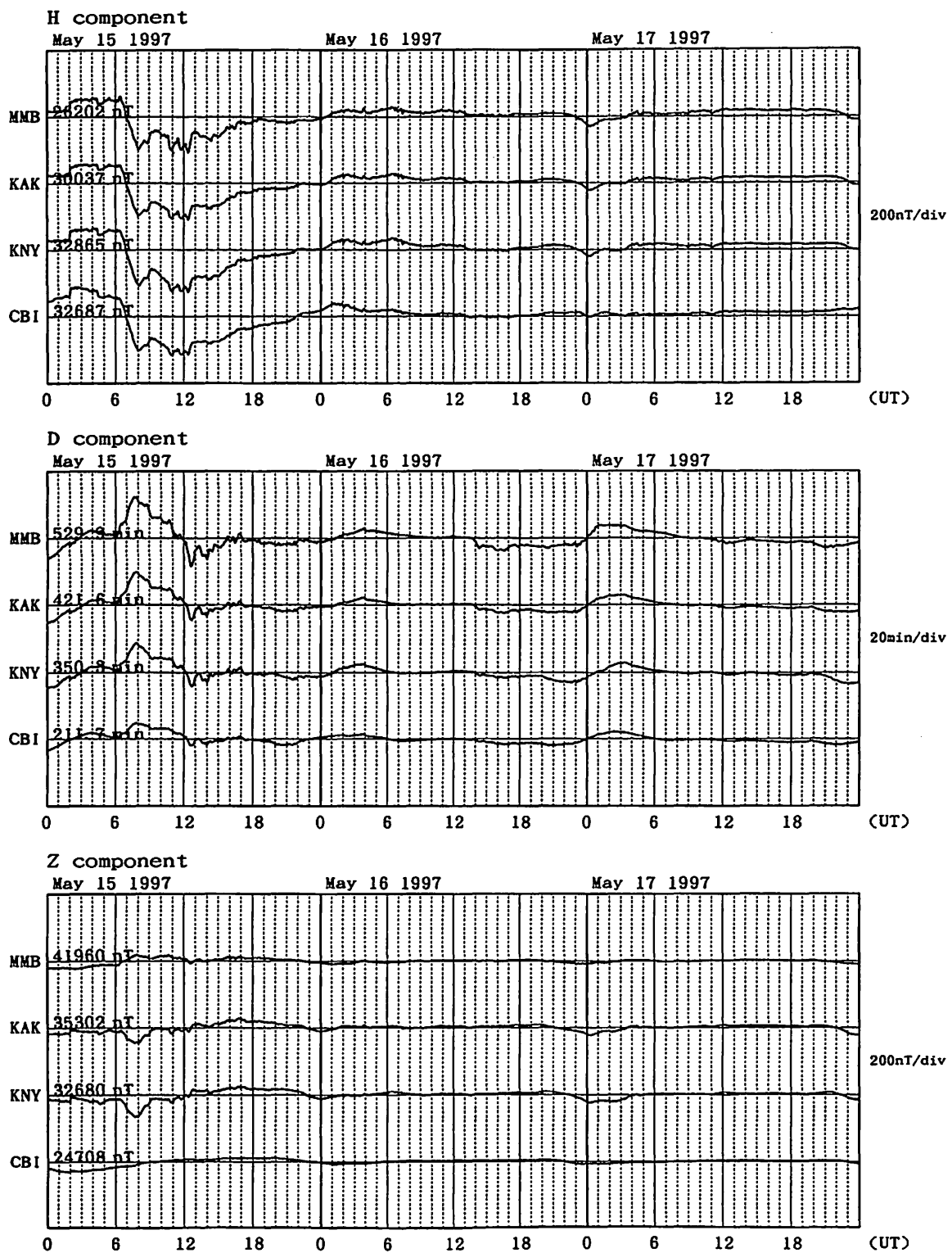


Fig. A-78 Magnetic records at MMB, KAK, KNY and CBI for the geomagnetic storm of May 15, 1997.

Magnetogram for 1997 Nov. 22-24

at Memambetsu(MMB), Kakioka(KAK), Kanoya(KNY)

Upward: increase(H), westward(D), downward(Z)

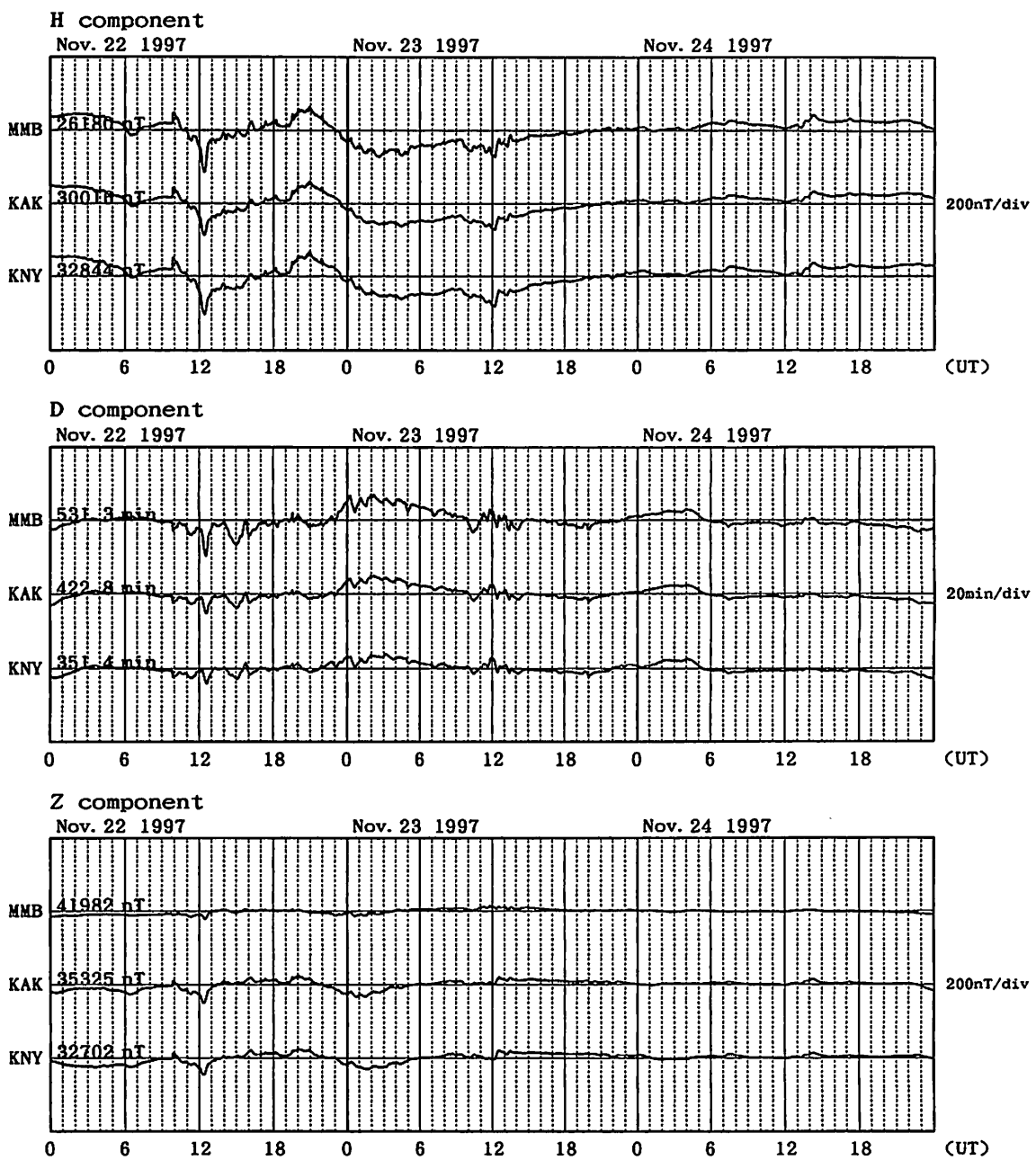


Fig. A-79 Magnetic records at MMB, KAK and KNY for the geomagnetic storm of November 22, 1997.

日本の地磁気観測データを用いた磁気嵐の研究

角村悟・外谷健・石井美樹・手島聰

概要

日本の地磁気観測点、女満別・柿岡・鹿屋で観測された磁気嵐の性質を、現象報告・毎分値を用いた統計・数値解析により調査した。柿岡および女満別における毎分値を SSC で開始する磁気嵐について重ね合わせてみると、一日またはより長い周期について、地球の電磁誘導による遮蔽効果によりいくぶん弱められてはいるものの、Z成分に環電流の直接の影響が見られる。その周期帯における H, Z 成分を比較して内部および外部起源の場の強さの比を概算したところ、力武・佐藤（1957）によって得られた数値とほぼ一致した。柿岡より局所的な C A 効果が小さい女満別の Z 成分は、環電流の強度を見積もるための即時的なモニターツールの一つとして使えるかも知れない。しかし、長期変化を吟味するには日本付近の複雑な Z 成分の永年変化が充分に解明されなければならないことが示される。柿岡における毎分値を地方時に分けて重ね合わせた記録に磁気嵐時における日変化パターンが見られた。それらは、沿磁力線電流およびそれによる電離層電流系によるものであろう。IGY 以来現在にいたるまでの間に観測された磁気嵐の中で、非常に大きな D 成分のレンジを記録した 1958 年 2 月 11 日の磁気嵐の変化パターンについて簡単な調査をした。SSC 直後に発生した H 成分の negative bay に対応して D 成分に現れた変化が D 成分のレンジを増加させるのに寄与していることが示される。昼間の時間帯の中低緯度において観測される negative bay を含め、磁気嵐のケーススタディが今後も重要であることが示唆される。